Modular Ammonia Production Plant

Student AIChE Design Competition
2019-2020

AIChE
The Global Home of Chemical Engineers

TABLE OF CONTENTS

Abstract

The following report provides a preliminary design analysis of a modular ammonia production plant proposed to be constructed in the Minnesota River Valley. One of the primary goals for the process engineering team was to design a plant capable of being carbon emission free, thus all design decisions were made prioritizing this goal. The process features ammonia synthesis via the Haber-Bosch process with a ruthenium-based which converts divalent hydrogen and nitrogen into ammonia at high temperature and pressure. The feed reactants are generated on site via electrolysis of water for the hydrogen stream and an air separation membrane system for the nitrogen stream. Both reactant generation methods require no direct carbon input while all electricity is sourced from wind energy produced in the surrounding area. Due to the efforts to make the plant carbon-neutral, manufacturing costs were significantly high resulting in a unit price of $1,480/mt to make the plant break even after the 20-year lifetime at a 10% rate of return. More market research is required to determine a competitive unit price for the Minnesota River Valley area, but this is likely too high based on the wide estimate of $500-$2,000/mt based preliminary research. Further process modifications must be completed before a modular ammonia production plant that operates with zero carbon emissions can compete on the market. The accuracy of the capital and operating costs are limited by the present lack of heuristic knowledge regarding modular chemical production. There is potential for decreases in capital and operating costs by further optimizing minor equipment, but the capital cost is limited by the capital costs of hydrolysis. Despite these economic concerns, the process engineering team has concluded that a carbon-free ammonia production plant is possible.

Introduction

The main objective of this project was to develop a preliminary design for a modular ammonia production plant capable of producing 50 metric tons per day of anhydrous ammonia for fertilizer. With the market size for ammonia projected to exceed $75 billion by 2025, now is the perfect time to start installing a plant [1]. In order to stay ahead of the curve for energy usage and production, the process engineering team has completed the following preliminary design with a major goal of being carbon neutral. The plant will be constructed in the Minnesota River Valley where there is underused wind availability for renewable energy generation to power the ammonia plant [2]. Attempting to reduce installed costs of large equipment, five smaller modules each capable of synthesizing 10 metric tons of the total 50 metric tons per day capacity were selected for the production plant. An analysis of module size is included to determine an optimum module size. While other processes have larger production capacities, the hope is that the module design will enable the plant to increase production with demand in the point-of-use location. The Minnesota River Valley is also part of the US corn belt, which is a major consumer of ammonia fertilizer. The point-of-use installation site has the added benefit of reduced shipping and insurance costs.

One of the primary goals of this ammonia production plant is to be environmentally sustainable by designing a system that is carbon neutral. The equipment and operational costs increased as a result of carbon neutral design elements—which decreases profitability—but ultimately is a small price to pay for more sustainable operation. Hydrogen was produced with electrolysis rather than the natural gas steam reformation traditionally used, which uses non-renewable resources to generate the product. The design team also decided to only use renewable energy to power process equipment. This includes generated steam (from excess heat) on-site to be used for energy generation in a steam turbine as well as wind energy. The availability of stranded wind in the area provides economical and sustainable energy for production.

Several non-traditional ammonia synthesis methods are considered here which include reactive separation and non-thermal plasma catalysis for ammonia production at near-ambient conditions. The traditional Haber-Bosch process is also investigated as an option, and the modern ruthenium-based catalysts are considered as well. It was decided that the non-traditional methods were underdeveloped and/or too energy intensive or complex at their current capabilities for commercial implications. The preliminary design here uses a traditional Haber-Bosch process with a modern ruthenium-based catalyst which allows for lower operating temperature and pressure with commercially viable single-pass conversions.

Hydrogen is produced in this design with an alkaline electrolysis system. This method of hydrogen production is relatively new, especially when compared to steam methane reforming (SMR). With this is mind, it was expected that the operating costs would be higher than normal in this design. The goal of being carbon-neutral ultimately led to this design choice, as the design team believes protecting the environment from carbon emissions is worth the extra cost. Also, the availability of stranded wind energy in the Minnesota River Valley encouraged the use of clean electricity. Alkaline electrolysis cells and proton exchange membrane (PEM) electrolysis cells were considered in this design, and the alkaline electrolysis was eventually chosen, as it is known to be a more straight-forward design, with a lower capital cost [3]. Another key design choice for the hydrogen production method is to use pure nickel electrodes in the electrolysis cells, and treat the

electrodes with hot-dip-galvanization in molten zinc [4]. After extensive economic analysis, it was decided that the electrolysis design was detrimental to the economics of the project. The design of this section must be considered more carefully, to reduce capital and operating costs, before moving forward with the project.

A membrane system was chosen in order to produce the nitrogen feed stream for the reactor due its simple design, reduced utility costs, and ability to remain carbon neutral. By employing a membrane system, on-site nitrogen generation is made possible with the only utility costs coming from the compressor and heat exchanger used to increase the pressure and decrease the temperature respectively. Key considerations that played a role in determining which membrane was selected included finding a membrane that is highly selective for oxygen (such that the small fraction of oxygen in air can be removed and disposed of) without a significant decrease in overall permeability (such that the material can handle the required flow rate). The chosen experimental porphyrin-based oxygen carrier membrane is not yet on the market, but recent research on T(*p*-OCH_3)PPCoCl infused TFC membranes indicate promise toward expansion for large-scale studies and eventual patents. Pressure-swing adsorption was identified as another viable option for on-site air separation in case of significant delays or unexpected costs related to the membrane.

The following report details each of the three major sections required for the production of ammonia using the Haber-Bosch process: the electrolysis cells (section 100), the membrane system (section 200), and the catalytic reactor (section 300). Relevant sample calculations, process flow diagrams, costing, and other forms of analysis are included for each section. Ultimately, the process engineering team was successful at designing a carbon neutral modular production plant capable of producing 50 metric tons per day.

Process Description

This section includes a complete description for each of the major sub-processes featured in a single module. Although there has been some research into alternative reaction schemes or reactor conditions, the process engineering team ultimately decided to utilize the traditional Haber-Bosch process of artificial nitrogen fixation at high temperature and pressure. The first task the team addressed was sourcing the reactants of hydrogen and nitrogen for the Haber-Bosch process. The purified hydrogen stream was generated via electrolysis of water and the purified nitrogen stream was generated via a membrane system. The use of these processes enabled both the reactants to be generated on-site, thus eliminating additional raw material costs. Once the reactant feed streams were generated, their temperature and pressure were increased before being fed into a ruthenium-based catalyst reactor. Finally, the separation process was designed to be capable of recovering 99% of the ammonia produced with the remaining ammonia removed from the purge stream via a scrubber for subsequent incineration. The current process features storage tanks capable of holding a week's worth of anhydrous ammonia production at 200 psia.

Hydrolysis Cell for Hydrogen Feed

Electrolysis of water with alkaline electrolysis cells was chosen as the method for hydrogen production. The electricity used will be sourced from stranded wind, making this section of the design carbon neutral. The basis of the electrolysis cell is the hydrogen gas input requirement to the ammonia synthesis reactor, see the Process Flow Diagram and Material Balance section above. The required hydrogen gas flow rate was used to design the size of each modular electrolysis cell system and find the required amount of electrical energy for the steady-state process.

It is recommended that the electrolysis section should be designed with monopolar, alkaline electrolysis cells. Each electrolysis cell has two reservoirs, in which an electrode is suspended in an aqueous solution of 30 wt% potassium hydroxide. There is a membrane separator between the reservoirs which allows only water and hydroxide ions to cross. The monopolar design implies that each individual cell has distinct electrodes, and the cells operate in parallel, each producing a pure stream of hydrogen and oxygen [3]. This design decision was made because monopolar cells are simpler, and it allows one cell to be shut down while the others continue to run. Shutting one cell down in the "series" bipolar design would cause the entire unit to shut down.

One common issue with electrolysis cells is providing enough electrode surface area to catalyze the electrochemical reaction at a high enough rate [5]. To mitigate this issue, it is recommended that the electrolysis cells are built with pure nickel electrodes, and the electrodes should be treated with a hot dip galvanization method to increase the specific surface area of the material [4]. When galvanized in molten zinc, nickel electrodes have been shown to increase in specific surface area by a factor of 1000 [4]. For this design, it is assumed that this treatment method will increase the active catalytic surface area of each electrode by a factor of 10. This assumption decreased the geometric area needed for each electrode, leading to a more compact electrolysis cell design.

Each modular electrolysis cell system was designed as a cube, with the side length of the cube being calculated to meet the required surface area to meet the needed 43 kg-moles of hydrogen gas produced per hour. Each cell within the cubic system was designed with a width of 20 cm (each

reservoir 10 cm wide) to provide room for the electrodes and an adequate amount of alkaline solution. The electrolysis cell design includes a heat exchanger to preheat the water to 80 °C and a cooling jacket on the cell to absorb excess heat released.

When determining the capital and operating expenses for this process, industrial heuristic values were used. The design was centered around a current density value of 0.5 A/cm^2, which has been shown to lead to an energy usage rate of 4.2 – 4.8 kW-hr per normal meter cubed of hydrogen produced [3]. For this design, a value of 5.0 $kW\text{-}hr/Nm^3$ was used. To determine the capital cost of each unit, a value of $800 per kg of hydrogen produced per day was used [6]. See the Equipment Cost Summary for an in-depth explanation of this costing estimation.

Membrane Separation of Air for Nitrogen Feed

The second required reactant for the Haber-Bosch process is nitrogen, which is readily available in air. Initially, two options were considered when investigating how the modular process would achieve this nitrogen feed stream for the reactor: separation via either a pressure awing adsorption (PSA) or membrane system. A primary benefit of pressure swing adsorption systems is that they are less sensitive to process parameters (mainly pressure and temperature conditions) when compared to membrane systems, although if process parameters can be appropriately controlled, membranes provide a very consistent unit [7]. Furthermore, PSA processes require a higher initial investment in addition to more energy consumption throughout their lifetime; thus, the decision was made to utilize a membrane for producing the nitrogen feed stream [8]. Assuming a stoichiometric ratio of reactants, a material balance was used to determine the required nitrogen feed in order to accomplish the process specifications for ammonia production. The process engineering team decided that to reduce concerns of undesired build-up in the reactor section, the nitrogen stream should have a 99% purity; therefore, selecting a specialized membrane with the appropriate permeability and selectivity was imperative to ensuring the correct flow and composition of the nitrogen feed.

The membrane recommended to produce this 99% pure nitrogen stream uses a novel approach to oxygen/nitrogen separation by employing a porphyrin-based oxygen carrier. A research group led by Jiuli Han of the Chinese Academy of Sciences concluded that thin film composite (TFC) membranes with the addition of a small amount of T(*p*-OCH_3)PPCoCl increases the membrane's selectivity for oxygen without a significant compromise in permeance [8]. This cobalt porphyrin forms relatively strong hydrogen bonds with the primary thin film Pebax-2533 material while interacting reversibly with oxygen to facilitate radial transport [8]. It was ultimately decided that radial diffusion would provide the simplest geometry of design and consistent oxygen transport through the walls of a tube composed of the membrane material. The proposed system will feature a residual stream of purified nitrogen (the feed stream into the reactor) and a permeate stream that is essentially a 50/50 mol% mixture of nitrogen and oxygen (vented to the atmosphere). Selecting a membrane that is highly selective for oxygen was an obvious choice due to its lower relative composition in air and the feasibility of finding a suitable molecule to interact with the more electronegative oxygen. Furthermore, while other membranes have been successful at separating nitrogen/oxygen, the process engineering team decided that using a highly selective membrane for oxygen would be critical for removing as much oxygen as possible from the residual stream.

Similar to the electrodes in the electrolysis section, the surface geometry of the membrane increases the available surface area for diffusion; thus, it was assumed that the geometry of the membrane increased the specific surface area by a factor of 100. With a diameter of 6 cm and thickness of 0.01 cm, it was determined using the experimental membrane selectivity and permeability that a membrane tube 26.6 m long would be capable of achieving the desired process specifications, though it is recommended that a single module is constructed with a 27 m tube that winds back and forth. Preliminary design of the membrane apparatus incudes a chamber that quickly vents the permeate to the atmosphere from the tube which winds back and forth to maximize space allocation. Specializing the membrane tube design for the specific purpose of this separation scheme provides the benefit of efficiency, but over time the material will need to be replaced.

To increase the efficiency of the membrane such that it processes less air to produce the nitrogen stream, the optimal temperature of 18 ºC and pressure of 4.17 bar (according to Han's research team in China) will be used for the feed stream. Assuming the air enters the system at atmospheric conditions, achieving the high optimal pressure requires a rotary screw compressor, which heats the air stream. To cool the stream, a heat exchanger employing refrigerated water will be used assuming isobaric operation. Utilizing these optimal feed conditions decreases the load on the membrane, thus, increasing its life expectancy. Another precaution taken to protect the membrane from unnecessary damage is a pretreatment system used to filter out air particulates and remove humidity. Water or other contaminants in the air can clog or degrade the membrane. Replacing the filter and desiccant in the pretreatment system will be a cheaper option than replacing the primary membrane.

With the recommended membrane not currently on the market, predicting the cost was a challenge that was overcome by requesting a quote for a PSA system capable of operating at the same process conditions from Compressed Gas Technologies Incorporated [9]. Generally, membrane systems reduce the initial capital investment, thus the $60,000 estimate for a single module was considered a conservative estimate for the membrane cost. Installing the compressor was the most significant capital cost for this section due to the need to quadruple the pressure, but due to a high heat transfer potential using refrigerated water, the heat exchanger was relatively small resulting in a low capital cost.

Ammonia Synthesis Reactor

Several novel process intensification designs were considered for the ammonia synthesis reactor. The designs considered were reactive separation and a non-thermal plasma catalyst. An article by Malmali et. al. investigated the effectiveness of reactive separation [10]. Some major advantages of reactive separation are the potential for low pressure synthesis and reducing or elimination of a recycle stream. Both of these would result in a process that is less expensive and less hazardous [10]. Malmali et. al. showed that high conversion is possible with reactive separation, and Himstedt et. al. was able to achieve >90% conversion via reactive separation [11]. However, reactive separation for ammonia synthesis is still a new technology, and large scale designs have not been implemented. The reactive separation process requires cycling of the system to remove the absorbed ammonia. Thus, the system is only producing ammonia approximately half the time, and

more equipment would be required to meet the production demand. The novelty and complexity of the cyclic process were ultimately the deterrents away from reactive separation.

Non-thermal plasma catalysts for ammonia synthesis were also investigated, and it has the potential to reduce the reaction conditions to near ambient [2]. A summary of energy requirements in lab-scale research from Peng et al showed that a minimum of about 2,000 GJ/mt are required to produce ammonia via non-thermal plasma catalysis. This would likely become more efficient at large scales, but large scales have not been attempted. Current, high-efficiency ammonia synthesis via the Haber-Bosch process has been able to produce ammonia at only 28 GJ/mt [12]. Thus, the current understanding of non-thermal plasma assisted ammonia synthesis was deemed too novel and too energy intensive to pursue at this point in time.

This led to the investigation of a small-scale Haber-Bosch process. A report by Reese et. al. laid out the design and performance of a small-scale Haber-Bosch process [13]. The modern, high-efficiency ruthenium-based catalyst developed by British Petroleum was also investigated to determine high throughput potential of a small-scale Haber-Bosch process [14], [15]. Ruthenium-based catalysts have proven to be about 20 times more active than the original promoted iron catalyst, and ruthenium-based catalysts have been used world-wide for more than 25 years [15]. Ruthenium-based catalysts have also lowered the reaction temperature and pressure significantly while still achieving commercially-viable ammonia yields [14], [15]. Based on this research, the ammonia synthesis reactor was chosen to be a Haber-Bosch style process using a ruthenium-based catalyst.

Reaction conditions and parameters were based on three sources. Brown reported the ruthenium-based catalysts could achieve nitrogen conversions of 26% or 55% at reaction conditions of 86 bar, 380 °C or 138 bar, 400 °C, respectively, when using a 1.5:1 ratio of hydrogen to nitrogen [15]. Lin et. al. reported ammonia synthesis rates on ruthenium-based catalysts ranging from 7 to 9.8 $\mathrm{mmol_{NH_3}\,g_{cat}^{-1}h^{-1}}$ that increased with pressure from 10 bar to 100 bar and became asymptotic around 80 bar [14]. This reaction data was generated using a stoichiometric feed of 3:1 hydrogen to nitrogen. Lastly, the review article Pattabathula reported that modern, high efficiency ammonia plants achieve a 20-21% single pass conversion using a more common 3:1 hydrogen to nitrogen ratio [12]. This is significantly different than the conversions reported in Brown, but the difference is likely due to the non-stoichiometric reactant ratio reported in Brown [15]. Lower reaction pressure and temperature are desirable from a capital cost and safety perspective. The demonstrated reaction rates from Lin also fall in the range of the lower reaction condition from Brown [14], [15]. Therefore, reaction conditions of 86 bar and 380 °C were chosen for the ammonia synthesis reactor. A conservative single pass conversion of 20% was chosen based on the information reported in Brown and to align with Pattabathula [12], [15]. A stoichiometric reactant ratio was chosen with a conservative reaction rate of 9.5 $\mathrm{mmol_{NH_3}\,g_{cat}^{-1}h^{-1}}$.

Reactor design was discussed in Pattabathula and Reese which influenced the reactor design here [12], [13]. Pattabathula describes a low-pressure drop, axial-radial reactor from Ammonia Casale [12]. A similar reactor with a central, cylindrical catalyst bed that uses radial flow was described in Reese, and the reactor design used here is based on a similar concept. Lastly, Reese used AmoMax 10 ammonia synthesis catalyst from Clariant, but minimal physical properties could be

found for AmoMax 10 [13]. Instead, the ruthenium on alumina catalyst, Ru-Cat 402, from Vesta Chemicals will be used as a model, which has an approximate bulk density of 850 kg/m^3 [16].

A reactor with catalyst filled tubes will be used in place of a single, cylindrical packed bed. Gas will flow into the catalyst filled tubes before being able to flow radially out of the tubes and leave the reactor. A catalyst tube length of 2.0 m and diameter of 10 cm was chosen to achieve a small reactor footprint. This gave a corresponding shell diameter of 2.1 m and requires 178 tubes to hold an adequate amount of catalyst to meet the module productivity requirement of 10 mt/day [17]. The reactor was assumed to have hemispherical ends, which gave an overall volume of 11.8 m^3 when using the multitube design. This footprint was chosen to meet typical semi-trailer dimensions [18]. The reactor will be equipped with an evaporative cooling jacket to control the reaction temperature and recover energy from the process. For this preliminary design, the reactor is assumed to be isothermal and isobaric.

In a single cylinder packed bed design (traditional axial-radial reactor), it is unknown how much larger the outer shell must be compared to the catalyst bed. If the outer shell is double the diameter of the single cylinder packed bed (catalyst bed dimensions: 2 m long, 1.33 m in diameter), then the reactor volume is 21.0 m^3. However, if the shell is only 1.5 times larger than the single cylinder packed bed, then the reactor volume is only 10.4 m^3. Because of this uncertainty in the reactor shell diameter requirement, the tubular sizing calculations will be used to approximate the reactor size. The tubular design may also lead to a lower pressure drop through the reactor since gas flows radially through 10 cm diameter tubes instead of a single, 1.33 m diameter catalyst bed. This may result in better overall performance. Detailed catalyst requirements and reactor sizing calculations can be seen in Appendix I.

Ammonia Separation

The outlet of the ammonia reactor needed to be purified because it's only 29 weight percent ammonia and the product specification is 99.5 weight percent. The hot product stream passes through a valve and series of heat exchangers that reduce the pressure and cool the reactor outlet down to a point just before the ammonia would condense at the pressure that the anhydrous ammonia would be stored at (-16 °C, 200 psia). The cooled reactor outlet stream then enters a flash drum, which rapidly removes energy to generate a liquid product stream at 200 psia and -33 °C of 99.5 weight percent anhydrous ammonia and a gas stream that is heated, compressed, and recycled to the reactor. The materials of construction in this section were designed to be stainless steel 316 because carbon steel and stainless steel 304 were not completely compatible with the ammonia in the process stream [19].

The reactor outlet first passes through an expansion valve to reduce the pressure from 1247 psia to 200 psia. The reasoning for having the valve immediately after the reactor outlet is to make the process inherently safer. Although expanding the stream reduces the heat capacity which would mean more heat exchanger area may be required, Aspen HYSYS simulated that the heat capacity would only decrease by 0.07 kJ/kmol—°C. This difference in energy saved is not worth the safety risk of leaving the stream pressurized through heat exchangers. Immediately reducing the pressure before the stream passes through heat exchangers reduces the damage that would occur if a heat exchanger tube ruptured.

The first heat exchanger that the reactor outlet passes through is one that is a double pipe heat exchanger in contact with the recycle stream that runs counter-currently, HX-306. The reasoning for having the recycle stream pass through a heat exchanger that comes into contact with the reactor outlet is because it eliminated the need for a high temperature heat transfer fluid that would heat up the recycle to the reactor temperature. After the recycle stream is compressed from 200 psia to 1247 psia (the reactor pressure condition), the temperature of the stream was 380 °C (the reactor temperature condition). The temperature of the reactor outlet stream changes from 380 °C to 290 °C. The heat transfer surface area of HX-306 is 7.0 m^2.

The reactor outlet then passes through two double pipe heat exchangers running counter-currently that use de-ionized water to reduce the temperature from 290 °C to 190 °C. The de-ionized water is vaporized into saturated steam at 5 bar and 152 °C, which is to be used in energy generation. The product stream passes through HX-307 first and decreases temperature from 290 °C to 247°C. The product stream then passes through HX-308 to decrease the temperature from 247°C to 183 °C. The de-ionized water pumped through the heat exchangers is initially at 6.5 bar to ensure the steam would be generated at 5 bar because a 0.75 bar pressure drop is assumed for liquid across heat exchangers. The water passes through the opposite order that the product stream passes through the heat exchangers to maintain a greater temperature difference and reduce heat exchanger area. The heat exchangers generate 356 kg/hr of saturated steam at 5 bar. HX-307 and HX-308 have surface areas of 9.6 and 12.4 m^2, respectively.

The next heat exchanger that the reactor outlet passes through is HX-309, which is a U-Tube HX that runs counter-currently. The heat exchanger fluid is a high performance, low temperature coolant which was specified to the material properties of the Jeffcool E100 60 volume percent heat transfer fluid [20]. The heat transfer fluid enters the heat exchanger at -43 °C and leaves at -33 °C. The outlet of the product stream of the heat exchanger was -16 °C, just before the dew point of the mixture. This temperature was chosen to prevent pressure changes that could result in hydraulic shock. The heat exchanger area is 50.6 m^2.

The outlet of HX-309 enters the flash drum, which has a U-Tube heat exchanger that cools the stream to -33 °C. This temperature was chosen to generate a liquid outlet stream of 99.9 weight percent anhydrous ammonia. The purity was chosen to generate a product that would meet or exceed the minimum specification of 99.5 weight percent. The heat transfer fluid is also modeled to be the Jeffcool E100 60 volume percent mixture with the same temperature change from -43 °C to -33°C. The liquid outlet is transported toward the storage section while the vapor outlet is sent back to the reactor section. The heat exchanger area was 161 m^2.

A three percent and one percent loss of the vapor stream was assumed as a result of the purge stream and imperfect sealing, respectively. The purpose of purging the air is to prevent a buildup of ammonia and maintain stoichiometric ratios of the reactants. The recycle stream enters the first heat exchanger discussed in this section before going through a compressor. The compressor, C-306, increases the pressure of the stream from 200 psia to 1247 psia. The inlet and outlet temperature of the compressor are 74 °C and 380°C, respectively. The compressor consumed 639 kW of power, which was the basis used to cost the compressor.

The flash drum was sized based upon an economical L/D ratio of 5 and a 30 minute stream capacity [21]. The volume flowing into the flash drum was 8.2 sm^3/hr, which translated to a 4.1 m^3 vessel that had a diameter of 1.0 m and length of 5.1 m. However, the minimum allowable velocity, which is designed to be 10% of the maximum velocity, is about 0.2 m/s higher than the flash drum would be able to hold. The density of the gas and liquid was calculated using Aspen HYSYS and the k value was assumed to be 576 m/hr, which is used for a vessel without a mesh separator [21]. For this reason, we suggest designing a hold up tank that would be on top of the flash drum to ensure proper performance. The flash drum wall thickness and weight were calculated using hoop and longitudinal stress guidelines provided in [22]. A 2.0 mm corrosion and 80% welding efficiency were assumed to provide a safety buffer for the process. The wall thickness and weight of the vessel were 11 mm and 1540 kg, respectively.

Ammonia Storage Vessels

The liquid, anhydrous ammonia must be stored onsite until it is sold and shipped to a customer. There is demand for ammonia in this form, so it is recommended to end the processing of the product once it is purified. Pressurized storage vessels were designed to contain up to seven days of product to provide sufficient time for sales and transportation. In the base design with 5 modules, each with a 10 mtpd capacity of ammonia, one module needs space to store 70 metric tons of ammonia. It was also assumed that 85% of the tank volume was used to hold the product, with 15% vapor space.

Storage vessels for the ammonia product were designed to operate at 200 psia and rated to withstand a Maximum Allowable Working Pressure (MAWP) of 250 psig. According to the ASME Boiler and Pressure Vessel Code, a safety factor of either 25 psig or 10% of the MAWP (the highest of these two) should be added to the MAWP. In this case, either method results in a safe design pressure of 275 psig. Due to material compatibility issues between ammonia and 304 stainless steel (as well as carbon steel), the storage vessels were designed to be constructed with 316 stainless steel.

With ease of construction and transportation in mind, the storage vessels were designed to fit on a semi-truck trailer. Therefore, a vessel diameter of 2.5 m (8.2 ft) was defined. An aspect ratio (L:D) of 3 was chosen, making the height of one vessel 7.5 m (25 ft). With these dimensions, four vessels are needed to provide enough storage space for one 10 mtpd module, meaning the entire plant will need 20 storage vessels to store one week of product. The number of total storage vessels can be adjusted if it is determined that one week of product storage is inappropriate.

Hoop stress and longitudinal stress calculations were used to determine the wall thickness of the storage vessels, see Appendix I – Storage Vessels. The tensile strength of 316 stainless steel is 20 ksi [22], a welding efficiency of 0.8 was assumed, and a 2.0 mm corrosion buffer was used (similar as previously described for the flash drum). After accounting for these considerations, the wall thickness for the storage vessels was determined to be 22.0 mm. In the current design, the mass of one storage vessel shell is 13,100 kg.

Process Flow Diagram and Material Balance

Included below are detailed process flow diagrams for each of the major sections in the production process. Note that each PFD represents the designated section for a single module.

Electrolysis: Section 100

Figure 1: In this section, an alkaline electrolysis cell converts water (feed stream) into pure hydrogen and oxygen streams. A shell-and-tube heat exchanger uses steam to heat the water to the operating temperature of the cell, 80 °C. A centrifugal pump is used to overcome the pressure drop induced by the heat exchanger. Heat is given off in the electrolysis cell due to ohmic resistance, and this heat is absorbed by a cooling water stream flowing through the external jacket of the cell. Potassium hydroxide, the electrolyte used in this cell, is mixed into the feed water stream during start-up, but is not used during steady-state operation.

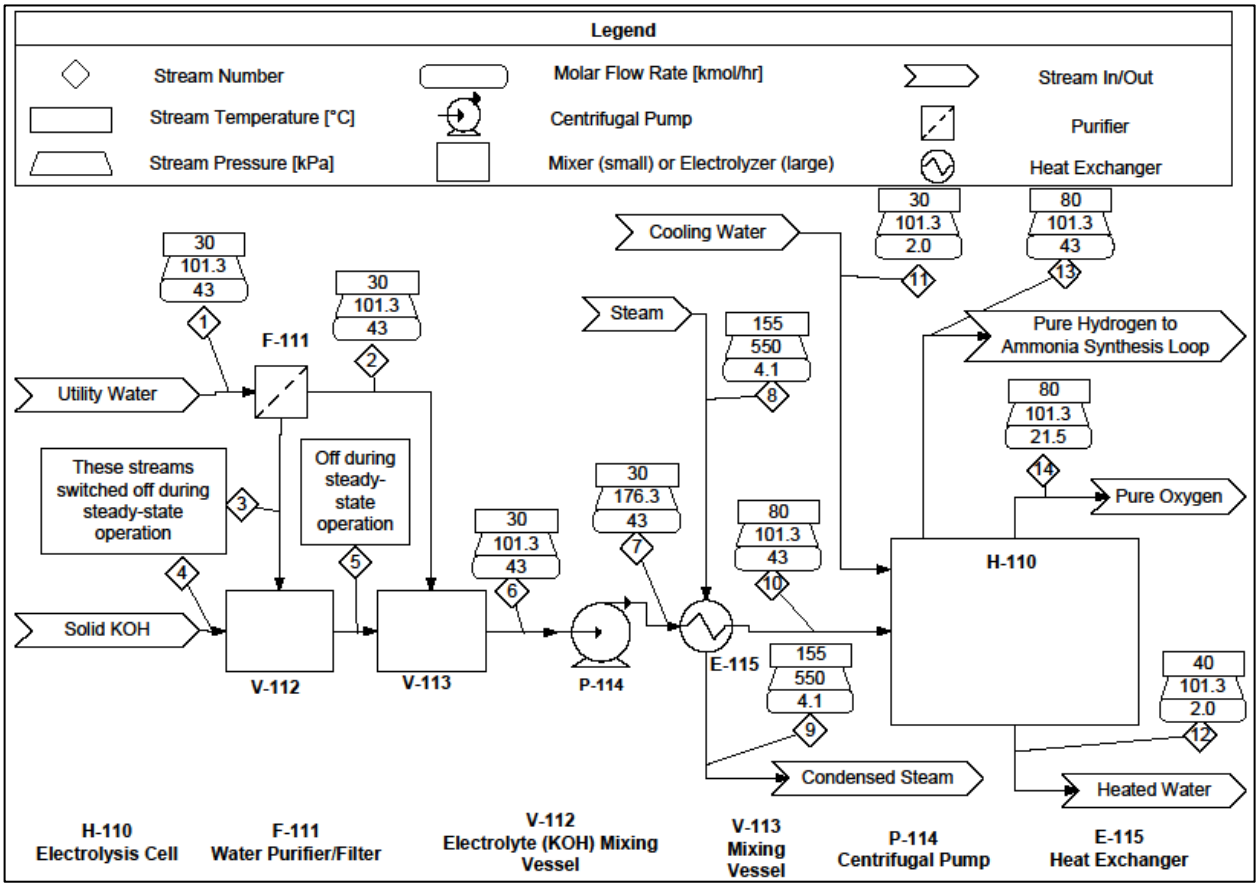

Electrolysis Material Balance

The material balance for the electrolysis section is based on the hydrogen gas requirement to the ammonia synthesis loop. The following calculations correspond to a single module within the 50 mtpd plant—the single module produces 10 mtpd of ammonia. Shown below is the conversion from 10 mtpd into an hourly molar flow rate of ammonia.

$$\dot{n}_{NH_3} = 10\frac{metric\ tons}{day} * 1000\frac{kg}{metric\ ton} * \frac{1\ kmol}{17.031\ kg} * \frac{1\ day}{24\ hr} = 24.5\frac{kmol\ NH_3}{hr}$$

An onstream efficiency of 88% was assumed, and a stoichiometric ratio was used to relate ammonia flow to hydrogen flow. Also, assuming a 97% conversion and recovery rate for the ammonia production process, the required steady-state inlet hydrogen gas flow rate can be calculated as follows.

$$\dot{n}_{H_2} = 24.5\frac{kmol\ NH_3}{hr} * \frac{1\ hr}{0.88\ hr\ on} * \frac{3\ kmol\ H_2\ cons.}{2\ kmol\ NH_3} * \frac{1\ kmol\ H_2\ prod.}{0.97\ kmol\ H_2\ cons.}$$

$$\therefore \dot{n}_{H_2} = 43\frac{kmol\ produced}{hr}$$

As hydrogen and oxygen are generated in the electrolysis cell, water is consumed. Knowing the stoichiometry of this process (shown below), the required flow rate of hydrogen can be used to solve backwards and obtain the required inlet water flow rate. This calculation is shown below.

$$2H_2O(l) \leftrightarrow 2H_2(v) + O_2(v)$$

$$\rightarrow \dot{n}_{H_2O,in} = 43\frac{kmol\ H_2}{hr} * \frac{2\ kmol\ H_2O}{2\ kmol\ H_2} = 43\frac{kmol\ H_2O}{hr}$$

Alternatively, we can represent the required water flow rate as a mass flow or volumetric flow. This is shown below.

$$\dot{m}_{H_2O,in} = 43\frac{kmol\ H_2O}{hr} * 18.02\frac{kg}{kmol} = 775\frac{kg}{hr}$$

$$F_{H_2O,in} = 775\frac{kg}{hr} * \frac{1\ m^3}{997\ kg} * 1000\frac{L}{m^3} * \frac{1\ hr}{60\ min} = 13\ LP$$

Membrane: Section 200

Figure 2: The membrane section takes in atmospheric air and generates a nitrogen reactant feed stream for the reactor. For a detailed sample calculation for determining the required air flow into this section in order to achieve the required flow rate of nitrogen, see Appendix I.

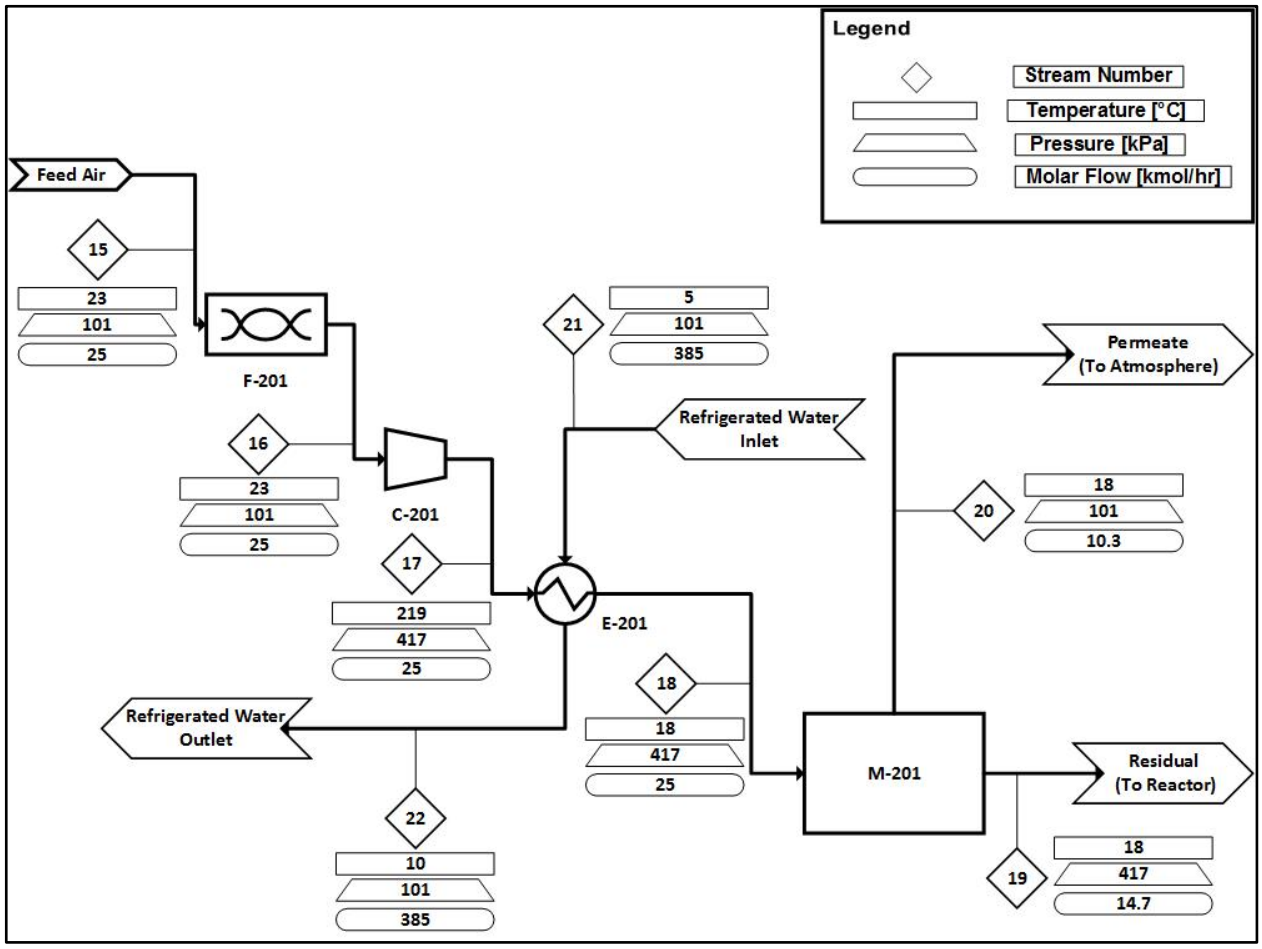

Membrane Material Balance

The overall material balance provided in the ammonia production section determined the required feed of nitrogen into the reactor was 14.5 $\frac{kmol}{hr}$ based on the desired ammonia production. This nitrogen flow rate was used to work backwards and determine the required flow rate of air into the membrane section considering the experimental selectivity and permeance values for the T(*p*-OCH_3)PPCoCl TFC membrane found in literature. The oxygen/nitrogen selectivity value was estimated to be 7.6 $\frac{O_2\ Permeance}{N_2\ Permeance}$ while the permeability for oxygen was $9.5 * 10^{-6} \frac{cm^3 * cm}{cm^2 * s * cmHg}$ when the membrane thickness was 0.01 cm. The following calculation was performed using an equation from Chapter 8 of *Membrane Technologies and Applications* to determine the mole fraction of oxygen in the permeate stream where y_{O_2} is the mole fraction of oxygen, φ is the pressure ratio, and $\propto$ is the membrane selectivity [23]. It was assumed that the average composition of air contains 21 mol% oxygen.

$$\varphi = \frac{Feed\ Pressure\ [bar]}{Permeate\ Pressure\ [bar]} = \frac{4.175\ bar}{1.013\ bar} = 4.12$$

$$y_{O_2,P} = \frac{\varphi}{2}\left[y_{O_2,F} + \frac{1}{\varphi} + \frac{1}{\alpha - 1} - \sqrt{(y_{O_2,F} + \frac{1}{\varphi} + \frac{1}{\alpha - 1})^2 - \frac{4\alpha y_{O_2,F}}{(\alpha - 1)\varphi}}\right]$$

$$y_{O_2,P} = \frac{4.12}{2}\left[0.21 + \frac{1}{4.12} + \frac{1}{7.6 - 1} - \sqrt{\left(0.21 + \frac{1}{4.12} + \frac{1}{7.6 - 1}\right)^2 - \frac{4(7.6)(0.21)}{(7.6 - 1)(4.12)}}\right]$$

$$\therefore y_{O_2,P} = 0.52$$

The mole fraction of oxygen in the permeate stream can be used to determine the partial pressure of oxygen in the permeate stream assuming the permeate side of the membrane is exposed to atmospheric conditions. The difference in partial pressures across the membrane can then be used with the permeance of oxygen to determine the average flux of oxygen through the membrane, J_{O_2}. For calculating the permeance from the permeability, it was assumed that the membrane thickness used was the same as the one used in literature of 0.01 cm.

$$p_{O_2,F} = y_{O_2,F} * p_{Total,O_2,F} = 0.21 * 4.175\ bar * \left(\frac{1\ cmHg}{0.0133\ bar}\right) = 65.92\ cmHg$$

$$p_{O_2,P} = y_{O_2,P} * p_{Total,O_2,P} = 0.52 * 1.013\ bar * \left(\frac{1\ cmHg}{0.0133\ bar}\right) = 39.52\ cmHg$$

$$Permeance\ (P)\ \frac{cm^3}{cm^2 * s * cmHg} = \frac{Permeability\ \frac{cm^3 * cm}{cm^2 * s * cmHg}}{Thickness\ (t) cm}$$

$$P_{O_2} = \frac{9.25 * 10^{-6}\ \frac{cm^3 * cm}{cm^2 * s * cm}}{0.01\ cm} = 9.25 * 10^{-4}\ \frac{cm^3}{cm^2 * s * cmHg}$$

$$J_{O_2}\ \frac{cm^3}{cm^2 * s} = P_{O_2}\frac{cm^3}{cm^2 * s * cmHg} * \left(p_{O_2,F}\ cmHg - p_{O_2,P}\ cmHg\right)$$

$$J_{O_2}\ \frac{cm^3}{cm^2 * s} = 9.25 * 10^{-4}\frac{cm^3}{cm^2 * s * cmHg} * (65.92\ cmHg - 39.52\ cmHg)$$

$$\therefore J_{O_2} = 0.027\ \frac{cm^3}{cm^2 * s}$$

To calculate the permeate flow of oxygen, the surface area of transfer needed to be calculated in order to use the flux value calculated above. The Excel solver function was used to determine a total surface area that would enable a residual stream of 99% nitrogen by using the membrane material balance (to follow) in an iterative loop. Solver estimated that a total surface area of approximately 500 m^2 was required to facilitate the desired separation. Note that when calculating the size of the membrane tube this value was reduced by a factor of 100 to account for the geometry of the membrane surface being very rough. The following equation was used to determine the permeate flow rate at STP and then adjusted to determine the flow rate at the membrane's operating conditions.

$$F_{STD,O_2,P}\ \frac{cm^3}{min} = J_{O_2}\frac{cm^3}{cm^2 * s} * A\ cm^2 * \frac{60\ s}{min} = 0.027\ \frac{cm^3}{cm^2 * s} * (5.015 * 10^6\ cm^2) * \frac{60\ s}{min}$$
$$\approx 8.2 * 10^6 \frac{cm^3}{min}$$

$$F_{O_2,P}\frac{cm^3}{min} = F_{STD,O_2,P}\frac{cm^3}{min} * \frac{P_{STD}\ [psi] * T_{Sys}\ [K]}{P_{Sys}[psi] * T_{STD}[K]} = \left(8.2 * 10^6 \frac{cm^3}{min}\right) * \left(\frac{(14.7\ psi)(291\ K)}{(60.6\ psi)(273\ K)}\right)$$
$$= 2.12 * 10^6\ \frac{cm^3}{min}$$

$$F_{O_2,P} = 2.12 * 10^6\ \frac{cm^3}{min} * \frac{1\ L}{1000\ cm^3} = 2.12 * 10^3 \frac{L\ O_2}{min}$$

$$\therefore F_{O_2,P} = 2.12 * 10^3\ \frac{L\ O_2}{min}$$

In order to complete a material balance around the membrane, this volumetric flow rate must be converted to a molar flow rate assuming oxygen behaves as an ideal gas. The conditions of the permeate side of the membrane were used to solve for the molar flow rate.

$$n_{O_2,P}\ \frac{mol}{min} = \frac{(P_P\ atm)\left(F_{O_2,P}\ \frac{L}{min}\right)}{\left(R\ \frac{L * atm}{mol * K}\right)(T_P\ K)}$$

$$n_{O_2,P}\ \frac{mol\ O_2}{min} = \frac{(1\ atm)\left(2.12 * 10^3\ \frac{L}{min}\right)}{\left(0.0821\ \frac{L * atm}{mol * K}\right)(291\ K)} = 88.74\ \frac{mol\ O_2}{min}$$

$$n_{O_2.P} = 88.74\ \frac{mol\ O_2}{min} * \frac{1\ kmol}{1000\ mol} * \frac{60\ min}{1\ hr} = 5.34\ \frac{kmol\ O_2}{hr}$$

$$\therefore n_{O_2,P} = 5.34\ \frac{kmol\ O_2}{hr}$$

With this molar flow rate of oxygen and the previously determined vapor mole fraction of oxygen in the permeate stream, the total molar flow in the permeate can be determined.

$$n_P\ \frac{kmol}{hr} = \frac{n_{O_2,P}\ \frac{kmol\ O_2}{hr}}{y_{O_2,P}} = \frac{5.34\ \frac{kmol\ O_2}{hr}}{0.52} = 10.3\ \frac{kmol}{hr}$$

$$\therefore n_P = 10.3\ \frac{kmol}{hr}$$

This total flow rate can be used to determine the amount of nitrogen that diffuses through the membrane to the permeate side. The required nitrogen feed flow rate of nitrogen can be used as the residual flow rate of nitrogen for a nitrogen material balance such that the total molar feed flow rate can be determined.

$$n_{N_2,P} = n_P - n_{O_2,P} = 10.3\ \frac{kmol}{hr} - 5.34\ \frac{kmol}{hr} = 4.96\frac{kmol}{hr}$$

$$n_F * y_{N_2,F} = n_P * y_{N_2,P} + n_R * y_{N_2,R}$$

$$n_F * (0.78) = 4.96\frac{kmol}{hr} + 14.5\frac{kmol}{hr} \rightarrow n_F = \frac{19.46\frac{kmol}{hr}}{0.78}$$

$$\therefore n_F = 25\ \frac{kmol\ air}{hr}$$

Now that the total molar flow rates in the feed and permeate streams are known and fully defined, the total molar flow rate in the residual stream (the stream that feeds into the reactor) can be determined. With the molar composition fully defined in all streams, the mole fractions of each component can be used to determine the flow rate of that species in a given stream, as seen in Table 1.

$$n_R = n_F - n_P = 25\ \frac{kmol}{hr} - 10.3\frac{kmol}{hr} = 14.7\ \frac{kmol}{hr}$$

$$\therefore n_R = 14.7\ \frac{kmol}{hr}$$

Table 1: Fully defines all flow rates in and out of the membrane system. The feed air stream comes directly from the atmosphere and is compressed and cooled before being fed into the membrane system. The permeate stream vents directly to the atmosphere. The residual stream (what is left from the initial feed) is the concentrated nitrogen stream that is fed to the reactor. Pressures and temperatures for each stream are also included.

Stream	**Temperature K**	**Pressure Bar**	**Total Flow Rate** $\frac{kmol}{hr}$	**Nitrogen Mole Fraction**	**Oxygen Mole Fraction**	**Nitrogen Flow Rate** $\frac{kmol}{hr}$	**Oxygen Flow Rate** $\frac{kmol}{hr}$
Feed	291	4.17	25	0.78	0.22	19.5	5.5
Permeate	291	1.01	10.3	0.48	0.52	5.0	5.3
Residual	291	4.17	14.7	0.99	0.01	14.5	0.2

Reactor and Ammonia Separation: Section 300

The reactor and ammonia separation section pressurizes the hydrogen and nitrogen feed streams from the electrolysis and membrane sections—respectively—and feeds the two streams into the reactor at the design reaction conditions (380 °C, 86 bar). A ruthenium-based catalyst is used to increase the conversion of the ammonia formation reaction. The reactor outlet is then de-pressurized, cooled, and fed into a flash drum. The flash drum separates anhydrous ammonia from the process stream by condensing it out of the process stream. The liquid anhydrous ammonia of high purity is then fed into storage vessels while the gas outlet is heated and re-pressurized before being recycled back into the reactor. Equipment sizing sample calculations may be found in Appendix I. This section was modeled in Aspen HYSYS and good agreement was found between the simulation and hand calculations. For this reason, the stream tables from Aspen HYSYS were used in this section because the program used more rigorous methods to calculate stream compositions. The Aspen HYSYS flow sheet may be found in Appendix II.

Table 2: Stream table for the ammonia synthesis and separation portion of the design.

Stream Name		23	24	25	26	27	28	29	30	31	32	33	34	35	36
Vapor Fraction	[-]	1	1	1	1	1	1	1	0	0	0.3053	0.8699	1	1	1
Temperature	[°C]	80	448.7	150	449.6	170	442.8	380	20	20.06	162	157.2	18	411.4	270
Pressure	[bar]	1.013	6.5	6.5	25.5	25.5	86	86	1.013	7.25	6.5	5.75	4.17	43	43
Molar Flow	[kmol/hr]	49.5	49.5	49.5	49.5	49.5	49.5	49.5	19.48	19.48	19.48	19.48	16.5	16.5	16.5
Mass Flow	[kg/hr]	99.79	99.79	99.79	99.79	99.79	99.79	99.79	351	351	351	351	462.2	462.2	462.2
Liquid Volume Flow	[m^3/hr]	1.428	1.428	1.428	1.428	1.428	1.428	1.428	0.3517	0.3517	0.3517	0.3517	0.5732	0.5732	0.5732
Heat Flow	[kJ/hr]	7.764E+04	6.083E+05	1.774E+05	6.114E+05	2.077E+05	6.071E+05	5.156E+05	-5.559E+06	-5.558E+06	-5.127E+06	-4.724E+06	-3.916E+03	1.925E+05	1.198E+05
Stream Name		37	38	39	40	41	42	43	44	45	46	47	48	49	50
Vapor Fraction	[-]	1	1	0	0	0.629	1	1	1	1	1	1	1	0	1
Temperature	[°C]	436.1	380	20	20.07	157.2	152	380	381.7	290.6	246.9	182.9	-16.01	-33.15	-33.15
Pressure	[bar]	86	86	1	6.5	5.75	5	86	13.79	86	13.79	13.79	13.79	13.79	13.79
Molar Flow	[kmol/hr]	16.5	16.5	2.14	2.147	2.147	2.147	272.9	272.9	272.9	272.9	272.9	272.9	27.4	245.5
Mass Flow	[kg/hr]	462.2	462.2	38.7	38.68	38.68	38.68	2725	2725	2725	2725	2725	2725	466.6	2259
Liquid Volume Flow	[m^3/hr]	0.5732	0.5732	0.3876	3.876E-02	3.876E-02	3.876E-02	8.151	8.151	8.151	8.151	8.151	8.151	0.7575	7.394
Heat Flow	[kJ/hr]	2.059E+05	1.765E+05	-6.125E+05	-6.125E+05	-5.397E+05	-5.104E+05	8.853E+05	8.853E+05	9.534E+04	-2.964E+05	-8.43E+05	-2.502E+06	-1.948E+06	-1.325E+06
Stream Name		51	52	53	54	55	56	57	58	Reactor Jacket Cooling Water		Reactor Jacket Steam			
Vapor Fraction	[-]	1	1	0	0	0.4631	1	1	1	0		1			
Temperature	[°C]	74.44	380.2	20	20.05	157.2	152	152	74.44	20		152			
Pressure	[bar]	13.79	86	1.013	6.5	5.75	5	5	13.79	1.013		5			
Molar Flow	[kmol/hr]	235.2	235.2	19.74	19.74	19.74	19.74	19.48	9.722	29.68		29.68			
Mass Flow	[kg/hr]	2163	2163	355.6	355.6	355.6	355.6	351	89.43	534.7		534.7			
Liquid Volume Flow	[m^3/hr]	7.082	7.082	0.3563	0.3563	0.3563	0.3563	0.3517	0.2928	0.5357		0.5357			
Heat Flow	[kJ/hr]	-5.186E+05	1.678E+06	-5.631E+06	-5.631E+06	-5.084E+06	-4.693E+06	-4.632E+06	-2.144E+04	-8.467E+06		-7.056E+06			

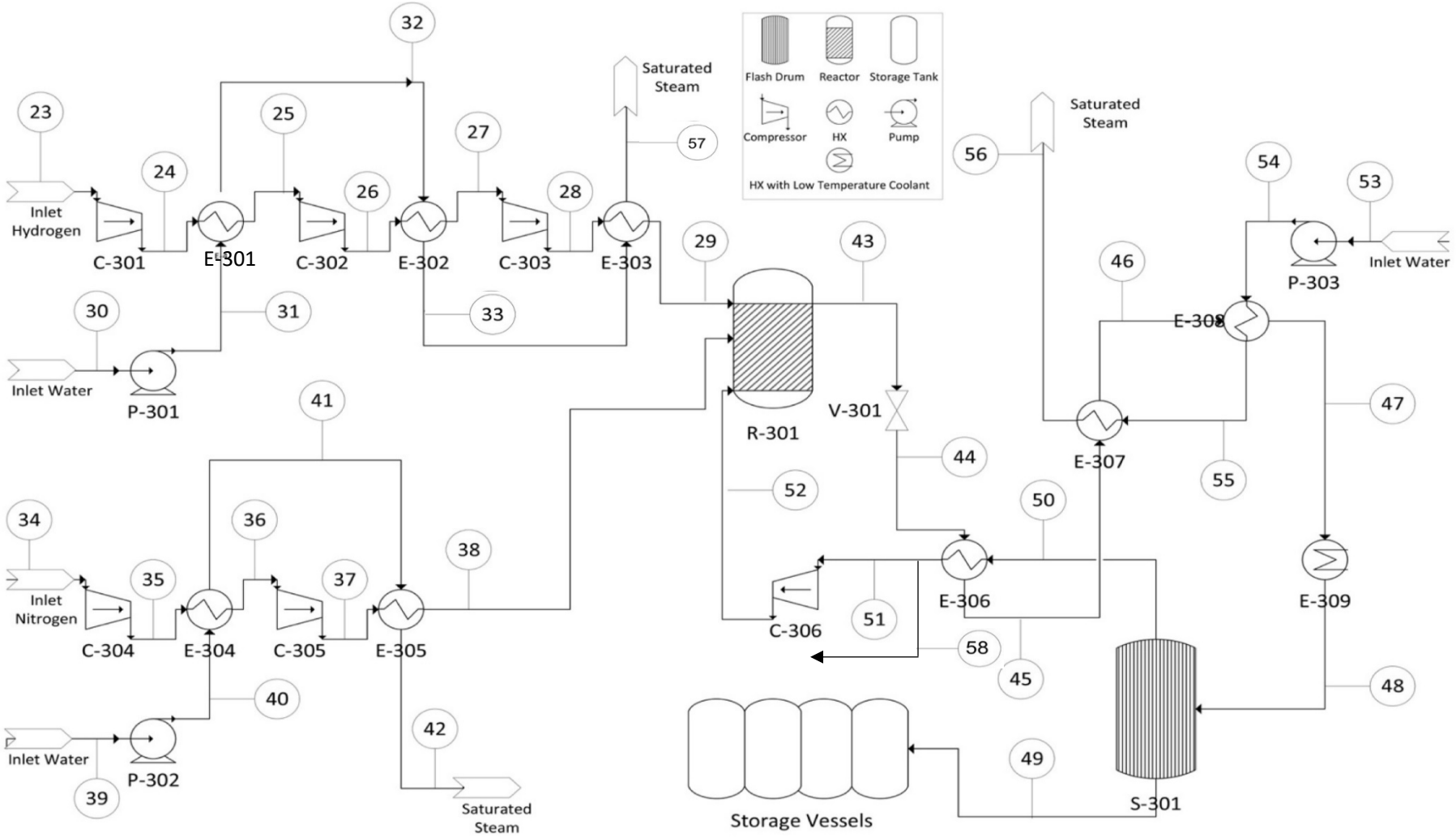
Flash Drum
Reactor
Storage Tank
Compressor
HX
Pump
HX with Low Temperature Coolant
Inlet Hydrogen
C-301
E-301
C-302
E-302
C-303
E-303
Saturated Steam
Inlet Water
P-301
R-301
V-301
Inlet Nitrogen
C-304
E-304
C-305
E-305
Inlet Water
P-302
Saturated Steam
C-306
E-306
E-307
E-308
P-303
Inlet Water
E-309
S-301
Storage Vessels

Reactor and Ammonia Separation Section Material Balance via Hand Calculations

The modular ammonia synthesis plant has been designed to produce 10 metric tons per day of ammonia. Therefore, five modules will be used to meet the 50 metric tons per day production capacity.

Several assumptions and design constraints were made to complete the material balance. First, the fresh hydrogen and nitrogen feed was designed to be at a 3:1 hydrogen to nitrogen ratio. This is a stoichiometric ratio, and it will be maintained throughout the synthesis loop. The total nitrogen conversion was assumed to be 97%, and the separator was assumed to condense 99% of the ammonia fed to it. The plant was assumed to have an on time of 88%. The single pass reactor conversion was approximated as 20% - a detailed discussion of how this approximation was made can be found in the process description section.

The following schematic shows the main streams in the ammonia synthesis loop with all minor equipment removed. In this schematic, the fresh nitrogen and hydrogen feed is already mixed in stream one.

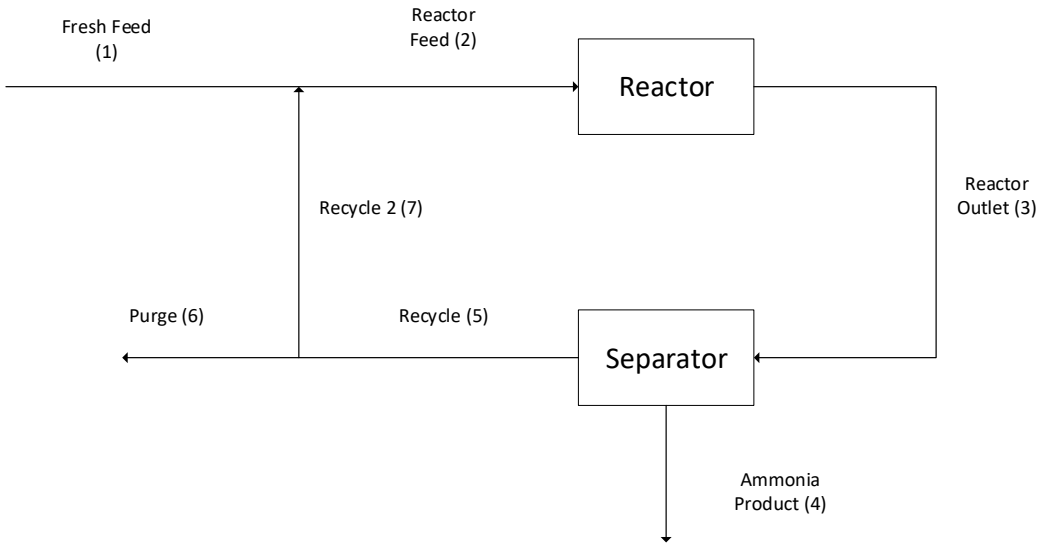

The following calculations were used to determine the hourly ammonia production rate and the fresh feed requirements for the overall system.

$$F_{NH_3,4} = \frac{Productivity}{0.88\ MW_{NH_3}}$$

$$F_{NH_3,4} = \frac{(10\ mt\ NH_3)\left(1000\frac{kg}{mt}\right)}{(0.88\ day)\left(17.03\frac{kg\ NH_3}{kmol\ NH_3}\right)\left(24\frac{hr}{day}\right)} = 27.8\frac{kmol\ NH_3}{hr}$$

The stoichiometric reaction ratio and the total nitrogen conversion were used to determine the fresh nitrogen feed requirement where ν_{N_2} is the stoichiometric coefficient for ammonia in the ammonia synthesis reaction.

$$F_{N_2,1} = \frac{F_{NH_3,4}}{0.97\ \nu_{N_2}}$$

$$F_{N_2,1} = \frac{27.8 \frac{kmol\ NH_3}{hr}}{0.97\ \left(2 \frac{kmol\ NH_3}{kmol\ N_2}\right)} = 14.5 \frac{kmol\ N_2}{hr}$$

Since the fresh reactants are feed at a stoichiometric ratio, the fresh hydrogen feed can be calculated as follows.

$$F_{H_2,1} = 3\ F_{N_2,1}$$

$$F_{H_2,1} = \left(3 \frac{kmol\ H_2}{kmol\ N_2}\right)\left(14.5 \frac{kmol\ N_2}{hr}\right) = 43.4 \frac{kmol\ H_2}{hr}$$

Next, the ammonia recovery rate can be used to determine how much ammonia must be leaving the reactor.

$$F_{NH_3,3} = \frac{F_{NH_3,4}}{0.99}$$

$$F_{NH_3,3} = \frac{27.8 \frac{kmol\ NH_3}{hr}}{0.99} = 28.1 \frac{kmol\ NH_3}{hr}$$

The overall conversion of nitrogen was used next, which allowed for the purge stream to be determined.

$$F_{N_2,6} = (1 - 0.97) F_{N_2,1}$$

$$F_{N_2,6} = (0.03)\left(14.5 \frac{kmol\ N_2}{hr}\right) = 0.434 \frac{kmol\ N_2}{hr}$$

The stoichiometric ratio of hydrogen to nitrogen is maintained throughout the system, so…

$$F_{H_2,6} = 3 F_{N_2,6}$$

$$F_{H_2,6} = 3\left(0.434 \frac{kmol\ H_2}{hr}\right) = 1.30 \frac{kmol\ H_2}{hr}$$

This means that $14.1\frac{kmol\ N_2}{hr}$ is consumed to produce the $28.1\frac{kmol\ NH_3}{hr}$ in the reactor effluent. An extent of reaction (ξ) will be used to determine the internal flows in the system where…

$$\xi = 14.1\frac{kmol\ N_2}{hr}$$

The following equation can be used to determine the nitrogen flow in the reactor effluent.

$$F_{N_2,3} = F_{N_2,2} - \xi$$

The single pass conversion is also needed to eliminate an unknown flow rate.

$$F_{N_2,3} = (1 - 0.2)F_{N_2,2}$$

Combining these two equations to eliminate $F_{N_2,2}$ and solve for $F_{N_2,3}$ yields the following result.

$$F_{N_2,3} = \frac{-\xi}{1 - \left(\frac{1}{1-0.2}\right)}$$

$$F_{N_2,3} = \frac{-14.1\frac{kmol\ N_2}{hr}}{1 - \left(\frac{1}{0.8}\right)} = 56.2\frac{kmol\ N_2}{hr}$$

The reactor influent and effluent flows can now be specified using these equations and the stoichiometric ratio of hydrogen and nitrogen. The last stream to specify is the ammonia lost in the purge. To do this, the ratio of nitrogen lost in the purge can be applied to the ammonia lost in the vapor leaving the separator, which gives the following equation.

$$F_{NH_3,6} = F_{NH_3,5}\frac{F_{N_2,6}}{F_{N_2,5}}$$

The separator is assumed to only condense ammonia, so the nitrogen and hydrogen molar flows entering the separator are equal to the molar flows leaving the separator. This specifies ammonia in stream five (and hydrogen due to the stoichiometric ratio).

$$F_{N_2,5} = F_{N_2,3} = 56.2\frac{kmol\ N_2}{hr}$$

Ammonia leaving is stream five can be specified as well.

$$F_{NH_3,5} = F_{NH_33} - F_{NH_3,4}$$

$$F_{NH_3,5} = 28.1\frac{kmol\ NH_3}{hr} - 27.8\frac{kmol\ NH_3}{hr} = 0.281\frac{kmol\ NH_3}{hr}$$

Finally, ammonia lost in the purge stream can be specified.

$$F_{NH_3,6} = \left(0.3\,\frac{kmol\ NH_3}{hr}\right)\left(\frac{0.434\,\frac{kmol\ N_2}{hr}}{56.2\,\frac{kmol\ N_2}{hr}}\right) = 2.17 * 10^{-3}\,\frac{kmol\ NH_3}{hr}$$

All remaining streams can be specified using equations previously shown, the stoichiometric ratio of hydrogen to nitrogen, or simple accounting. The table below gives all molar flow rates in the simplified system diagram.

Table 3: Molar flow rates for each species in the simplified process flow diagram. These are the values determined by hand calculations. Stream numbers here correspond to the simplified flow diagram, and there is no relation to the actual process flow diagrams.

Stream	**Nitrogen** $\left(\frac{kmol}{hr}\right)$	**Hydrogen** $\left(\frac{kmol}{hr}\right)$	**Ammonia** $\left(\frac{kmol}{hr}\right)$	**Total** $\left(\frac{kmol}{hr}\right)$
1	14.5	43.4	0.0	57.9
2	70.2	211	0.279	281
3	56.2	169	28.1	253
4	0.0	0.0	27.8	27.8
5	56.2	169	0.281	225
6	0.434	1.30	$2.17 * 10^{-3}$	1.74
7	55.7	167	0.279	223

Energy Balance and Utility Requirement

Each section of the production plant required some unique energy balance calculations, though all sections relied on heat exchangers and compressors to modify the temperature and pressure, respectively, of various streams. This section includes a discussion and sample calculation for these two key pieces of equipment used throughout the process followed by detailed descriptions and calculations for some of the more complicated pieces of equipment.

Heat Exchangers

Heat exchangers employing a variety of heating/cooling fluids were used to modify the temperature throughout the process in order to achieve the optimal temperature for various unit operations. The following calculation determines the coolant flow rate and required heat transfer area of the heat exchanger that cools the air feed into the membrane section after heating up during compression.
First, the required heat load to cool the air is determined based on the known incoming temperature (T_{In}), the desired outlet temperature (T_{Out}), and the total flow rate of air (m_{air}) determined in the membrane calculations (Appendix I).

$$Q_{HX}\frac{kJ}{hr} = m_{air}\frac{kg}{hr} * C_{p,air}\frac{kJ}{kg*K} * (T_{Out}\,K - T_{In}\,K)$$

$$Q_{HX}\frac{kJ}{hr} = 721.3\frac{kg}{hr} * 1.005\frac{kJ}{kg*K} * (291\,K - 492\,K) = -146141.2\,\frac{kJ}{hr}$$

$$\therefore 146{,}141\,\frac{kJ}{hr}\ must\ be\ removed\ from\ the\ air\ stream$$

This heat duty will also be used to estimate the cost of the heat exchanger and the utility cost of the refrigerated water used as a coolant. This utility enters the heat exchanger at 5 ^{O}C and exits after absorbing heat at 10 ^{O}C making it a suitable coolant to bring down the air stream temperature to 18 ^{O}C before flowing through the membrane. This change in temperature and the previously calculated heat load were used to determine the required flow rate of refrigerated water to achieve the desired outlet stream.

$$Q_{HX}\frac{kJ}{hr} = m_{Ref.Water}\frac{kg}{hr} * C_{p,water}\frac{kJ}{kg*K} * (T_{Out}\,K - T_{In}\,K)$$

$$146141.2\frac{kJ}{hr} = m_{Ref.Water}\frac{kg}{hr} * 4.2\frac{kJ}{kg*K} * (283\,K - 278\,K)$$

$$m_{Ref.Water}\frac{kg}{hr} = \frac{146141.2\frac{kJ}{hr}}{4.2\frac{kJ}{kg*K} * (283\ K - 278\,K)} = 6960\,\frac{kg}{hr}$$

A summary of the total energy transfer, required flow rate of heat exchange fluid, and heat exchange area (see Appendix I for sample calculation) for all heat exchangers in a single module of the production plant is included in Table 4, below.

Table 4: Summary of calculated values for all heat exchangers featured in the process. Please note that these values are all based on a single module basis. Additionally, note that the use of deionized water to cool the hydrogen and nitrogen feeds enabled the production of steam which can be sold for credit (see costing calculations and summary).

Section	Unit Number	Heat Transfer Fluid	Total Energy Transfer $\frac{kJ}{hr}$	Heat Transfer Fluid Flow Rate $\frac{kg}{hr}$	Size m^2
Electrolysis (100)					
	E-115	Steam	155,000	74	0.54
Membrane (200)					
	E-201	Refrigerated Water	146,000	6,960	5.6
Synthesis Loop (300)					
	E-301	Deionized Water	387,000	314[(a)]	3.6
	E-302	Deionized Water	363,000	314[(a)]	8.4
	E-303	Deionized Water	86,700	314[(a)]	0.62
	E-304	Deionized Water	71,400	38[(b)]	0.50
	E-305	Deionized Water	29,900	38[(b)]	0.21
	E-306	Internal Loop	790,000	N/A	7.0
	E-307	Deionized Water	392,000	355[(c)]	9.6
	E-308	Deionized Water	547,000	355[(c)]	12.4
	E-309	Refrigerant (60% Jeffcool E100 w/ water)	1,660,000	198,000	50.6

(a) = Shared coolant for nitrogen feed, (b) = Shared coolant for hydrogen feed, (c) = Shared coolant for post-reactor cooling of product

Compressors

Compressors are used throughout the ammonia production module. The power requirement for each compressor was determined through hand calculations and modeled in Aspen HYSYS. The hand calculations were performed using the following equations for shaft work, outlet temperature, and actual outlet temperature.

$$\widehat{W}_s = \frac{RT_{in}k}{\eta(k-1)}\left[\left(\frac{P_{out}}{P_{in}}\right)^{\frac{k-1}{k}} - 1\right]$$

$$T_{out} = T_{in}\left(\frac{P_{out}}{P_{in}}\right)^{\frac{k-1}{k}}$$

$$\eta = \frac{T_{out} - T_{in}}{T_{out,actual} - T_{in}}$$

Where R is the gas constant, $k = \frac{C_p}{C_v}$ of the species being compressed, η is the combined motor and turbine efficiency, $\widehat{W}_s$ is the shaft work in $\frac{J}{mol}$. The inlet temperature and pressure and outlet pressure were all specified when designing the compressors for the ammonia production module. Finally, the third equation presented here was rearranged to determine the actual outlet temperature of the compressed gas.

$$T_{out,actual} = \frac{T_{out} - T_{in}}{\eta} + T_{in}$$

The first compressor in the fresh hydrogen feed section, C-301, was sized based on an inlet temperature of 80 °C, inlet pressure of 1.01 bar, and a desired outlet pressure of 6.50 bar. The k for hydrogen is 1.41 [22]. The motor efficiency and turbine efficiency for all compressors were assumed to be 0.90 and 0.75, respectively, giving an overall efficiency of 0.675 (η). Thus, the shaft work for C-301 was…

$$\widehat{W}_s = \frac{\left(8.314\frac{kJ}{kmol*K}\right)(353K)(1.41)}{(0.675)(1.41-1)}\left[\left(\frac{6.50\ bar}{1.01\ bar}\right)^{\frac{1.41-1}{1.41}} - 1\right] = 10{,}700\frac{kJ}{kmol}$$

Next, the molar flow rate of hydrogen in this section of the plant could be used to determine the energy requirement of the compressor in kilowatts.

$$W_s = \widehat{W}_s * \dot{n}_{H_2}$$

$$W_s = \left(10{,}700\frac{kJ}{kmol}\right)\left(43.4\frac{kmol\ H_2}{hr}\right)\left(\frac{1\ hr}{3600\ s}\right) = 129\ kW$$

Next, the perfect efficiency outlet temperature can be calculated to then determine the actual outlet temperature. The actual outlet temperature is needed to specify downstream processes.

$$T_{out} = (353\ K)\left(\frac{6.50\ bar}{1.01\ bar}\right)^{\frac{1.41-1}{1.41}} = 606\ K$$

Finally, the actual outlet temperature can be calculated as follows.

$$T_{out,actual} = \frac{606\ K - 353\ K}{(0.90 * 0.75)} + 353\ K = 728\ K$$

A summary of the sizing for each compressor in the 10 metric ton per day module can found in the table below.

Table 5: Summary of the sizing calculations for all compressors in the 10 metric ton per day ammonia production module. All compressors were calculated using a motor efficiency of 0.9 and turbine efficiency of 0.75, which gives an overall efficiency of 0.675. The power input column represents the energy requirement determined by hand (see calculations above), and the Aspen HYSYS column represents the results from the Aspen HYSYS model.

Compressor	Location	Pressure Change (bar)	Power Input (kW)	Temperature Change (ºC)
C-201	Air feed to membrane separation	1.01 → 4.17	44.0	23 → 220
C-301	1st fresh hydrogen feed compressor	1.01 → 6.50	129	80 → 449
C-302	2nd fresh hydrogen feed compressor	6.50 → 25.5	105	150 → 450
C-303	3rd fresh hydrogen feed compressor	25.5 → 86.0	95.9	170 → 443
C-304	1st fresh nitrogen feed compressor	4.17 → 43.0	47.9	18 → 411
C-305	2nd fresh nitrogen feed compressor	43.0 → 86.0	20.6	270 → 436
C-306	Recycle compressor	13.8 → 86.0	639	74 → 380

Electrolysis Cell Energy Balance

In the electrolysis section, hydrogen gas is produced with a system of alkaline electrolysis cells. Within each electrolysis cell, an oxidation reaction occurs at the anode, and a reduction reaction occurs at the cathode. The combination of these two reactions is simply the conversion of water into hydrogen gas and oxygen gas. These reactions are shown below.

Oxidation at Anode: $4OH^-(aq) \leftrightarrow O_2(v) + 2H_2O(l) + 4e^-$

Reduction at Cathode: $4H_2O(l) + 4e^- \leftrightarrow 2H_2(v) + 4OH^-(aq)$

Overall Reaction: $2H_2O(l) \leftrightarrow 2H_2(v) + O_2(v)$

The overall reaction is endothermic, and energy is needed to be supplied for the conversion to happen at steady state. Energy supplied to this reaction via the current applied across the cell, which drives each electrochemical reaction. However, the current must also overcome energy losses due to ohmic resistance (in addition to the energy absorbed by the reaction). A conservative value of 5.0 kW-hr/Nm^3 of hydrogen produced was used in this design, with the typical range being 4.2 – 4.8 kW-hr/Nm^3 [3]. Below, the electricity requirement for the electrolysis cell system is calculated. The first step is to convert the molar flow rate of hydrogen into a normal volumetric flow rate.

$$F_{H_2} = \frac{43000\frac{mol}{hr} * 8.314\frac{J}{mol * K} * 273.15\ K}{100000\ Pa} = 976\frac{Nm^3}{hr}$$

$$W = 976\frac{Nm^3}{hr} * 5.0\frac{kW * hr}{Nm^3} = 4882\ kW$$

The energy lost to resistance is absorbed by the alkaline solution as heat, and must be transferred to cooling water in the cooling jacket to avoid an increase in temperature. The heat load through the cooling jacket can be calculated with a steady-state energy balance as shown below. Note: the reaction term is negative because it is drawing energy out of the system.

$$\Delta H = 0 = -\dot{n}_{H_2O} * \Delta H_{rxn} + Q + W$$

$$\therefore Q = -W + \dot{n}_{H_2O} * \Delta H_{rxn} = -4882\frac{kJ}{s} + \left[\left(43000\frac{mol}{hr} * 284\frac{kJ}{mol}\right) * \frac{1\ hr}{3600\ s}\right]$$

$$\rightarrow Q = -1490\ kW$$

With the heat load calculated, the flow rate of cooling water required can be calculated as seen in the heat exchanger energy balances above. In this case, 36 kg/hr of cooling water is needed per module. Cooling water is supplied at 30 °C, and is heated to 40 °C.

Reactor Energy Balance

The ammonia synthesis reaction is exothermic, and the heat evolved must be removed to maintain the reaction conditions and safe operation. For this preliminary design, the reactor is assumed to be isothermal and isobaric at 380 °C and 86 bar. Deionized water will be fed to the reactor cooling jacket, which will evaporate in the jacket to remove heat from the system. The water feed will be pumped to 5 bar to reduce the temperature difference between the vaporizing water and the reactor and minimize stress due to thermal expansion of the material. The steam created in the jacket can then be used elsewhere in the plant or for credit. Sample calculations for the reactor energy balance can be found in Appendix III – Other Supplementary Information.

A hypothetical path was used to determine that $-2.76 * 10^6$ kJ/hr of heat must be removed from the reactor to maintain isothermal operation. In this calculation, the heat capacities of each species were assumed to be relatively independent of temperature, and a high and low value for the heat capacity were averaged and used in calculations. The heat capacity was also assumed to be independent of pressure, and the small amount of ammonia in the feed was assumed to have a negligible effect on the energy balance.

Finally, it was determined that 1,300 kg/hr of deionized water at 5 bar would need to be evaporated in the reactor jacket to maintain isothermal operation of the reactor. These calculations can also be found in Appendix III – Other Supplementary Information. This hand calculation is about twice as much steam generation compared to the Aspen HYSYS model. This discrepancy may be due to the hand calculation's lack of dependence on pressure. The more conservative steam generation will be used in costing because it will give a more conservative cost estimate by reducing the steam credits earned.

Flash Drum

The energy balance on the flash drum was simulated in Aspen HYSYS and verified with hand calculations. The energy balance is used to calculate the energy requirement of the heat exchanger in the flash drum. The molar enthalpies—which were based on composition, temperature, and pressure—as well as the molar flow rate were the basis for the calculations. The UNIQUAC equation of state was used in the Aspen HYSYS simulation for the flash drum section.

$$\dot{n}_{flash,in} h_{flash,in} = \dot{n}_{flash,vap\ out} h_{flash,vap\ out} + \dot{n}_{flash,liq\ out} h_{flash,liq\ out} + q_{flash\ HX}$$

$$273 \frac{kmol}{hr} * -9178 \frac{kJ}{kmol - °C} = 246 \frac{kmol}{hr} * -5398 \frac{kJ}{kmol - °C} +$$

$$27.4 \frac{kmol}{hr} * -71{,}100 \frac{kJ}{kmol - °C} + q_{flash,HX}$$

$$\therefore q_{flash,HX} = -768{,}300 \frac{kJ}{hr} = -\mathrm{q}_{\mathrm{coolant}}$$

The energy requirement of the flash drum heat exchanger is then used to calculate the mass flow rate of coolant required using a simple energy balance calculation using the heat capacity of the heat transfer fluid as well as the temperature change of the heat transfer fluid. The heat transfer fluid was assumed to change from 230 K to 240 K. The heat capacity was assumed to be that of the Jeffcool E100 heat transfer fluid 60 volume percent water mixture [20].

$$q_{coolant} = \dot{m}_{coolant} C_{p\ coolant} \Delta T_{coolant}$$

$$768{,}300 \frac{kJ}{hr} = \dot{m}_{coolant} * 0.38 \frac{\mathrm{kJ}}{\mathrm{lb - K}} * (240\mathrm{K} - 230\mathrm{K})$$

$$\therefore \dot{m}_{coolant} = 201{,}657 \frac{lb}{hr}$$

Equipment List and Unit Descriptions

Table 6: Brief descriptions for each piece of equipment in a single module.

Equipment Number	Unit Description
Electrolysis: Section 100	
H-110	This is the system of electrolysis (or hydrolysis) cells which produces the pure hydrogen stream needed in the ammonia synthesis loop. It contains multiple electrolysis cells, each with two electrodes. Current is applied across the electrodes to drive the reduction and oxidation reactions, and a cooling water jacket is used to maintain a system temperature of 80 °C.
F-111	Filtration and purification system used to keep unwanted contaminants and obstructions out of the electrolysis cell. Utility water is sent through this system before it is heated and flowed into the electrolysis cell system.
V-112	The mixing vessel used to dissolve the solid electrolyte, potassium hydroxide. This vessel is not used in steady-state operation, only when electrolyte must be added to the system (during startup).
V-113	Mixing vessel used to dilute the concentrated solution from the electrolyte mixing vessel. During steady-state operation, this simply acts as a holding tank for the purified water before it is pumped into the electrolysis cell.
P-114	Centrifugal pump used to overcome the 75 kPa pressure drop through the heat exchanger and pump the water into the electrolysis cell.
E-115	Shell-and-tube heat exchanger used to preheat the water inlet to the steady-state operating temperature of 80 °C. Pressurized (550 kPa) saturated steam is used as the shell fluid, which heats the tube-side water inlet stream.
Membrane: Section 200	
F-201	Filtration system used to protect the membrane from potential contaminants. Includes a polyester filter to remove particulates and silica gel beads as a desiccant to remove water vapor from the air.
C-201	According to our literature review, the optimal feed pressure for the membrane to operate most efficiently is about 4.17 bar. Because the feed air is taken directly from the atmosphere, this compressor is tasked with quadrupling the pressure.
E-201	The compression of the air stream increases the temperature to about 220 ^{o}C; thus, a significant decrease in temperature is required to achieve the optimal operating temperature for the membrane of 18 °C. For this vapor stream, it is assumed that heat exchange is perfectly isobaric.
M-201	The membrane itself used to a nitrogen stream that is 99% pure to be fed into the reactor section (while the permeate stream is vented to the atmosphere). The basic design includes a chamber open to the atmosphere a pipe coiled within composed of the membrane material with the feed stream flowing through it.
Ammonia Synthesis and Separation: Section 300	
C-301	This is the first compressor following the electrolysis section. The compressor increases the inlet hydrogen feed stream. The pressure increases to a point at least 50 °C before the autoignition point.

C-302	This is the second compressor following the electrolysis section. The compressor increases the pressure of the outlet stream of the E-301 heat exchanger. The pressure increases to a point at least 50 °C before the autoignition point.
C-303	This is the third compressor following the electrolysis section. The compressor increases the pressure of the outlet stream of the E-302 heat exchanger. The pressure and temperature increases to the reactor conditions and a point at which the stream is at least 50 °C before the autoignition point, respectively.
C-304	This is the first compressor following the membrane separation section. The compressor increases the inlet nitrogen feed stream. The pressure increases to about the same temperature as the C-301 outlet temperature.
C-305	This is the second compressor following the membrane separation section. The compressor increases the outlet of E-304 heat exchanger. The pressure increases to the reactor operating conditions.
C-306	This is the compressor on the recycle stream. It increases the pressure of the E-306 outlet from the pressure in S-301 to the reactor operating pressure.
E-301	This is the first heat exchanger following the electrolysis section. The heat exchanger utilizes de-ionized water to cool the stream after C-301 to a safe operating temperature before C-302 to prevent auto-ignition of hydrogen, which occurs at 500 °C. The inlet water is that of the outlet de-ionized water pump P-301. The outlet water is partially vaporized.
E-302	This is the second heat exchanger following the electrolysis section. The heat exchanger utilizes de-ionized water to cool the stream after C-302 to a safe operating temperature before C-303 to prevent auto-ignition of hydrogen, which occurs at 500 °C. The inlet water is that of the outlet de-ionized water from E-301. The outlet water is partially vaporized.
E-303	This is the third heat exchanger following the electrolysis section. The heat exchanger utilizes de-ionized water to cool the stream after C-303 the reactor conditions. The inlet water is that of the outlet de-ionized water from E-302. The outlet water is saturated steam at 5 bar.
E-304	This is the first heat exchanger following the membrane separation section. The heat exchanger utilizes de-ionized water to cool the stream after C-304 to a safe operating temperature before C-302. The inlet water is that of the outlet de-ionized water pump P-302. The outlet water is partially vaporized.
E-305	This is the second heat exchanger following the membrane separation section. The heat exchanger utilizes de-ionized water to cool the stream after C-305 to the reactor conditions. The inlet water is that of the outlet de-ionized water of E-304. The outlet water of this heat exchanger is saturated steam at 5 bar.
E-306	This is the heat exchanger following V-301 after the reactor. The heat exchanger utilizes the outlet of S-301 to cool the post-reactor stream before entering into a series of heat exchangers that cool it before the flash drum.
E-307	This is the heat exchanger following the E-306 outlet process stream. The heat exchanger has an inlet de-ionized water flow rate from E-308 that is partially vaporized. The outlet de-ionized water is saturated steam at 5 bar.

E-308	This is the heat exchanger following the E-307 outlet process stream. The heat exchanger has an inlet de-ionized water flow rate from P-303, which is used to cool the process stream. The process stream partially vaporizes the cooling water, which enters at room temperature.
E-309	This is the heat exchanger following the E-308 process stream. The heat exchanger utilizes the Jeffcool E100 60 volume percent fluid to cool the process stream down just before its dew point.
Flash Jacket	This is the cooling jacket/heat exchanger used within the flash drum. The heat exchanger cools down the outlet from E-309 to a point at which would generate a liquid stream with the specified purity of 99.5 wt percent ammonia.
P-301	This is the pump that feeds de-ionized water to E-304 and E-305. The pump takes water at STP and increases the pressure such that the outlet out of E-305 would be saturated steam at 5 bar. The liquid pressure drop across each heat exchanger is assumed to be 0.75 bar.
P-302	This is the pump that feeds de-ionized water to E-301, E-302, and E-303. The pump takes water at STP and increases the pressure such that the outlet out of E-303 would be saturated steam at 5 bar. The liquid pressure drop across each heat exchanger is assumed to be 0.75 bar.
P-303	This is the pump that feeds de-ionized water to E-307 and E-308. The pump takes water at STP and increases the pressure such that the outlet out of E-307 would be saturated steam at 5 bar. The liquid pressure drop across E-307 and E-308 is assumed to be 0.75 bar.
R-301	This is the reactor vessel which converts nitrogen and hydrogen into ammonia with a Ru based catalyst. The temperature and pressure of the reactor is maintained at 380 °C and 86 bar, respectively. The outlet of C-306, E-303, and E-305 enter the reactor. The outlet of the reactor goes into V-301.
Reactor Jacket	This is the jacket of the R-301 reactor. It produces saturated steam from de-ionized water fed into the system.
S-301	This is the flash drum, which is a vessel used to isolate liquid ammonia out of the E-309 outlet process stream. The flash drums were designed to generate a total of 50,000 metric tons of 99.5 wt percent anhydrous ammonia between all of the modules.
V-301	This is the expansion valve immediately after the reactor section. The valve is a throttling valve that decreases the pressure from the reactor conditions to that at which the anhydrous ammonia product would be stored at.

Equipment Specification Sheets

Table 7: Specifications for all equipment featured in plant which was ultimately used for costing. For sizing calculations see Appendix I. The material of construction used was also considered.

Equipment Number	Characteristic Size - 1	Characteristic Size - 2	Material of Construction
Electrolysis: Section 100			
H-110	$Width, w = 2.3\ m$	$Volume, V = 11.6\ m^3$	Shell: Stainless Steel 316 Electrodes: Hot-Dip (in Zinc) Galvanized Nickel
F-111	$\dot{n}_{H_2O} = 43 \frac{kmol\ H_2O}{hr}$	N/A	Carbon Steel, Polyester
V-112	$Volume, V = 1\ m^3$	N/A	Stainless Steel 316
V-113	$Volume, V = 1\ m^3$	N/A	Stainless Steel 316
P-114	$W = 0.01\ kW$	N/A	Stainless Steel 316
E-115	$Q = 43\ kW$	$A = 0.54\ m^2$	Stainless Steel 316
Membrane: Section 200			
F-201	$n_{air} = 25 \frac{kmol\ air}{hr}$	N/A	Filter: Polyester Desiccant: Silica Gel
C-201	$W = 44\ kW$	$\Delta P = 316\ kPa$	Carbon Steel
E-201	$Q = 41\ kW$	$A = 5.6\ m^2$	Carbon Steel
M-201	$L = 27\ m$	$V = 502\ cm^3$	Pebax-2533 TFC w/ T(p-OCH_3)PPCoCl
Ammonia Synthesis and Separation: Section 300			
C-301	W = 129 kW	1.01 → 6.50	Carbon Steel
C-302	W =105 kW	6.50 → 25.5	Carbon Steel
C-303	W = 95.9 kW	25.5 → 86.0	Carbon Steel
C-304	W = 47.9 kW	4.17 → 43.0	Carbon Steel
C-305	W = 20.6 kW	43.0 → 86.0	Carbon Steel
C-306	W = 639 kW	13.8 → 86.0	Carbon Steel
E-301	Q = 120 kW	A =3.57 m^2	Stainless Steel 316
E-302	Q = 112 kW	A =8.37 m^2	Stainless Steel 316
E-303	Q = 25.0 kW	A =0.62 m^2	Stainless Steel 316
E-304	Q = 20.0 kW	A =0.50 m^2	Stainless Steel 316
E-305	Q = 8.10 kW	A =0.21 m^2	Stainless Steel 316
E-306	Q = 219 kW	A =6.97 m^2	Stainless Steel 316
E-307	Q = 109 kW	A =9.62 m^2	Stainless Steel 316
E-308	Q = 152 kW	A =12.4 m^2	Stainless Steel 316
E-309	Q = 461 kW	A =50.6 m^2	Stainless Steel 316
Flash Jacket	Q = 213 kW	A =161 m^2	Stainless Steel 316
R-301	D = 2.1 m	P = 86 bar	Stainless Steel 316
Reactor Jacket	Q = 392 kW	N/A	Stainless Steel 316
S-301	L = 5.1 m	D = 1.0 m	Stainless Steel 316

Process Safety Considerations

Waste Treatment

There are two waste streams in each modular ammonia production facility: the purge stream coming off of the recycle loop in the ammonia synthesis section as well as the oxygen rich air stream coming off of the electrolysis section.

Ammonia gas is toxic and poses a threat to climate change because it is a greenhouse gas [24]. For these reasons, the ammonia needs to be removed from the gas stream prior to environmental release. The purge stream stemming from the recycle loop contains about 15 weight percent ammonia. An ammonia packed bed gas scrubber will be used to treat this stream. In the scrubber, a sulfuric acid mixture with water will be used to strip ammonia gas out of the air stream before it is released to the environment. Since the gas scrubber would be small as it only has to treat about 90 kg/hr of gas, the gas scrubber cost is included in the budget used for miscellaneous equipment. The scrubbing blowdown fluid may be sold as a crude fertilizer to local farmers [25].

In addition to high levels of ammonia in the purge stream, there is also about 15 weight percent hydrogen. This hydrogen in the air stream poses a flammability concern. To mitigate this risk, the hydrogen rich stream following the ammonia packed bed scrubber will be sent to an incinerator stack with the stream described in the following paragraph.

The oxygen rich air stream stemming from the electrolysis section is about 50% inert gasses (argon and nitrogen) and 50% oxygen. The main risks that the oxygen rich stream poses is a flammability risk if the stream is near fuel as well as oxygen poisoning if the gas outlet is not in a well ventilated area. To deal with this, the oxygen rich stream will be sent through an incinerator stack with the outlet of the ammonia packed bed scrubber that would oxidize the hydrogen rich stream to form water.

Health Risk Mitigation

Table 8: Table with the key health risks and steps taken to mitigate these.

Health Risk	Risk Mitigation
Ammonia Gas Exposure	Provide operators with sufficient training on how to respond to gas leaks in the process stream. Also have ammonia gas alarms at various points along the process stream, especially around areas prone to leaking. The purge stream will also be treated with a packed bed scrubber to prevent emission of the toxic gas. Lock out tag out procedures will also be in place to ensure proper operation and maintenance of valves and other equipment controlling this hazard. Equipment will be regularly monitored and maintained in effort to prevent excursions or failures.
High Oxygen Level Exposure	Provide operators with sufficient training on how to respond to gas leaks in the process stream. The oxygen rich stream coming from the electrolysis section will be sent to an incinerator stack (electric of course to maintain carbon neutrality) with the hydrogen rich packed bed scrubber outlet. Oxygen alarms will also be present at various points along the process stream,

	especially around areas prone to leaking. Lock out tag out procedures will also be in place to ensure proper operation and maintenance of valves and other equipment controlling this hazard. Equipment will be regularly monitored and maintained in effort to prevent excursions or failures.
Suffocation from excess exposure to nitrogen	Provide operators with sufficient training on how to respond to gas leaks in the process stream. The oxygen gas alarms will also be a good indicator of nitrogen levels. If the oxygen levels are too low, this would be indicative of potential suffocation from overexposure to nitrogen. Lock out tag out procedures will also be in place to ensure proper operation and maintenance of valves and other equipment controlling this hazard. Equipment will be regularly monitored and maintained in effort to prevent excursions or failures.
Flammability	Provide operators with sufficient training on how to respond to gas leaks in the process stream. Hydrogen gas sensors will be located along the process streams. The hydrogen rich purge stream will be treated by oxidizing it in an incinerator stack (electric powered) with the oxygen rich stream from the electrolysis section. Lock out tag out procedures will also be in place to ensure proper operation and maintenance of valves and other equipment controlling this hazard. Equipment will be regularly monitored and maintained in effort to prevent excursions or failures.
Sulfuric acid and potassium hydroxide exposure	Provide operators with sufficient training on how to respond to handle these hazardous chemicals as well as respond to leaks in the process streams. A containment and secondary containment area will be used around sulfuric acid tanks and scrubbers. PPE will be provided to operators working on equipment that contains sulfuric acid. Lock out tag out procedures will also be in place to ensure proper operation and maintenance of valves and other equipment controlling this hazard. Equipment will be regularly monitored and maintained in effort to prevent excursions or failures.
Pressurized gas	Provide operators with sufficient training on how to respond to gas leaks as well as ruptured lines. Pressure relief valves (vacuum and high pressure) and rupture disks will be on pressurized systems. In addition to that, system controls will be designed to prevent rapid pressure changes resulting from condensing gas by ensuring that no areas with hot gasses in them will be filled with cold gasses during a defrosting cycle. Strict system controls will be put in place to prevent the mixture of hot and cold streams in process piping that would be at risk of condensing and generating a vacuum. Isolation valves will be placed on each pressurized system and vessel to ensure that if one system or vessel had an emission event, only the contents of that specific system or vessel would be released. Lock out tag out procedures will also be in place to ensure proper operation and maintenance of valves and other equipment controlling this hazard. Equipment will be regularly monitored and maintained in effort to prevent excursions or failures.
Pinch points	Provide operators with appropriate training about how to avoid pinch points as well as PPE to help protect them when operating around pinch points. Lock out tag out procedures will also be in place to ensure proper operation and maintenance of valves and other equipment controlling this hazard.

Height risks	Provide operators with appropriate training about how to use a ladder and work at heights properly as well as PPE to help protect them from fall risks when working at heights. Lock out tag out procedures will also be in place to ensure proper operation and maintenance of valves and other equipment controlling this hazard. Equipment will be regularly monitored and maintained in effort to prevent excursions or failures.
Electric shock	All process lines will be grounded to prevent the buildup of static electricity. This will prevent electrical arks that could harm people or pose a fire risk. Lock out tag out procedures will also be in place to ensure proper operation and maintenance of valves and other equipment controlling this hazard. Equipment will be regularly monitored and maintained in effort to prevent excursions or failures.

Relevant Knowledge from Other Chemical Plants –Relevant lessons learned from the industry and a summary of how these have been incorporated in the design

Millard Event in Theodore, AL

An anhydrous ammonia production plant in Theodore Alabama, owned by Millard, was a frozen poultry export facility. The chemical that caused the explosion was anhydrous ammonia. The explosion occurred as a result of hydraulic shock, which released 32,000 pounds of anhydrous ammonia into the surrounding area [26].

The plant lost power on August 22nd, which caused issues around the plant with start-up. The cooling coils responsible for condensing ammonia into liquid had lost power for seven hours. On August 23rd, an operator was working on troubleshooting startup issues when he manually cleared the alarms in the refrigeration coils. The refrigeration system was in the process of a defrosting cycle in which hot ammonia is put through the coils to melt the ice on the outside of the coils. When he cleared the alarm it reset the refrigeration system, which caused the system to go into a refrigeration cycle. This put cold, liquid anhydrous ammonia into the coils, which condensed the hot ammonia and generated a vacuum rapidly. This sudden change in pressure resulted in a piping failure due to hydraulic shock (a sudden localized pressure surge). Instead of initiating an emergency shutdown, the decision was made to isolate the piping failure during operation. This led to increased stress on the roof mounted manifold above the piping system that failed which ultimately caused it to catastrophically fail [26].

The failure was easily preventable in a number of ways. Manually interrupting the defrosting cycle was the primary cause of the disaster, which could be prevented by ensuring that control systems are equipped with security devices that only trained and authorized personnel may manually override. Along with that, this process could be made inherently safer by reducing the number of evaporator coils connected to the same valve. Only one of the coil systems failed, but the contents of four evaporator coil systems were released since they were connected to one valve [26]. By putting a valve on each coil individually, this will limit the damage if a release event were to occur. The process also could have been made safer by installing interruption of service logic in the control system. If the control system had been programmed to automatically remove contents in

the coil before restarting a refrigeration cycle, the hydraulic shock even could have been prevented because there would be no hot cause in the system to condense and cause a rapid pressure change.

The failure released 32,000 pounds of anhydrous ammonia in the area, which traveled a quarter mile to a site where 800 contractors were working on cleaning up the Deepwater Horizon oil spill. A total of 153 people were exposed to toxic levels of anhydrous ammonia. 32 off-site workers required hospitalization and four required ICU admittance [26]. The ammonia also caused significant environmental damage to the aquatic species in the area. The aquatic species in the area were already stressed due to the oil pollution and the release caused a spike in unionized ammonia that is significantly toxic to marine populations [27]. Along with affecting the local community and environment, this failure also set a precedent for how release events are legally handled. Millard had previously had an ammonia release due to hydraulic shock at the same site three years before. Millard was found guilty in violating the Clean Air Act and ultimately was evicted from the site in addition to receiving a $3 million fine [28]. This affected the chemical industry by providing another example of what can happen if corrective actions aren't taken and the severe legal implications of chemical plant failures that are the result of negligence [26]. Events like these make chemical engineering negatively viewed in the public eye. Out of specification events or plant failures would be costly to the company and could shut down the ammonia plants all together.

Goodyear Heat Exchanger Explosion

Another relevant lesson to ammonia production is that of heat exchanger explosion which occurred at a Goodyear rubber synthesis facility. The heat exchanger in utilized latent heat from anhydrous ammonia latent heat to cool a process stream. On June 10th, 2008, a Goodyear employee closed the isolation valve to the pressure relief system on the ammonia side of the heat exchanger to replace a ruptured rupture disk. However, the employee never reopened the isolation valve to allow the pressure relief system to work properly. On June 11th, 2008, a Goodyear employee closed the block valve to the ammonia-side pressure control valve before cleaning the process side of the heat exchanger with steam. The ammonia side of the heat exchanger was isolated from the pressure control valve and the pressure relief system, which caused the heat exchanger to pressurize until it violently exploded. The explosion killed one employee and injured six others. The employee tracking system failed, and the fatally injured employee was not found for hours after the explosion. The explosion also resulted in the release of toxic ammonia vapors [29].

Based on the CSB report, the heat exchanger had been properly designed and equipped with pressure control and relief devices. The issues that lead to the over pressurization, explosion, and unaccounted employees was a result of poor protocols and lack of practice/commitment to the protocols. The major takeaways from this incident are that headcount drills must be practiced routinely, and headcount procedures must have contingency plans if automatic headcount systems fail. Headcount practice drills should also simulate the failure of automatic headcount systems. The maintenance completion protocols were also not followed, and the protocols were not taken seriously. Proper lockout-tagout procedures need to be followed for all maintenance work. Maintenance protocols also need to follow the proper ASME Boiler and Pressure Vessel Code, which include designating an individual to monitor and have control over vessel pressure when a pressure relief system is isolated. The heat exchanger explosion could have been avoided at the Goodyear rubber facility if proper lockout-tagout procedures had been followed during regular maintenance. Implementing these procedures and safeguards is essential before plant operation.

Safety, Health, and Environmental Considerations

Extreme safety precautions must be taken designing this plant as significant hazards are present. Among the safety hazards include flammable gases, hydraulic shock, ammonia exposure, oxygen toxicity, asphyxiation, sulfuric acid exposure, potassium hydroxide exposure, pressurized gas, pinch points, working at heights, and electric shock. In addition to all of those health considerations, chemicals in the process also pose environmental threats like accelerating the Greenhouse Effect as well as poisoning organisms in the surrounding area if waste streams are not properly treated.

A few general safety practices will be used to mitigate the above safety risks for on-site personnel. Operators will be adequately trained how to handle chemicals used in each system, operate safely around pressurized gas risks, perform lock out tagout procedures, and operate safely at heights. Along with that, operators will be properly trained how to maintain equipment as well as operate equipment. Operators will also be provided with appropriate PPE to mitigate inherent risks associated with operating and maintaining each piece of equipment. This includes—but is not limited to—acid/base protective suits, helmets, safety glasses, gloves, fall protection, closed toed boots, respirators, and ear protection. In addition to that, equipment maintenance and inspections will be performed regularly to ensure proper function of equipment. Evacuation routes will be posted in visible locations and regular evacuation drills will be performed so that everyone on site will know the quickest and most effective way to evacuate during a potential excursion. Noise measurements will be taken around the plant to find areas where ear protection should be required. Red and yellow tape with documentation will be used to restrict personnel from entering areas that are temporarily hazardous, while physical barriers and guard rails will be used to prevent accidental entry into an area deemed inherently hazardous.

The plant will also have devices and practices to make the systems inherently safer. Process pipelines and vessels will be equipped with pressure relief valves so that pressurized and vacuum systems don’t fail. Rupture disks will be put in place prior to pressure relief valves to reduce wear and extend life. Spill kits and fire extinguishers will be located around the plant in case of emergency. For pressurized gas systems, each pressurized vessel will have a blast gate or isolation valve to prevent the contents of more than one vessel from releasing during an excursion. In addition to that, controls will be put in place to prevent an accidental mixture of cold and hot streams that could result in hydraulic shock if the hot stream rapidly cooled and condensed. All systems containing gases and liquids with the potential to generate static electricity will be properly grounded to reduce the risk of arc and electrocution. To prevent flammability risks associated with hydrogen, heat exchangers will be used to ensure that hydrogen never exceeds a temperature within 50 °C of its autoignition temperature.

Environmental sustainability was one of the primary drivers when designing this plant. Our goal to remain carbon neutral was achieved by using electrolysis rather than steam reformation to generate hydrogen along with using stranded wind energy instead of non-renewable sources of energy. Waste streams will be properly treated prior to release to ensure the health of neighbors and the surrounding environment. Ammonia is toxic as well as a greenhouse gas that can also form into NOx if it is oxidized, which is a more potent greenhouse gas. For this reason, process equipment will be used to reduce ammonia emissions around the plant. The purge stream of the

ammonia synthesis loop will be treated to strip out ammonia and hydrogen with a scrubber and stack as discussed in the previous section to minimize the release of toxins in the surrounding environment. In addition to that, the blowdown of the ammonia scrubber—which is rich in ammonium sulfate—will be given away as a crude fertilizer to reduce the amount process waste.

Equipment Cost Summary

Various costing correlations were used while estimating the installed costs of the major equipment featured throughout the modular process. While some equipment types were used in multiple sections and required simpler costing correlations (such as the compressors and heat exchangers), others required a more complicated calculation. Below are explanations and example applications of the costing correlations used for costing the general equipment followed by detailed descriptions of the more complicated equipment with references to Appendix I where the full sample calculation can be found. For a complete equipment cost summary, see Table 8 at the end of this section.

Compressor Costing

For adjusting the system pressure of gas streams, rotary screw compressors were used because this type of compression device is more durable, is safer to operate, and is easier to maintain [30]. The simplest costing correlation for rotary screw compressors was found on matches.com which has a database of costing correlations for a wide range of chemical plant equipment. While acknowledged as a "black-box" method for costing estimation, the website recommends using this JavaScript correlation for a project's "early development and budgeting" [31]. This particular correlation requires a range of 5 to 450 horsepower for the compressor power and simply uses the compressor power to estimate the purchased cost in 2014 as follows. The following example is taken from the compressor used to increase the feed pressure of the air into the membrane section.

$$P_{Comp}\ hP = 44\ kW\left(\frac{1.34\ hp}{1\ kW}\right) = 59\ hp$$

$$59\ hp\ Compressor \xrightarrow{>125\ psi, Carbon\ Steel} \$53{,}700\ in\ 2014$$

Please also note that for costing the storage vessels, the same website was used based on the pressure vessel size. For detailed sizing calculations for the storage vessels see Appendix I.

To convert the cost of the rotary screw compressors in 2014 dollars to 2020 dollars, the chemical plant cost indexes for each year were used. The values for 2010 and October of 2019 (used as estimate for 2020) were found on www.chemengonline.com/pci [17]. The final cost in 2020 dollars is the estimate for the compressor in a single module.

$$CEPCI_{2014} = 576.1\ \&\ CEPCI_{2020} = 599.5$$

$$C_{e,2019} = \left(C_{e,2014}\right)\left(\frac{CEPCI_{2020}}{CEPCI_{2014}}\right)$$

$$C_{e,2020} = (\$53{,}700)\left(\frac{599.5}{576.1}\right) = \$55{,}900\ in\ 2020$$

Heat Exchanger Costing

Throughout the ammonia production process, temperature changes were required at various points to ensure the optimal temperature was being used for a given unit operation. To remain consistent, the following purchased cost correlation from *Chemical Engineering Design* from Towler and Sinnott was used for all heat exchangers where "a", "b", and "n" are all constants unique to the piece of equipment while "S" is the characteristic size parameter unique to that piece of equipment [22]. Note that this correlation predicts the cost for the piece of equipment in 2010 and will need to be adjusted for a current estimate. The following example comes from the purchased cost estimation for the 5.6 m^2 heat exchanger used in the membrane section. We acknowledge that some of the smaller heat exchangers fell out of the range given by Towler and Sinnott and we are unsure how this will affect the accuracy of the calculation, but decided that the correlation would be used as a preliminary estimate in order to remain consistent.

$$C_e = a + bS^n$$

$$For\ double - pipe\ heat\ exchangers: a = 1900, b = 2500, and\ n = 1$$

$$C_{e,2010} = 1900 + 2500(5.6\ m^2)^1 = \$15{,}900\ in\ 2010$$

Although most heat exchangers used a double-pipe configuration, the flash drum employed a U-tube shell and tube heat exchanger which uses the same correlation though slightly different constants to calculate the cost of the heat exchanger. Please also note that the flash drum, used in the ammonia recovery process, also used this costing correlation using the constants for a vertical pressure vessel.

To convert the cost of the heat exchangers in 2010 dollars to 2020 dollars, the chemical plant cost indexes for each year were used. The values for 2010 and October of 2019 (used as estimate for 2020) were found on www.chemengonline.com/pci [17]. The final cost in 2020 dollars is the estimate for the heat exchanger in a single module.

$$CEPCI_{2010} = 532.9\ \&\ CEPCI_{2020} = 599.5$$

$$C_{e,2019} = (C_{e,2010})\left(\frac{CEPCI_{2020}}{CEPCI_{2010}}\right)$$

$$C_{e,2020} = (\$15{,}900)\left(\frac{599.5}{532.9}\right) = \$17{,}900\ in\ 2020$$

Electrolysis Costing Summary

It is difficult to find methods to estimate capital costs of electrolysis cells as this is a relatively new type of technology. A few costing methods exist, but there is not a well-known costing model for electrolysis cells that is as comprehensive as the models used for more common equipment (e.g. heat exchangers, compressors). In a review article on water electrolysis for hydrogen production, the authors agreed upon a linear cost model for electrolysis cells that produce less than 1,000 kg per day of hydrogen [6]. Several case studies were explored in the article, finding that a scale of $800 in capital expense (purchased cost) per kg of hydrogen produced per day was an appropriate, conservative estimate. The scale of the electrolysis cell is within the given range, as one cell produces 190 kg of hydrogen per day. Eleven cells are built in the same structure (per module) in this design, producing a total of 2,100 kg of hydrogen per day. This costing method is shown below, for a calculation for one 10 mtpd module.

$$C_{e,2005} = \frac{800\ 2005\ USD}{kg\ H_2\ per\ day} * \frac{43\ kmol}{hr} * \frac{2.01\ kg}{kmol} * \frac{24\ hr}{1\ day} = \$1.66M$$

This capital expense value is in 2005 reference dollars, so a CEPCI scaling calculation must be performed to obtain the appropriate expense for today's economy. This scaling calculation is shown below.

$$C_{e,2020} = (\$1.66M\ 2005\ USD) * \frac{599.5\ CEPCI_{2020}}{468.2\ CEPCI_{2005}}$$

$$\therefore C_{e,2020} = \$2.13M$$

More in-depth characterization of the electrolysis cell design, including sizing calculations, can be found in Appendix I.

Membrane Costing Summary

Because the selected membrane is still in a developmental stage and the recent research using porphyrin-based oxygen carrier membranes still requires further testing for large-scale production, predicting the cost for the material itself was a challenge, not to mention the added complexity the tube geometry requires. While the process engineering team is confident that membranes employing this technology will eventually hit the market for efficient air separation systems, the cost for purchasing the material in bulk at that time is an unknown until further research into the market is performed. Literature review yielded no consistent estimation for the cost of such a membrane, so the team decided to go a different route for a preliminary cost by acquiring a quote from Compressed Gas Technologies Inc. for a pressure-swing adsorption unit capable of accomplishing the desired flow rate and purity of nitrogen at the designated process conditions. The estimate they provided of $60,000 for a single module was considered a conservative estimate

for the cost of the membrane since the original motivation for choosing a membrane separation (as opposed to PSA) was the reduced capital investment that membrane alternatives often offer. Assuming the Pebax-2533 TFC w/ T(p-OCH_3)PPCoCl membrane ultimately hits the market, a complete economic and market analysis can be performed in order to determine whether this trend of cheaper membrane options holds true. If after further review choosing the membrane option is not deemed financially viable, switching to a PSA would require further technical analysis, but we would already have a cost estimation for such a switch.

For a preliminary design estimate, we deemed this quote an acceptable starting cost range for the process, but there are several questions that still need to be answered. Such as how often will the membrane need to be replaced. While precautions are set in place to protect the membrane via the pre-filter and desiccant apparatus, wear-and-tear for such a thin material is likely to occur. This will require further research that is not currently obtainable for this specific membrane. Since this form of air separation is a novel approach, out plant may serve as a case study for such parameters of operation.

Membrane material is often sold based according to its required mass, which was calculated to be 502 g in Appendix I for a single module (thus about 2.5 kg for the entire plant). Note that this calculation is based on an estimated density of $1\frac{g}{cm^3}$, since the actual density of the Pebax-2533 with the active chemical was not found during literature review. This metric, whether volume or mass, could become useful once the membrane can be purchased and an active market exists for the product. A more thorough discussion on the consideration of intellectual property and the potential for paying royalties on the membrane is discussed in the *Other Important Considerations* section of this report.

Reactor Costing Summary

The ammonia synthesis reactor purchase cost was determined by comparing three different cost estimates. Two cost estimates came from Towler and Sinnott, and the third came from the Matches online cost correlations. The reactor was initially cost using the Towler and Sinnott correlation for a jacketed, agitated reactor, which gave a purchase cost of a single reactor at $332,000 in Oct. 2019 dollars [22]. This cost would end up being relatively low, and the equipment described by the correlation is inaccurate because the reactor is not agitated. The correlation also fails to account for operating pressure. The reactor was then cost using the horizontal pressure vessel correlation from Towler and Sinnott so that internal pressure was considered. This proved to be far too high of an estimate at $2,620,000 for a single reactor in Oct. 2019 dollars. Finally, a cost correlation from Matches online cost correlations for a jacketed, non-agitated reactor that was dependent on internal pressure was used to cost a single reactor at $488,000 in Oct. 2019 dollars. This gave a middle price point, and the equipment description and pressure dependence made this estimate seem the most accurate. A detailed discussion of these calculations and decisions can be found in the reactor costing section of Appendix I.

Extraneous Equipment Costing (10% of Total Capital Cost)

For minor/supplementary equipment and other cost considerations in addition to the major components of the process, it was decided that for a preliminary estimate to include an additional 10% of the total purchased costs of all other equipment [17]. This value was determined to be just over $600,000 which was considered a reasonable estimate for the following extraneous costs. Such equipment included the pump used in the membrane section, a scrubber for removing the small amount of ammonia from the purge stream, and a small incinerator to dispose of this waste ammonia stream. This incinerator will use a high current ignition source in order to ensure the process remains carbon neutral as outlined in the explanation of our goals. Alternative solutions for dealing with the waste ammonia stream (as discussed in the *Process Safety Consideration* section) may replace the incinerator in updated versions of the design. Another potentially significant cost that fell into this category was the cost of the ruthenium-based catalyst in the reactor. The mass of catalyst required was calculated in Appendix I to be 2365 kg. A quote from a supplier may be the best approach moving forward for a more accurate cost of the catalyst. One final consideration included in this section of the costing was the potential for heat exchangers costing more than the correlations suggested due to high pressure conditions, and other precautions related to high pressure conditions. The reactor, flash drum, storage vessels, and all other major equipment was costed considering the pressure, though in some cases the design pressure was above the recommended range in the Towler and Sinnott correlation. To ensure safe operation, pressure relief valves and appropriate system control should also be evaluated and is assumed to fall into this category for cost estimation.

Purchased Equipment Cost Summary

Table 8: Capital cost summary table for a single module producing 10 metric tons per day.

Unit Number	Design Metric	Cost Correlation	Purchase Cost (USD)
Electrolysis			
E-115	0.54 m^2	Matches – double pipe, small	$ 940
H-110	2,090 kg H_2/day	National Renewable Energy Lab (Ruth, 2009)	$ 2,130,000
		Total	**$ 2,131,000**
Membrane Section			
C-201	44.1 kW	Matches – screw compressor	$ 55,900
E-201	5.6 m^2	Towler & Sinnott Double-pipe, CS	$ 17,800
M-201	300 g 3 m^2	Quote from Compressed Gas Technology Inc.	$ 60,000
		Total	**$133,700**
Ammonia Synthesis Loop			
C-301	129 kW	Matches – screw compressor	$ 119,800
C-302	105 kW	Matches – screw compressor	$ 103,500
C-303	95.9 kW	Matches – screw compressor	$ 97,200
C-304	47.9 kW	Matches – screw compressor	$ 59,200
C-305	20.6 kW	Matches – screw compressor	$ 32,600

E-301	3.57 m^2	Towler & Sinnott Double pipe, 304ss	$ 12,200
E-302	8.37 m^2	Towler & Sinnott Double pipe, 304ss	$ 25,700
E-303	0.62 m^2	Towler & Sinnott Double pipe, 304ss	$ 3,900
E-304	0.50 m^2	Towler & Sinnott Double pipe, 304ss	$ 3,500
E-305	0.21 m^2	Towler & Sinnott Double pipe, 304ss	$ 2,700
R-301	D = 2.1 m L = 4.1 m P = 1400 psig	Matches – jacketed, non-agitated	$488,000
C-306	1,000 psi 639 kW	Matches – Centrifugal, 316ss	$ 1,460,000
E-306	6.97 m^2	Towler & Sinnott Double pipe, 316ss	$ 32,600
E-307	9.62 m^2	Towler & Sinnott Double pipe, 316ss	$ 43,800
E-308	12.4 m^2	Towler & Sinnott Double pipe, 316ss	$ 55,400
E-309	50.6 m^2	Towler & Sinnott U-Tube, 316ss	$ 57,400
S-301	161 m^2	Towler & Sinnott U-tube Shell&Tube, 316ss	$ 87,900
S-301	1,540 kg	Towler & Sinnott Vertical Pressure Vessel, 316ss	$ 97,500
		Total	**$ 2,783,000**
Storage Vessels			
	23,500 lb	Matches Column, no internals, medium	$ 256,000
	23,500 lb	Matches Column, no internals, medium	$ 256,000
	23,500 lb	Matches Column, no internals, medium	$ 256,000
	23,500 lb	Matches Column, no internals, medium	$ 256,000
		Total	**$ 1,024,000**
Miscellaneous			
	10% of total		$ 607,000
		Total Purchase Cost	***$ 6,679,00***

Fixed Capital Investment Summary

The Lang Factor is used to approximate the installed cost of equipment. This is different than the purchase cost because the installed cost accounts for the additional costs associated with making the equipment fully operational. The Lang Factor was first introduced by Lang in 1948, and heuristics have been used to determine appropriate Lang Factors ever since the introduction. For this modular plant design, the Lang Factor requires careful consideration because the majority of heuristic knowledge applies to stick-built plants. The text by Towler and Sinnott discusses installation factors with a range for stick built, mixed fluid Lang Factors of 3.3 to 6.0 [22]. However, this is far greater than the Lang Factor of 1.7 used by Weber and Snowden-Swan for a modular plant design [32]. Unfortunately, this article was not fully accessible, and a thorough analysis of a Lang Factor for a modular plant could not be investigated. Therefore, a Lang Factor of 1.7 will be used here. An analysis of the Lang Factor's effect on the ammonia sales price will be performed in the Economic Analysis section. This sensitivity analysis will allow for a discussion of the how important the Lang Factor is to the plant's success.

Using the Lang Factor of 1.7 results in the first-of-a-kind (FOAK) module installed cost of $11.4 million. As discussed in the project memo, the learning rate for modular manufacturing will be approximated at 20%. This means the module cost reduces by 20% every time the production quantity doubles. The cost of the nth module will be calculated with the following equation.

$$k_n = k_1 n^{\log_2 p}$$

Where k_n is the cost of the nth module, k_1 is the FOAK cost, n is the module number, and p is 0.8 which represents the learning rate of the modular production. The table below shows the cost of each module of the five modules used in this design.

Table 9: Cost of all five, 10 mt/day modules at a learning rate of a 20%. This means the module production cost decreases by 20% every time the number of modules produced doubles. As mentioned, the Lang factor used was 1.7 to convert the purchased cost into an installation cost prediction.

	Installed Cost (USD)
FOAK (k_1)	$ 11,400,000
Module # (n)	
1	$ 11,400,000
2	$ 9,080,000
3	$ 7,970,000
4	$ 7,270,000
5	$ 6,760,000
Total Installed Cost	**$ 42,400,000**

Table 9 shows that the total installed cost of the five-module plant with a 50 mt/day capacity is $42.4 million. An analysis and discussion of adjusting the module size and number of modules used to meet the 50 mt/day capacity can be found in the Economic Analysis section.

A discussion of the plant construction and installation timeline can now be done since the total installed cost has been approximated. The project memo discusses a six-month waiting period that

must be allocated for the permit acceptance process. For the purposes of this preliminary design, a conservative approach will be taken for the timeline, so no investment or construction will happen until after the permit process is complete. The project memo also mentions a 30-34 month construction and installation period for a modular plant, compared to 36-40 months for a stick built plant. It is assumed that the plant construction and assembly period will be assumed to take 30 months, which sets the total permitting, construction, and installation period at 36 months.

The 36 month timeline described above can be broken into six-month periods to give a general timeline for plant construction and installation. The modular construction has the benefits of beginning operation once a single module is installed. Therefore, construction and installation should focus on one module at a time. A rough approximation of six-months per module can be used to lay out a preliminary timeline. However, module construction can begin off-site on its own timeline, but installation will follow general schedule laid out below. It is likely that the first module installation will take more than six-months, but the subsequent modules will likely be installed more quickly. This is likely similar to the learning curve applied to the module installation cost above. The six-month installation period given to each module is likely inaccurate, but this inaccurate should balance out over the full construction and installation period. A preliminary construction and installation timeline is shown in the table below.

Table 10: Construction and installation timeline for the five module, 50 mt/day ammonia plant. No investment or construction will begin until permits are obtained. Production can begin in each module once installation is complete. It is likely that the FOAK module will take longer to install than subsequent modules. For simplicity, the timeline will show each module installation over the same time allotment for each.

Time Period (months)	Task or Construction/Installation Completed	Total Amount Invested (USD)
0 – 6	Environment and building permits applied for at month zero. Six-months allotted for permit approval.	$ 0
6 – 12	First-of-a-kind module is constructed and installed. Can begin operation at 10 mt/day at the end of month 12.	$ 11,400,000
12 – 18	Second module is constructed and installed. Can begin operation at 20 mt/day at the end of month 18.	$ 20,500,000
18 – 24	Third module is constructed and installed. Can begin operation at 30 mt/day at the end of month 24.	$ 28,500,000
24 – 30	Fourth module is constructed and installed. Can begin operation at 40 mt/day at the end of month 30.	$ 35,700,000
30 - 36	Fifth module is constructed and installed. Can begin operation at 50 mt/day at the end of month 36.	$ 42,400,000

Manufacturing/Operating Costs

The manufacturing/operating costs for the ammonia plant are made up of five different factors – utilities, operating labor, labor related costs, capital related costs, and sales related costs. Minimal raw materials are required at the plant, and those costs have been lumped into a miscellaneous utility cost. It is also being assumed that sufficient capital is available to construct the plant, and no interest will have to be paid. However, interest payments would significantly increase operating costs, and interest will need to be factored in if sufficient capital is not available.

The utilities included in this project are cooling water, refrigerated water, deionized water, steam, electricity, and low temperature coolant. Unit cost ranges for cooling water, refrigerated water, and deionized water were estimated as \$(6.7 – 20)/1000 m^3, \$8.30/GJ, and \$(1.0 – 1.2)/ 1000 kg, respectively [17]. These estimates were provided for a similar project, and they provide relatively wide ranges and conservative estimates for the related operating costs. The high unit cost for each range was used to ensure an overall conservative estimate. Steam was both used and produced at 550 kPa and 155 °C. Similar to the process water costs, steam costs were assumed to be \$20/1000 kg, and the same rate was applied as credit for steam produced by waste heat [17]. Electricity was priced with a range of values found for recent wind energy costs. A range of \$(11 – 45)/MW-hr was used, with a baseline estimate of \$20/MW-hr [33], [34]. Electricity was a dominant factor in the analysis for operating costs, so the price was adjusted within this range when performing sensitivity analyses. The low temperature coolant used to cool and condense the reactor products was priced at a rate of \$13.11/GJ [21]. The price for the coolant was accepted as reasonable, as it is roughly 60% more expensive than the rate for refrigerated water. A miscellaneous utility cost of \$0.03/kg NH_3 produced was included to account for minor raw materials and unaccounted utilities such as KOH for the electrolysis cells, H_2SO_4 for the ammonia scrubber, and other utilities [17].

Table 11: Summary of all utility requirements for a single, 10 metric ton per day ammonia production module. Yearly costs given here are based on the high estimate of each utility's unit cost range except for electricity, which is cost at $20/MW-h.

Utility	Unit Number	Unit Type	Amount	Cost (USD/yr)
Cooling Water				
	E-115	Heat Exchanger	0.81 m^3/hr	$ 125
Deionized Water				
	E-304, E-305	Heat Exchangers	38.0 kg/hr	$ 350
	E-301, E-302, E-303	Heat Exchangers	314 kg/hr	$ 2,900
	R-301	Reactor Jacket	535 kg/hr	$ 4,950
	E-307, E-308	Heat Exchanger	356 kg/hr	$ 3,290
Electricity				
	C-110	Electrolysis Cell	4880 kW	$ 752,000
	C-201	Compressor	44 kW	$ 6,800
	C-301	Compressor	130 kW	$ 20,000
	C-302	Compressor	105 kW	$ 16,200
	C-303	Compressor	96 kW	$ 14,800
	C-304	Compressor	48 kW	$ 7,400
	C-305	Compressor	21 kW	$3,200
	C-306	Compressor	639 kW	$ 98,500
Refrigerated Water				
	E-201	Heat Exchanger	146 MJ/hr	$ 9,360
Refrigerant				
	E-309	Heat Exchanger	1,660 MJ/hr	$ 191,000
	S-301	Heat Exchanger	768 MJ/hr	$ 88,300
Steam (and credit)				
	E-115	Heat Exchanger	74 kg/hr	$ 11,400
	E-304, E-305	Heat Exchangers	38.0 kg/hr	-$ 48,400
	E-301, E-302, E-303	Heat Exchangers	314 kg/hr	-$ 5,840
	R-301	Reactor Jacket	535 kg/hr	-$ 82,400
	E-307, E-308	Pre-Chillers	356 kg/hr	-$ 54,800
Misc.				
			10,000 kg NH_3/day	$ 120,000
			Single Module Utility Cost	**$ 1,160,000**

The required operating labor is traditionally determined by the different equipment in use at the plant. However, these estimates are for stick built plants operating at production levels much higher than 50 mt/day. Therefore, some adjustments were made to the traditional operator estimates. Five modules that each produce 10 mt/day will be used at the plant, but each module

should not require the traditional number of operators as a high production, stick build plant. The number of operators for a single module based on traditional operator requirements is shown in the table below. The operator requirement for the five-module plant will be assessed after this calculation.

Table 12: Determination of the number of operators needed per module (10 mt/day) based on traditional operator requirements for a stick built plant. The traditional operators per unit per shift recommendation comes from **[17]**.

Equipment Type	Number of Units per Module	Traditional Operators per Unit per Shift	Number of Operators
Separators	1	0.5	0.5
Reactors	1	0.5	0.5
Heat Exchangers	11	0.1	1.1
Blowers/Compressors	7	0.2	1.4
Cooling Tower	1	1	1
Separators	1	0.5	0.5
		Total Operators per Shift per Module	**5**

The traditional determination of operators per unit gave five operators required per module per shift. This would mean 25 operators are required per shift to run the plant. Unfortunately, this way of determining the number of operators required is independent of production capacity, and 25 operators per shift is an extremely high number for a small plant producing 50 mt/day. Instead, the an approximation of two operators per module per shift will be used. This gives 10 operators per shift for the entire plant. The next section shows how inaccuracies of this approximation could affect the operating costs of the plant.

The plant will operate using four different operator shifts. Operators will work twelve-hour shifts, and there will be a day shift and a night. This means the day shift will work Monday through Thursday in the first week, followed by Monday through Wednesday in the second week. The other day shift will cover Thursday through Sunday in the first week, and Friday through Sunday in the second week. Two night shifts will alternate in this way as well.

This means a total of 40 operators will be required on staff for normal operation. An operator average salary is estimated at $50,000 per year. This equates to $2,000,000 in operator salaries, which will be referred to as operating labor costs. Labor related costs are also estimated at an additional 60% of the operating labor costs, which accounts for health insurance, retirement, vacation, disability, payroll overhead, and supervisor labor costs [17].

The capital related costs portion of the operating cost is used to account for recurring costs in the form of maintenance, operating supplies, insurance, waste treatment, local taxes, and overhead. Plant depreciation is not considered in the capital related costs because it will be accounted for in the Net Present Value analysis in the following Economic Analysis section. The capital related operating cost estimate for this project will be taken as 15% of the installed cost of the plant. This is on the lower end of the general range because the equipment has a small footprint and production

capacity compared to stick-built plants, so a lower estimate for categories like maintenance is more appropriate [17]. The installed cost of the 50 mt/day ammonia plant was shown to be $42,400,000 in the Fixed Capital Investment Summary. This will be used to determine the capital related operating costs.

The sales related operating costs are used to account for reoccurring costs related to patents and royalties, packaging, distribution, marketing and sales, and administrative costs. This is where the membrane and electrolysis intellectual property is accounted. The sales related costs will be taken as 20% of the annual sales of ammonia. A summary of the five different operating cost considerations can be seen below.

Table 13: Summary of the five different factors considered in the operating cost of the 50 mt/day modular ammonia plant. Yearly costs are given for the full, 50 mt/day ammonia production capacity. The installed cost of the plant is estimated at $42,400,000. Ten operators are required per shift. The annual sales are determined through a circular reference, and this calculation is shown after this table so the percentage is included here only.

Operating Cost Factor	Determination	Yearly Cost (USD/yr)
Utilities (U)	Breakdown by utility time and equipment requirements.	$ 5,800,000
Operating Labor (OL)	Baseline set at two operators per module; salary of $50,000/yr.	$ 2,000,000
Labor Related (LR)	Set at 60% of the operating labor cost,	$ 1,200,000
Capital Related (CR)	Set at 15% of the installed cost of the ammonia plant.	$ 6,370,000
Sales Related (S)	Set at 20% of the annual sales generated from ammonia.	0.2 x annual sales

With these operating costs determined, the annual sales requirement can be determined. A profit margin of 10% will be used for this calculation, and further analysis of the profit margin is performed in the Economic Analysis section. The annual sales requirement is determined through the following cyclic relationship.

$$Sales = (1 + PM)(U + OL + LR + CR + 0.2Sales)$$

Where PM is the profit margin, U is the annual utility cost, OL is the annual operating labor cost, LR is the annual labor related cost, and CR is the annual capital related cost. $0.2Sales$ represents the annual sales related cost. This equation can be solved for $Sales$ to determine the annual sales income.

$$Sales = \frac{(1 + PM)(U + OL + LR + CR)}{1 - 0.2(1 + PM)}$$

$$Sales = \frac{(1 + 0.1)(\$5.8M + \$2.0M + \$1.2M + \$6.37M)}{1 - 0.2(1 + 0.1)}$$

$$Sales = \$21{,}700{,}000/yr$$

This shows the annual sales income must be $21,700,000. This value can now be used to determine the sales price of the ammonia, which will help determine if the plant can produce and sell ammonia at a competitive price. The plant produces 50 mt/day, which is equivalent to 18,250 metric tons of ammonia per year. The sales price per metric ton is determined as follows.

$$Sales\ Price = \frac{Sales}{Production}$$

$$Sales\ Price = \frac{\$21{,}700{,}000/yr}{18{,}250\ mt\ NH_3/yr} = \$1{,}190/mt\ NH_3$$

This means the plant would need to sell the ammonia at $1,190 per metric ton to break even and have a profit margin of 10%. The Independent Commodity Intelligence Service gave a price of ammonia from 2014 at approximately $500 per metric ton [35]. This price point is outdated, but more recent information from the University of Illinois shows the price point of ammonia remained relatively stable around $500/ton for 2018, equivalent to about $550/mt [36]. In contrast to this, liquid ammonia can be purchased for $1,100 to $2,220 per metric ton through Alibaba [37]. The low end of this final estimate is likely more accurate to the small-scale market that this plant will target. More discussion to the competitiveness of the plant will be given in a later section.

Economic Analysis

Sales Price Sensitivity Study

The units sales price calculated in the previous section is dependent on several key assumptions. The purpose of this section is to analyze the effects that an inaccurate assumption could have on the successfulness of this project. Here, project success is measured by the sales price per metric ton that would be required for the ammonia produced at the plant to achieve a profit margin of 10%. This discussion is meant to be separate from a Net Present Value analysis, Internal Rate of Return analysis, and modularity analysis.

The assumptions and decisions that were identified as critical to the success of the plant are the Lang Factor, capital related manufacturing costs, electricity costs, and labor related costs. Also, the profit margin was investigated to determine its effect on the sales price.

The Lang Factor baseline was chosen to be 1.7, but this was based on minimally available information for modular plant Lang Factors. This Lang Factor was chosen because a paper by Weber and Snowden-Swan used this value in their economic analysis of numbering up a chemical process [32]. However, this paper was not accessible, and other detailed discussions of the Lang Factor for modular plants were few and far between. Therefore, this sensitivity analysis looks at how different Lang Factor values would affect the operating costs of the plant. Lang Factors of 0.85, 1.7, 3.4, and 5.1 were chosen for this analysis. For each Lang Factor, the installed cost of the plant was recalculated, which subsequently effected the yearly capital related costs which are taken as 15% of the plant installed cost.

Electricity costs were found from several different sources, and their cost estimates spanned a wide range. Forbes reported high and low estimates for wind energy at $45/MWh and $11/MWh, respectively [31]. However, GreenTechMedia reported the national average for wind-derived energy at $20/MWh [34]. Lastly, lecture notes from Dr. AuYeung and Dr. Mallette reported a high-end electricity cost of $75/MWh [17]. The $20/MWh national average was chosen for the baseline, but electricity is the largest utility at 79% of the yearly utility cost when the baseline is used. The sale price sensitivity to electricity cost was analyzed to see the potential effects of the wide range of electricity costs, the potential for fluctuations in electricity cost, and the large portion of utility costs incurred by electricity.

The labor related costs were analyzed due to the uncertainty of the number of operators required per shift. There is a well-established number of operators required for a traditional stick-built plant, which would typically have a much larger capacity than the 50 mt/day capacity of this modular plant design. However, the operator requirement is not well established for modular plant designs, therefore the number of operators required per shift is likely subject to some variability. A high estimate using the operator requirements for a stick-built plant requires 25 operators per shift. As discussed in the previous section, an estimate of 10 operators per shift will be used since the modular equipment is much smaller than a traditional plant – this gives two operators per module [17]. A low estimate of five operators per shift will also be considered in case the baseline is overestimated.

Lastly, profit margins of 5%, 10%, 20%, and 30% were used in this analysis with 10% being the baseline profit margin. This was done to show the sales price dependence on the profit margin.

The results of the sensitivity analysis can be seen in Figure 4 below. A high end sales price of $1,500/mt was used to show where the sales price begins to reach uncompetitive levels. A discussion of current market sales price can be found in the Manufacturing/Operating Costs section.

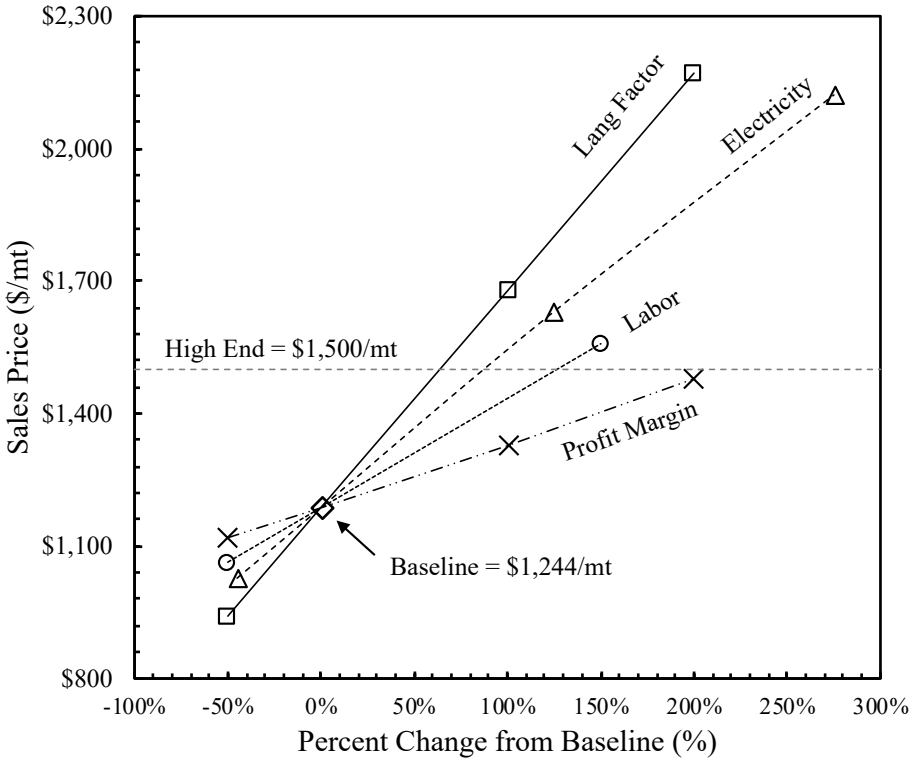

Figure 4: Sensitivity plot for the ammonia sales price to four different price factors – Lang Factor, electricity cost, labor costs, and the profit margin. The baseline is a Lang Factor of 1.7, electricity cost of $20/MWh, 10 operators per shift, and profit margin of 10%. The Lang Factor and profit margin were scaled by -50%, 0%, 100%, and 200% to Lang Factors of 0.85, 1.7 (baseline), 3.4, and 5.1 and to profit margins of 5%, 10% (baseline), 20%, and 30%. The sales price was calculated at 5, 10 (baseline), and 25 operators per shift, which corresponds to -50%, 0%, and 150% changes in the number of operators per shift from the baseline. The sales price was also calculated at electricity costs of $11/MWh, $20/MWh (baseline), $45/MWh, and $75/MWh, which corresponds to -45%, 0%, 125%, and 275% changes in the electricity cost from the baseline.

As seen in Figure 4 above, the Lang Factor is the biggest driver of the sales price. The Lang Factor determines the installed cost, which in turn determines the yearly capital related costs (maintenance, insurance, supplies, taxes, etc.). The capital related costs have been set at 15% of the total installed cost of the plant – a discussion of the capital related operating costs can be found in the Manufacturing/Operating Costs section. Unfortunately, there is little heuristic knowledge available for Lang Factors of modular plants, which makes it difficult to be certain that the baseline of 1.7 is accurate. What the plot does show is that an increase in the Lang Factor of ~50% could lead to a sales price that is too high to be competitive. A 50% increase would raise the Lang Factor

to about 2.5, which is still well below the stick built Lang Factor of about 4 for mixed fluid, stick built plants [17], [22]. This must be considered more thoroughly before moving forward with this project.

The next largest sales price driver for the plant is the cost of electricity. The cost of electricity varies by location, and the actual cost of electricity in the Minnesota River Valley should be investigated further. The Minnesota River Valley also has a high potential for wind energy generation [2]. However, it is unknown if that potential has been accessed. It is also unknown if the wind energy cost would fall near the national average. Based on the sensitivity analysis, the cost of electricity could increase to approximately $35/MWh before the sales price would become uncompetitive, which is $10/MWh below the high estimate given by Forbes [33]. This is concerning for the success of the plant because electricity costs can fluctuate, and there is not much room for upward adjustment from the national average [34].

The number of operators was found to have less effect on the sales price than the previous two price factors. The number of operators per shift could be doubled to 20 before the sales price would become uncompetitive. This price factor is also more stable than the previous two, as the number of operators per shift is unlikely to change during the lifetime of the plant. 20 operators of a 50 mt/day plant is also extraordinarily high for the low capacity of the plant. This price factor should be of little concern compared to the others discussed earlier.

The profit margin was found to have the lowest effect on the sales price, which has positive and negative attributes. The profit margin can be increased without the sales price changing significantly. However, this also means the profit margin cannot significantly reduce the sales price if other operating costs increase. This limits the ability of the sales price to be adjusted via the profit margin, which is one of the few independently adjustable factors in the sales price. Lack of adjustability in the sales price is a concern for the success of this project as well.

This analysis considers each price factor individually, but the real plant will be affected by simultaneous changes in price factors. The profit margin can be adjusted to a certain extent to accommodate changes in operating costs, but the effects of the profit margin are limited. Further investigation should be done into the possible range of Lang Factors that could be seen and the subsequent capital related costs that will be attributed to the plant. The cost and variability of electricity of the Minnesota River Valley should also be investigated further. These two price factors will be important in the success of the plant.

Net Present Value Analysis

The net present value of the plant was determined over a 20-year lifetime. It was assumed that environmental and building permits would take six months to be obtained from the onset of the project. It was also assumed that construction and installation would not begin until the permits were obtained, and that it would take 30 months for the plant to become fully operational. For simplicity and a more conservative estimate, it was assumed that sales do not begin until the plant is fully assembled. It is likely that production could begin in individual modules once they are constructed. However, as will be seen at the end of this analysis, it is unlikely that accounting for

below capacity production during the construction phase will change the results of this analysis very much.

The $42.4 million capital cost of the plant was spread evenly over the 30-month manufacture and assembly period. The annual gross profit is equal to the annual sales income less the total operating costs. Based on the $21.7 million annual sales income at a 10% profit margin (see Manufacturing/Operating Cost section), the annual gross profit is $1.97 million. A 20-year Modified Accelerated Cost Recovery System (MACRS) was used to account for depreciation, and the yearly depreciated value of the plant was used to determine the taxable profit. A corporate tax rate of 21% was used to determine how much was paid in taxes on the previous year's taxable profit. Finally, the annual cash flow was determined from the gross profit minus the taxes, which allowed the net present value (NPV) of the plant to be determined [17]. The minimum acceptable rate of return of 8% was used as mentioned in the project memo. The following equation was used to calculate the NPV of the plant.

$$NPV = \sum_{n} \frac{CF_n}{(1+i)^n}$$

Where n is the number of years, i is the acceptable rate of return, and CF_n is the cash flow in year n. A full breakdown of the NPV over the 20-year operating lifetime can be found in Appendix III.

As seen in Appendix III, the net present value of the plant over the 20-year lifetime is -$21.2 million, and the internal rate of return (IRR) was -0.7%. This means the project is very far from being a profitable endeavor. The negative IRR also shows that there is no time value of money that would make this project feasible in its current state.

Some further analysis was done to determine what the sales price would need to be for the NPV to break even. Excel solver was used to determine that the annual gross profit would need to be $6.28 million for the NPV to be zero with a 10% rate of return. The 10% rate of return was used in order to see what it would take for the plant to be better than the minimum requirement of 8%. The gross profit of $6.28 million corresponds to a 30% profit margin, and a sales price of $1,480/mt of ammonia. This sales price falls near the middle of the ammonia price estimate of $1,000-$2,000/mt from [37], but this is well above the price estimates of approximately $500/mt from [35] and [36].

Number of Modules Analysis

The preliminary design was performed using five equally sized modules capable of producing 10 metric tons per day. The following analysis was performed in order to determine whether increasing or decreasing the number of modules would decrease the overall cost of the plant. The six-tenths rule, below, was employed to scale the installed cost of the first year according to the production load for a single module.

$$C_{New} = C_{Original}\left(\frac{S_{New}}{S_{Original}}\right)^{0.6}$$

For this method, "C" represents the cost in USD and "S" represents the production load in metric tons per module. The first analysis performed was doubling the number of modules (therefore cutting the modular production in half from 10 mt to 5 mt). For the original cost, the FOAK capital cost for the five modular design of $11,353,780 was used.

$$C_{New} = \$11{,}353{,}780\left(\frac{5\ mt}{10\ mt}\right)^{0.6} = \$7{,}490{,}701$$

The cost of the first module, as expected, is 35% less expensive, though when considering the cost of all the modules with a learning rate of 20%, the total cost for installing more, smaller modules is consistently higher. Table 14 below shows the analysis for various number of module options using the six-tenths rule to scale the cost.

Table 14: Summary of the various number of module options. Three options for increasing the number of modules were considered, and, as a control, a study was done using a single, large module.

Number of Modules	Modular Production (mt)	First-of-kind Installed Cost (USD)	Total Installed Cost (USD)
5	10	$11,353,780	***$42,437,489***
10	5	$7,490,701	***$47,306,572***
20	2.5	$4,942,020	***$51,816,794***
50	1	$2,851,941	***$57,385,931***
1	50	$29,821,018	***$29,821,018***

Notice that while increasing the number of production modules causes an increase in total cost, using a single module actually decreases the cost, suggesting that modular design may not be a feasible option for this production plant. This is counter-intuitive because modular design for small chemical production plants should provide a decrease in total cost, with eventual diminishing returns once the number of modules increases [38]. According to this known trend seen in other production plants, the six-tenths rule scaling the installed cost according to the per module production may be an inadequate analysis. While the six-tenths rule is a common method for obtaining a rough estimate for a single piece of equipment, scaling up to an entire process likely makes this method an invalid approach.

A more advanced approach may be required for a proper analysis of the effect of modular size such as a design structure matrix using hybrid multidimensional scaling and clustering [39], [40]. This method clusters various costs and scales them differently, rather than using a simple equation like the six-tenths rule. This degree of analysis is outside the scope of the preliminary design, though with a cost value for a five-module design, the process engineering team has established a reference point for future analysis. Due to the inclusivity of this study, the team recommends employing a more powerful analytical tool, such as the suggested clustered matrix method, to acquire a more legitimate estimate for the effect of the number of modules.

Notice that while increasing the number of production modules causes an increase in total cost, using a single module actually decreases the cost, suggesting that modular design may not be a feasible option for this production plant. This is counter-intuitive because modular design for small

chemical production plants should provide a decrease in total cost, with eventual diminishing returns once the number of modules increases [38]. According to this known trend seen in other production plants, the six-tenths rule scaling the installed cost according to the per module production may be an inadequate analysis. While the six-tenths rule is a common method for obtaining a rough estimate for a single piece of equipment, scaling up to an entire process likely makes this method an invalid approach.

A more advanced approach may be required for a proper analysis of the effect of modular size such as a design structure matrix using hybrid multidimensional scaling and clustering [41, 42]. This method clusters various costs and scales them differently, rather than using a simple equation like the six-tenths rule. This degree of analysis is outside the scope of the preliminary design, though with a cost value for a five-module design, the process engineering team has established a reference point for future analysis. Due to the inclusivity of this study, the team recommends employing a more powerful analytical tool, such as the suggested clustered matrix method, to acquire a more legitimate estimate for the effect of the number of modules.

Other Important Considerations

There are a number of different aspects of the plant that could be considered that may reduce the capital cost and/or the operating costs. The capital cost is currently far too high for the plant to be successful. Several considerations are given below that could reduce the capital cost of the plant.

Capital and Operational Cost Considerations

A major capital cost factor in the plant is the use of 316 stainless steel in the ammonia synthesis loop and storage vessels. The Matches cost correlations accounted for this material directly in the correlations. However, the Towler and Sinnott correlations were mainly for carbon steel with some correlations for 304 stainless steel. Equipment costs determined through the Towler and Sinnott correlations for carbon steel were multiplied by 3x to obtain a cost in 316ss. Subsequently, correlations for 304ss were multiplied by 1.5x to obtain the cost in 316ss. These cost factor additions were justified through the relative cost of each type of material. However, the text by Towler and Sinnott describes on page 332 that the material cost factors relative to carbon steel are 1.3 for both 304ss and 316ss. This means the carbon steel correlations should only be multiplied by 1.3 to obtain the cost in 316ss, and the 304ss correlations are directly applicable to 316ss. However, this contradicts the general consensus that 316ss is more expensive than 304ss, which is due to the presence of molybdenum in 316ss but not in 304ss [43]. Molybdenum is the reason why 316ss is more expensive than 304ss, so the material cost factor shown in the Towler and Sinnott text is concerning. A more detailed investigation into the cost of 316ss relative to carbon steel and 304ss should be performed to justify or change the 3x cost factor relative to carbon steel used here. This could lead to a significant change in the capital cost of the plant.

The initial design of the ammonia synthesis loop used the lower temperature and pressure conditions reported by Brown et. al [15]. This reaction condition was chosen because the yield presented in [15] was closer to the typical single pass conversions presented in the summary article by Pattabathula [12]. The single pass conversion in the reactor means that a larger recycle stream is needed, but equipment does not have to handle as high of a temperature and pressure. It could be beneficial to the module capital or operating costs if the higher single pass conversion is used because the recycle stream can be reduced. However, it is unclear if the higher single pass conversion is actually achievable, and a redesign would be required to determine the capital and operating costs at the different reaction conditions. It is hard to tell how costs would balance between operating at lower flow rates but higher temperature and pressure. It is also hard to tell how equipment costs would change at higher temperature and pressure but lower material throughputs.

The design velocity of the flash drum was lower than the minimum velocity as shown in Appendix I. The upper L:D ratio of 5 for an economical design was decided upon to increase the operating velocity in attempt to reach the minimum required velocity. However, the minimum velocity was never achieved which gives rise to two potential options: increase the L:D ratio until the operational velocity is greater than the minimum velocity or add a holding tank on top of the flash drum. The latter was chosen because an L:D ratio an order of magnitude higher than 5 was needed to achieve the minimum velocity, which would not be economical [21]. A holdup tank above the

flash drum would help increase the operational velocity while maintaining an economical L:D ratio.

An additional consideration when building the plant is to break up some of the larger heat exchangers in the reactor section into smaller ones. This would decrease the large temperature differences in some of the heat exchangers. Large temperature differences could lead to a greater risk during operation if a system component were to fail. In the heat exchanger after the reactor with a hot process air stream that's cooled with the cold recycle stream, hydraulic shock may occur if the hot process stream slows significantly in a process failure event. In addition to that, splitting up some of the larger heat exchangers that use refrigerant would decrease the stress on the systems if a smaller temperature difference between the heat transfer fluid and working fluid are used.

The same idea of breaking up equipment into multiple pieces could be applied to reducing the power load required on the recycle compressor. The current design uses one compressor with a power load of 639 kW, whereas the other compressors in the module rarely need above 100 kW. Using several, smaller compressors may allow for a less expensive compressor type and lower overall energy requirement to perform the same compression.

Intellectual Property Costs

Intellectual property is a concern for the two separation sections of the process: both the electrolysis section and membrane section of the plant. For designing the electrolysis section, ideas from textbooks and scientific journals were used, and properly cited, in the design, though the final design is unique in structure and composition [3, 5, 4, 6]. The electrolysis cell design was not heavily dependent on any source, hopefully leading to minimal intellectual property issues.

Alternatively, the membrane section relied heavily on the research Jiuli Han and her research team of the Chinese Academy of Sciences has conducted on T(*p*-OCH_3)PPCoCl as a porphyrin-based oxygen carrier within a TFC membranes [8]. This study concludes that this method of separating oxygen and nitrogen can be effective, though its scalability is still in question. Regardless of the timeline for developing a refined product, purchasing a membrane using this novel technology (whether using the active carrier in this design or another option) will require the payment of royalties. Since the concern for intellectual property issues was greater for this section, costing for the membrane was based off a PSA alternative in order to evaluate whether the membrane, once purchasable, is a viable option economically. If the cost of the membrane is too high with the added concerns of IP issues, the savvy option may be to switch to a PSA based separation.

In anticipation of IP expenses, a 20% factor was added onto the total amount of sales, as an additional manufacturing cost to account for potential royalties and patents related to these two sections (see *Manufacturing/Operating Costs*). This factor has been added to account for the uncertain amount of intellectual property charges, and to make the manufacturing cost model more conservative.

Conclusions and Recommendations

The primary objective of this project was to generate a preliminary design for a 50 metric ton per day modular ammonia plant. The secondary goal of this preliminary design was to produce anhydrous ammonia without carbon emissions. Both of these goals were achieved in the design. The modular design took the form of five, 10 metric ton per day ammonia synthesis modules. The carbon emission-free design used water electrolysis to produce the high purity hydrogen feed stock and a membrane to form the high purity nitrogen feedstock from air. A traditional, high temperature and pressure Haber-Bosch synthesis loop was used with a modern ruthenium-based catalyst to form ammonia more efficiently. The ruthenium-based catalyst allowed for higher conversion at lower temperature and pressure compared to the original Haber-Bosch catalyst. The design then uses a condensation system and a flash drum to separate the ammonia before being stored at 200 psia.

The total installed cost of the plant was found to $42.4 million when a Lang Factor of 1.7 is used for the modular design. The operating costs for the plant were determined, and a price point of $1,190 per metric ton of ammonia is required to achieve a profit margin of 10%. A wide range of anhydrous ammonia price points were found, and more market analysis is required to determine a competitive price for the Minnesota River Valley area due to the geographical price variations of the product. The market analysis should consider the reduced shipping costs based on the point-of-us design used here. A sensitivity analysis was performed to analyze the price point's dependence on several factors with high uncertainty or high variability. The sensitivity analysis found that the price point is most dependent on the Lang Factor followed by the cost of electricity. The next most important factor analyzed was the number of operators required per shift followed by the profit margin.

The net present value (NPV) analysis of this preliminary design gave very concerning results. The gross annual profit at a profit margin of 10% was found to be $1.97 million. A 20-year MACRS depreciation was used along with a minimum acceptable rate of return of 8% in the NPV analysis. The net present value of this preliminary design was found to be -$21.2 million with an internal rate of return at -0.7%. This means the plant would be extremely unsuccessful in its current state, and significant design changes need to be made in order to reduce the current capital cost and increase the cash flow.

Since a competitive price point for ammonia in the Minnesota River Valley area is currently uncertain, some calculations were done to determine what price point would be required to make the plant successful in its current state. If ammonia can be sold at $1,480 per metric ton—which corresponds to a 30% profit margin—then the plant will have a high enough cash flow to break even after the 20-years of operation with a higher than required rate of return at 10%. However, this price point is likely uncompetitive for the Minnesota River Valley area based on U.S.-wide ammonia prices. It is important to remember that these price point calculations are highly dependent on the Lang Factor and cost of electricity as described in the sensitivity analysis.

A comparison to the current ammonia industry further confirms the two issues with this preliminary design. Giddey et. al. reports energy consumption in current ammonia production at about 38 GJ/mt when using natural gas reformation and about 48 GJ/mt when electrolysis is used

[44]. Pattabathula reports an efficiency as low as 28 GJ/mt [12]. In electricity alone, this preliminary design uses 45 GJ/mt, but this value does not account for the energy used to heat and cool process streams. This would increase the energy used per metric ton by 10-20 GJ/mt, which is higher than the current electrolysis average. A presentation by Linde showed that ammonia production plants can be built for $600k-$700k per metric ton per day capacity, and the per mtpd cost decreases with increasing capacity [45]. This means the 50 metric ton per day design should cost $30-$35 million without considering the cost reduction with increased capacity. This is significantly less than our preliminary cost of $42.4 million. This discrepancy means that certain costs were overestimated in the design process or that the design needs significant reductions in capital costs and energy consumption to meet current ammonia production capabilities.

Future work should begin with a market search to determine competitive price points for the Minnesota River Valley area. Subsequent work should be guided by the Other Important Considerations section. This preliminary design lays the groundwork for a modular ammonia production facility that is free of carbon emissions, but significant work is needed to ensure that the design profitable.

Acknowledgements

We dedicate this work to Dr. Natasha Mallette and Dr. Trevor Carlisle for their dedication and passion for teaching, student learning, and genuine relationships. Without either of you, our undergraduate educations would have been paltry at best. Your examples have set the groundwork for our professionalism and dedication to our craft and the ones we love. You will be missed, but never forgotten.

Bibliography

[1] "Ammonia Market Size Worth $76.64 Billion By 2025," Grand View Research, October 2017. [Online]. [Accessed 1 May 2020].

[2] P. Peng, P. Chen, C. Schiappacasse, N. Zhou, E. Anderson, D. Chen, J. Liu, Y. Cheng, R. Hatzenbeller, M. Addy, Y. Zhang, Y. Liu and R. Ruan, "A review on the non-thermal plasma-assisted ammonia synthesis technologies," *Journal of Cleaner Production,* vol. 177, pp. 597-609, 28 December 2017.

[3] M. Sankir and N. D. Sankir, Hydrogen Production Technologies, Beverly, MA: John Wiley & Sons, 2017.

[4] M. Schalenbach, O. Kasian and K. J. Mayrhofer, "An alkaline water electrolyzer with nickel electrodes enables efficient high current density operation," *International Journal of Hydrogen Energy,* vol. 43, no. 27, pp. 11932-11938, 5 July 2018.

[5] N. Mahmood, Y. Yao, J.-W. Zhang, L. Pan and X. Zhang, "Electrocatalysts for Hydrogen Evolution in Alkaline Electrolytes: Mechanisms, Challenges, and Prospective Solutions," *Advanced Science,* vol. 5, no. 2, February 2018.

[6] J. Genovese, K. Harg, M. Paster and J. Turner, "Current (2009) State-of-the-Art Hydrogen Production Cost Estimate Using Water Electrolysis," 30 September 2009. [Online]. Available: https://www.hydrogen.energy.gov/pdfs/46676.pdf. [Accessed 4 April 2020].

[7] C. A. Grande, "Advances in Pressure Swing Adsorption for Gas Separation," *International Scholarly Research Notices,* vol. 2012, pp. 1-13, 2012.

[8] J. Han, "Highly Selective Oxygen/Nitrogen Separation Membrane Engineered Using a Porphryin-Based Oxygen Carrier," *Membranes,* 2019.

[9] P. McCloskey, *Nitrogen Generator - CGT - Email,* Compressed Gas Technologies, 2020.

[10] M. Malmali, Y. Wei, A. McCormick and E. L. Cussler, "Ammonia Synthesis at Reduced Pressure via Reactive Separation," *Industrial & Engineering Chemistry Research,* vol. 55, p. 8922−8932, 25 July 2016.

[11] H. H. Himstedt, M. S. Huberty, A. V. McCormick, L. D. Schmidt and E. L. Cussler, "Ammonia Synthesis Enhanced by Magnesium Chloride Absorption," *AIChE Journal,* vol. 61, p. 1364–1371, 27 January 2015.

[12] V. Pattabathula and J. Richardson, "Introductino to Ammonia Production," *Chemical Engineering Progress,* September 2016.

[13] M. Reese, C. Marquart, M. Malmali, K. Wagner, E. Buchanan, A. McCormick and E. L. Cussler, "Performance of a Small-Scale Haber Process," *Industrial & Engineering Chemistry Research,* vol. 55, no. 13, pp. 3742-3750, 8 March 2016.

[14] B. Lin, L. Heng, B. Fang, H. Yin, J. Ni, X. Wang, J. Lin and L. Jiang, "Ammonia Synthesis Activity of Alumina-Supported Ruthenium Catalyst Enhanced by Alumina Phase Transformation," *ACS Catalysis,* vol. 9, no. 3, pp. 1635-1644, 2019.

[15] D. E. Brown, T. Edmonds, R. W. Joyner, J. J. McCarroll and S. R. Tennison, "The Genesis and Development of the BP Doubly Promoted Catalyst for Ammonia Synthesis," *Catalyst Letters,* vol. 144, no. 4, pp. 545-552, 2014.

[16] "Ru-Cat 402 CAS: 7440-18-8, Ruthenium on Alumina Catalyst," Vesta Chemicals, [Online]. Available: https://vestachem.com/chemicals/ruthenium-on-alumina-catalyst/. [Accessed 1 May 2020].

[17] N. Mallette and N. AuYeung, *ChE 431 - Chemical Plant Design Lecture Notes,* 2020.

[18] "SEMI-TRAILER DIMENSIONS," B&W Trailer Rental, [Online]. Available: https://www.bwtrailer.com/semi-trailer-dimensions/. [Accessed 1 May 2020].

[19] "Chemical Compatibility Database," Cole-Parmer, [Online]. Available: https://www.coleparmer.com/chemical-resistance. [Accessed 28 April 2020].

[20] Huntsman, "Industrial Coolants and Heat Transfer Fluids," Huntsman, 2013. [Online]. Available: https://www.huntsman.com/performance_products. [Accessed 11 April 2020].

[21] "3rd Year Design Flash System Design," Queens University, 16 October 2008. [Online]. Available: https://chemeng.queensu.ca/courses/integratedDesign/Resources/documents/flashsystemdesign.pdf. [Accessed 5 May 2020].

[22] G. Towler and R. K. Sinnott, Chemical Engineering Design - Principles, Practice and Economics of Plant and Process Design 2nd Edition, Elsevier, 2013.

[23] R. W. Baker, "Gas Separations," in *Membrane Technology and Applications*, John Wiley & Sons, 2004.

[24] D. Oonincx, J. van Itterbeeck, M. J. W. Heetkamp, H. van Den Brand, J. J. A. van Loon and A. van Huis, "An Exploration on Greenhouse Gas and Ammonia Production by Insect Species Suitable for Animal or Human Consumption," *PLoS ONE,* vol. 5, no. 12, p. e14445, 29 December 2010.

[25] C. Clark, "Pollution Control - Expense, or Profit?," Gulf Coast Environmental Systems, 26 September 2018. [Online]. Available: http://www.gcesystems.com/pollution-control-expense-or-profit/. [Accessed 15 April 2020].

[26] US Chemical Safety Board, "CSB Releases New Safety Video Entitled Shock to the System Offering Key Lessons for Preventing Hydraulic Shock in Ammonia Refrigeration Systems," US Chemical Safety Board, 26 March 2015. [Online]. Available: https://www.csb.gov/-csb-releases-new-safety-video-entitled-shock-to-the-system-offering-key-lessons-for-preventing-hydraulic-shock-in-ammonia-refrigeration-systems/. [Accessed 2 April 2020].

[27] Minnesota Department of Agriculture, "Ecological Effects of Ammonia," Minnesota Department of Agriculture, [Online]. Available: https://www.mda.state.mn.us/ecological-effects-ammonia. [Accessed 16 April 2020].

[28] United States Environmental Protection Agency, "Millard Refrigerated Services, LLC Clean Air Act (CAA) Settlement," 2 June 2015. [Online]. Available: https://www.epa.gov/enforcement/millard-refrigerated-services-llc-clean-air-act-caa-settlement. [Accessed 6 April 2020].

[29] "CASE STUDY Heat exchanger rupture and ammonia release in Houston, Texas (One Killed, Six Injured)," January 2011. [Online]. Available: https://www.csb.gov/assets/1/20/case_study.pdf?13960. [Accessed 8 May 2020].

[30] A. A. -. C. A. a. Vacuum, "What are the advantages of using a rotary screw compressor?," Ash Air. [Online]. [Accessed 30 April 2020].

[31] Matches, "Process Equipment Cost," [Online]. Available: https://www.matche.com/equipcost/Compressor.html. [Accessed 3rd May 2020].

[32] R. S. Weber and L. J. Snowden-Swan, "The economics of numbering up a chemical process enterprise," The Journal of Advanced Manufacturing and Processing, 2019. [Online]. Available: https://doi.org/10.1002/amp2.10011.

[33] S. Maracci, "Renewable Energy Prices Hit Record Lows: How Can Utilities Benefit From Unstoppable Solar And Wind?," Forbes Media LLC, 21 January 2020. [Online]. Available: https://www.forbes.com/sites/energyinnovation/2020/01/21/renewable-energy-prices-hit-record-lows-how-can-utilities-benefit-from-unstoppable-solar-and-wind/#1befb5272c84. [Accessed 22 April 2020].

[34] E. R. Merchant , "Average US Wind Price Falls to $20 per Megawatt-Hour," GreenTechMedia, 24 August 2018. [Online]. Available: https://www.greentechmedia.com/articles/read/us-wind-prices-20-megawatt-hour. [Accessed 9 May 2020].

[35] R. Ewing, "ICIS pricing," 10 January 2014. [Online]. Available: https://s3-eu-west-1.amazonaws.com/cjp-rbi-icis-globalassets/fertilizers-ammonia.pdf. [Accessed 8 May 2020].

[36] G. Schnitkey, "farmdocDAILY," 25 September 2018. [Online]. Available: https://farmdocdaily.illinois.edu/2018/09/fertilizer-prices-higher-for-2019-crop.html.

[37] "Liquid Ammonia," Alibaba, [Online]. Available: https://www.alibaba.com/product-detail/Liquid-ammonia-R717_60344159070.html?spm=a2700.galleryofferlist.0.0.107f3c93LpGb8i. [Accessed 13 May 2020].

[38] "10 Benefits of Modular Construction," 2020. [Online]. Available: https://www.green-modular.com/blog/benefits-of-modular-construction.

[39] L. Qiao, "Product modular analysis with design structure matrix using a hybrid approach based on MDS and clustering," *Journal of Engineering Design,* pp. 433-456, 2017.

[40] E. V. Voorthuysen, "Design for scalability of industrial processes using modular components," *Journal of Engineering Manufacture,* pp. 1-15, 2017.

[41] L. Qiao, "PRoduct modular analysis with design structure matrix using a hybrid approach based on MDS and clustering," *Journal of Engineering Design,* pp. 433-456, 2017.

[42] E. v. Voorthuysen, "Design for scalability of industrial processes using modular components," *Journal of Engineering Manufacture ,* pp. 1-15, 2015.

[43] "THE PROS AND CONS OF 304 VS 316 STAINLESS STEEL," Arthur Harris & Co., [Online]. Available: https://arthurharris.com/news/304-vs-316-stainless-steel/. [Accessed 14 May 2020].

[44] S. Giddey, S. Badwal and A. Kulkarni, "Review of electrochemical ammonia production technologies and materials," *International Journal of Hydrogen Energy,* pp. 14576-14594, 12 September 2013.

[45] C. Lalou, "Scaling Down Ammonia Production Modular solutions for constructability," Linde Engineering North America, [Online]. Available: https://www.globalsyngas.org/uploads/downloads/2017-presentations/s1-3-lalou.pdf. [Accessed May 2020].

Appendix I – Equipment Sizing and Costing Calculations

General Equipment Used for All Sections

Compressor Sizing/Costing Calculations

The actual sizes of the compressors were never calculated as the costing correlation used to determine the cost was based only on the power load. For a detailed energy balance used to determine the power load for a desired pressure change, and subsequent temperature change, see the *Energy Balance* section. Because compressors are acknowledged as a common piece of equipment seen in multiple section of the process, for costing, see the *Equipment Cost Summary* section for a detailed explanation of costing using matches.com.

Heat Exchanger Sizing Calculations

The following example for determining the heat exchange area comes from the heat exchanger used to preheat the air entering the membrane section. In order to determine the heat exchange area, the delta temperature log mean must be determined using the differences in temperature at either end of the co-current heat exchanger. The delta at the entrance for both fluids is ΔT_1 while the delta for the exit is denoted as ΔT_2.

$$\Delta T_{lm} = \frac{\Delta T_1 - \Delta T_2}{ln\left(\frac{\Delta T_1}{\Delta T_2}\right)}$$

$$\Delta T_{lm} = \frac{(492\ K - 278\ K) - (291\ K - 283\ K)}{ln\left(\frac{(492\ K - 278\ K)}{(291\ K - 283\ K)}\right)} = 62.85\ K$$

$$\therefore\ \Delta T_{lm} = 62.86\ K = 62.85\ ℃\ an\ estimated\ average\ temperature\ difference$$

Finally, the heat exchanger design equation was used to determine the heat exchange area required. An estimated overall heat transfer coefficient (U) for a liquid and gas system of 418.4 $\frac{kJ}{m^2 * hr * ℃}$ was used. Other heat exchangers in the process featured a liquid transferring heat to another liquid, such systems used an overall heat transfer coefficient of 2092 $\frac{kJ}{m^2 * hr * ℃}$. For a complete list of heat exchanger areas, see the Energy Balance and Utility Section.

$$Q_{HX}\ \frac{kJ}{hr} = U\ \frac{kJ}{m^2 * hr * ℃} * A\ m^2 * \Delta T_{lm}\ ℃$$

$$146141.2\ \frac{kJ}{hr} = 418.4\ \frac{kJ}{m^2 * hr * ℃} * A\ m^2 * 62.85\ ℃$$

$$A\ m^2 = \frac{146141.2\ \frac{kJ}{hr}}{418.4 \frac{kJ}{m^2 * hr * ℃} * 62.85\ ℃} = 5.56\ m^2$$

Because heat exchangers are acknowledged as a common piece of equipment seen in multiple sections of the process, for costing, see the *Equipment Cost Summary* section for a detailed explanation of costing heat exchangers using the Towler and Sinnott correlation method.

Electrolysis Cell Sizing Calculations: Section 100

The material balance around the electrolysis section is the starting point for the sizing calculations for this section. See the Process Flow Diagram and Material Balance section for detailed calculations. The material balance leads to a hydrogen production rate of 43 kmol/hr. Using reaction stoichiometry, this hydrogen value can be used to calculate the total current required across the electrodes for one module. See the calculation below.

Reaction catalyzed at hydrogen electrode: $4H_20 + 4e^- \leftrightarrow 2H_2 + 4OH^-$

$$I = 43 \frac{kmol\ H_2}{hr} * 1000 \frac{mol}{kmol} * \frac{4\ mol\ e^-}{2\ mol\ H_2} * \frac{1\ C}{1.036 * 10^{-5}\ mol\ e^-} * \frac{1\ hr}{3600\ s}$$

$$\therefore I = 2.31 * 10^6\ A$$

As explained in the Process Description for this section, it was assumed that the energy consumption in the electrolysis cell could be calculated with a rate of 5.0 kW-hr/Nm^3 of hydrogen produced. This energy rate is known to be a conservative estimate for electrolysis cells operating at current densities of 0.5 – 1.0 A/cm^2 [3]. Therefore, this mode of operation was assumed (0.5 A/cm^2) and used to calculate the required active electrode surface area. Also, the electrodes for the electrolysis cell were designed as pure nickel meshes, treated with a hot-dip-galvanization technique in molten zinc [4]. As explained in the Process Description, this technique leads to a ten-fold decreased geometric electrode surface area. See the surface area calculation below, which is based on the current calculated above, and the assumed value for current density.

$$A = \frac{2.31 * 10^6 A}{0.5\ A/cm^2} * \left(\frac{1\ m}{100\ cm}\right)^2 = 461\ m^2$$

$$\therefore A_{geometric} = 5\ m^2 \text{ (after the factor of 10 reduction)}$$

With the geometric electrode area known, the dimensions of the electrolysis cell can now be calculated. The electrolysis system for one module was designed as a cube, with multiple electrolysis cells stacked side-by-side. A system of equations was set up so the width of all cells combined was equal to the length and height of one cell (creating a cube shape). Also constrained within the equations, the number of cells multiplied by the geometric area of one electrode is set equal to 5 m^2. Only one side of each electrode is considered, as it has been observed that the

catalytic activity of the inner portion of the electrode (facing the other electrode) is much higher than that of the outer portion [5]. See below the system of equations, and their solution. The side lengths were rounded up from 2.15 m to 2.30 m to provide space for the electrodes at the edges of the tank, and to provide headspace above each electrode (making the cell taller than the electrodes themselves).

$$x = y = z \text{ (dimensions of cube)}$$

$$x = n * 0.2\ m \text{ (x = width, n = number of cells)}$$

$$n * x^2 = 5\ m^2 \text{ (area of all electrodes)}$$

$$\therefore x = 2.15\ m, \qquad n = 11$$

The methods for determining capital costs and operating costs for the electrolysis cell are shown and explained in the Electrolysis Costing Summary and Electrolysis Cell Energy Balance sections, respectively.

Membrane: Section 200

As previously discussed, an Excel solver function was used in conjunction with a material balance for the membrane to estimate a required surface area of membrane to achieve the desired separation. The process engineering team decided that a membrane in the shape of a tube (or pipe) would allow for consistent separation continuously operating, an efficient use of space, and a simple way to dispose of the waste permeate stream (composed only of oxygen and nitrogen). The estimated required surface area according to Excel and the material balance is 500 m^2, but because of the membrane's geometry, it was assumed that the specific surface area would increase by a factor of 100. Therefore, the membrane tube requires 5 m^2 of internal surface area in order to accomplish the molar flows defined in Table 2. This internal surface area was used to determine the length of pipe needed. A small pipe diameter of 6 cm (close to 2") was selected in order to ensure consistent diffusion which could be lost as the diameter increases due to inertial focusing.

$$A_i\ cm^2 = 50\ m^2 \left(\frac{100\ cm}{1\ m}\right)^2 = 500{,}000\ cm^2$$

$$L_p\ cm = \frac{A_i\ cm^2}{(r\ cm) * 2\pi} = \frac{500{,}000\ cm^2}{(3\ cm) * 2\pi} = 26{,}600\ cm$$

$$L_p\ m = 26{,}600\ cm \left(\frac{1\ m}{1000\ cm}\right) = 26.6\ m$$

$$\therefore \boldsymbol{L_p = 26.6\ m}$$

While costing for the membrane was based on a quote, if we are ultimately able to get access and purchase this particular membrane, it will likely be sold on the basis of total volume or mass. As a conservative estimate, a pipe length of 27 m will be used to determine the volume of membrane required when the thickness is 0.01 cm (0.0001 m).

$$V_m = \pi(r+t)^2 L_p - \pi(r^2)L_p$$

$$V_m = \pi(0.03\ m + 0.0001\ m)^2(26.6\ m) - \pi(0.03\ m)^2(26.6\ m) = 5.02 * 10^{-4}\ m^3$$

$$V_m\ cm^3 = 5.02 * 10^{-4} m^3 \left(\frac{100\ cm}{1\ m}\right)^3 = 502\ cm^3$$

$$\therefore \boldsymbol{V_m = 502\ cm^3}$$

Although the density of the membrane used in this system was not found during literature review, most membranes have a density close to 1 $\frac{g}{cm^3}$.

$$m_m = (V\ cm^3)\left(\rho\ \frac{g}{cm^3}\right) = (502\ cm^3)\left(1\frac{g}{cm^3}\right) = 502\ g$$

$$\therefore \boldsymbol{m_m = 502\ g}$$

No calculations were performed to determine the size of the pretreatment system which includes a filtration system and desiccant. It was assumed that a simple, in-line apparatus could be installed and replaced as needed without a significant effect on price. For sizing the heat exchanger and compressor that precede the membrane section, see *General Equipment Used for all Sections*, above.

Ammonia Synthesis Reactor Sizing Calculations

A thorough literature review lead to a reactor kinetics used in the sizing and design of the ammonia synthesis reactor – see Process Description section [15], [14]. The final catalyst choice was the promoted ruthenium based catalyst. Reaction conditions were chosen to be 86 bar and 380 °C, which gave a 26% yield in the article from Brown and others [15]. A more conservative single-pass conversion of 20% was used in the final design parameters, and a hydrogen to nitrogen ratio of 3:1 (stoichiometric) was used as well based on Pattabathula [12]. An appropriate reaction rate for the promoted ruthenium catalyst was determined to be 9.5 $\frac{mmol\ NH_3}{g_{cat} * hr}$ from the article by Lin et. al. [14]. A more in-depth discussion of these design choices is presented in the Process Description section.

Based on the material balance and ammonia production requirements of 10 metric ton per day per module, the reactor must take on a 56.2 kmol/hr feed of nitrogen and a total of feed of 281 kmol/hr. The mass of catalyst required to achieve the 20% single pass conversion based on the reaction rate was determined from the following equation [17]:

$$m_{cat} = \frac{F_{N_2,2} X_{N_2}}{r_{NH_3}}$$

Where m_{cat} is the required mass of catalyst in the reactor, $F_{N_2,2}$ is the molar flow rate of nitrogen fed to the reactor, X_{N_2} is the single pass conversion of nitrogen in the reactor, and r_{NH_3} is the rate of formation of ammonia in the presence of the catalyst. Inserting values gives the following result.

$$m_{cat} = \frac{\left(56.2\frac{kmol\ N_2}{hr}\right)(0.20)}{\left(9.5\frac{mmol\ NH_3}{g_{cat} * hr}\right)\left(\frac{1\ kmol\ N_2}{2\ kmol\ NH_3}\right)\left(\frac{1000\ g_{cat}}{1\ kg_{cat}}\right)\left(\frac{1\ kmol}{10^6 mmol}\right)} = 2{,}365\ kg\ of\ catalyst$$

An axial-radial reactor is typically used in ammonia synthesis to limit the pressure drop through the reactor [12]. Here, catalyst tubes will be used that allow the reactant feed to flow into the tubes and react on the catalyst before flowing radially out of the tubes and then out of the reactor. Many tubes will be used to keep the reactor footprint small. A size comparison will be shown here as well. The shell diameter of the multitube reactor design is determined with the following equations [17].

$$D_s = d_{tube}\sqrt{\frac{n_{tube}}{\Phi}}$$

And,

$$\Phi = \frac{\pi}{2\alpha^2\sqrt{3}}$$

Where D_s is the diameter of the reactor shell, Φ is the fraction of perforation, α is the tube spacing coefficient, n_{tube} is the number of tubes, and d_{tube} is the diameter of one tube. The number of tubes was determined by first choosing a catalyst tube diameter of 10 cm. The catalyst bulk density was found to be approximately 850 kg/m^3 based on the ruthenium on alumina catalyst sold by Vesta Chemicals [16]. The number of tubes needed to accommodate the mass of catalyst in the reactor was determined as follows.

$$n_{tubes} = \frac{\pi d_{tube}^2 L_{tube}}{4}\rho_{cat}$$

Where L_{tube} is the length of the catalyst tubes and ρ_{cat} is the density of the catalyst. A tube length of 2 m was chosen as an appropriate size for shipping and short tube length to more accurately represent an axial-radial catalytic reactor. Thus, the number of tubes is…

$$n_{tubes} = \frac{\pi(0.10\ m)^2(2.0\ m)}{4}\left(850\frac{kg}{m^3}\right) = 178\ tubes$$

A tube spacing coefficient of 1.5 was chosen as the final parameter needed to size the reactor shell. This means the spacing between the center of each tube is $1.5d_{tube}$. The fraction of perforation was determined to be…

$$\Phi = \frac{\pi}{2(1.5)^2\sqrt{3}} = 0.403$$

And the shell diameter was determined to be…

$$D_s = (0.10\ m)\sqrt{\frac{178}{0.403}} = 2.10\ m$$

The total length of the reactor was determine by assuming the ends were hemispherical, and one shell diameter length was added to the tube length to determine the total reactor length, L.

$$L = L_{tube} + D_s$$

$$L = 2.00\ m + 2.10\ m = 4.10\ m$$

The total volume of the reactor can now be determined as a cylinder the length of the tube section with two hemispherical ends. The hemispherical ends combine to be the volume of a sphere of diameter D_s.

$$V_{reactor} = \frac{\pi D_s^2 L_{tube}}{4} + \frac{4\pi\left(\frac{D_s}{2}\right)^3}{3}$$

$$V_{reactor} = \frac{\pi(2.10\ m)^2(2.00\ m)}{4} + \frac{4\pi(1.05\ m)^3}{3} = 11.8\ m^3$$

This reactor would then be jacketed to remove the heat of reaction during normal operation.

A reactor size calculation was also performed to show the difference in reactor footprint if a single catalyst-filled tube were used in an axial-radial reactor. Using the same bulk density and required mass of catalyst, the total volume of catalyst required is…

$$V_{cat} = \frac{m_{cat}}{\rho_{cat}}$$

$$V_{cat} = \frac{2365\ kg_{cat}}{850\frac{kg_{cat}}{m_{cat}^3}} = 2.78\ m_{cat}^3$$

The same 2.00 m catalyst bed length will be used, so the single catalyst bed diameter would then be…

$$D_{bed} = \left(\frac{4V_{cat}}{\pi L_{bed}}\right)^{0.5}$$

$$D_{bed} = \left(\frac{4(2.78\ m_{cat}^3}{\pi(2.0\ m)}\right)^{0.5} = 1.33\ m$$

From here, two different shell diameters were calculated to show the reactor volume dependence on the shell diameter. For a larger approximation, the shell diameter was chosen to be 2x times larger than the bed diameter, and for smaller approximation the shell diameter was chosen to be 1.5x times larger than the bed diameter. This gave a large and small shell diameter of 2.66 m and 2.00 m, respectively. Assuming the same hemispherical end design, the reactor volumes were determined as follows.

$$V_{reactor} = \frac{\pi D_s^2 L_{tube}}{4} + \frac{4\pi\left(\frac{D_s}{2}\right)^3}{3}$$

$$V_{reactor,large} = \frac{\pi(2.66\ m)^2(2.00\ m)}{4} + \frac{4\pi(1.33\ m)\text{^}3}{3} = 21.0\ m^3$$

$$V_{reactor,small} = \frac{\pi(2.00\ m)^2(2.00\ m)}{4} + \frac{4\pi(1.00\ m)\text{^}3}{3} = 10.4\ m^3$$

Ammonia Synthesis Reactor Costing Calculations

Three different costing methods were used for the reactor. Ultimately, the Matches online cost correlation for a jacketed, non-agitated reactor was used because it was a middle ground between the two other cost correlation results [31]. The other two methods were both from correlation presented in the textbook by Towler and Sinnott [22].

The first method from Towler and Sinnott was a cost correlation for a jacketed, agitated reactor, which was the closest similarity of the two reactor cost correlations presented in the text. The cost correlation is based on reactor volume with an applicable range of 0.5-100 m^3 – which the reactor falls within. The purchase cost with this method was determined with the following calculation.

$$C_{e,2010} = a + bS^n$$

$$C_{e,2010} = 61{,}500 + 32{,}500(11.8\ m^3)^{0.8} = \$296{,}000$$

The Towler and Sinnott cost correlations give purchase cost in 2010 dollars, so the purchase cost must be adjusted to 2019. The CEPCI for 2010 is 532.9 and the CEPCI for Oct. 2019 is 599.5 [17], [22]. Now the purchase cost can be adjusted to Oct. 2019 dollars.

$$C_{e,2019} = C_{e,2010}\frac{CEPCI_{2019}}{CEPCI_{2010}}$$

$$C_{e,2019} = (\$296{,}000)\left(\frac{599.5}{532.9}\right) = \$332{,}000$$

This cost method is inaccurate for this reactor because the cost correlation is not dependent on operating pressure or material of construction, and the correlation is for an agitated reactor when this reactor is not agitated. Next, the reactor was cost as a horizontal pressure vessel using the correlation in Towler and Sinnott. The correlations was for 304 ss, which was then converted to 316 ss.

The shell mass had to be determined first to use this cost correlation. Hoop stress and longitudinal stress calculations were performed to determine reactor shell thickness – see the pressure vessel calculations for an example of these calculations. An operating pressure of 1,210 psi and design pressure of 1,410 psi gave a required thickness of 15.5 cm thick 316 ss. This gave a total shell mass of 17,000 kg, which allowed for the following cost calculation to be performed which has an applicable range of 120-50,000 kg of 304 ss [22].

$$C_{e,2010} = a + bS^n$$

$$C_{e,2010} = 12{,}800 + 240(17{,}000\ kg)^{0.9} = \$1{,}550{,}000$$

Next, this value must be converted to 316 ss by multiplying the 304 ss cost by 1.5, and then the value must be converted to Oct. 2019 dollars.

$$C_{e,2010,316ss} = \$2{,}330{,}000$$

$$C_{e,2019,316ss} = (\$2{,}330{,}000)\left(\frac{599.5}{532.9}\right) = \$2{,}620{,}000$$

This cost seems extremely high, and the correlation likely includes considerations specific to pressure vessels rather than reactors. This lead to the Matches online cost correlations for jacketed, non-agitated reactors [31]. The material of construction could be chosen as 316 ss in this correlation, and the cost is dependent of reactor pressure. The design pressure of 1,410 psi could not be selected, but costs for internal pressures of 300 psi, 600 psi, and 900 psi could be obtained. These values were then plotted to determine if the correlation was linear or not, and if the cost could be extrapolated to the design pressure.

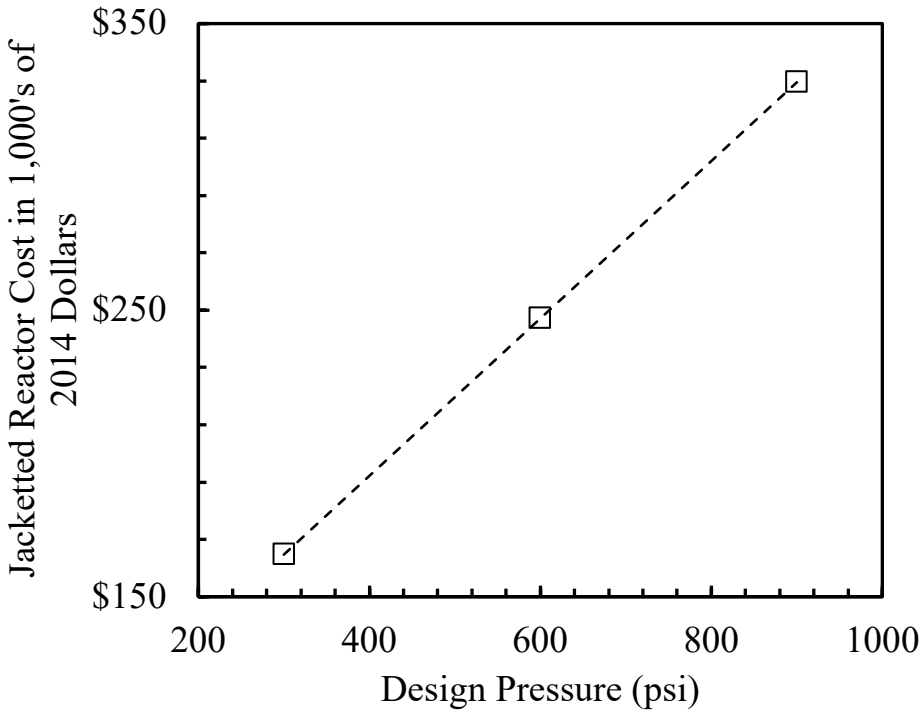

Figure 5: Cost of an jacketed, non-agitated reactor in 2014 dollars based on internal reactor pressure from Matches online cost correlations **[31]**. Reactor cost is for 316 ss, and the cost is shown in 1,000's of dollars. The trendline had an R^2 value of 1.

The trendline for this cost data was perfectly linear with an R^2 value of 1, which supports the viability of extrapolating this data the design pressure. However, this may be a sign that the cost correlation lacks some rigor. An equation for the line of fit to this data was determined and used to calculate the cost at the design pressure of 1,410 psi. The Matches online cost correlations are in 2014 dollars when the CEPCI was 576.1 according to chemengonline.com [17].

$$C_{e,2014} = 275P + 82{,}300$$

$$C_{e,2014} = 275(1{,}410\ psi) + 82{,}300 = \$469{,}000$$

$$C_{e,2019} = (\$469{,}000)\left(\frac{599.5}{576.1}\right) = \$488{,}000$$

The purchase cost of the reactor was chosen to be this value, $488,000, because the Matches online cost correlation equipment description most closely matches the reactor being described here. This value also seemed to be a balance between the low value given by the Towler and Sinnott reactor correlation and the extremely high value of the horizontal pressure vessel correlation also from Towler and Sinnott [22].

Flash Drum Sizing and Costing

The flash drum was designed to produce the specified 99.5 weight percent minimum ammonia production rate of 50,000 metric tons. The flash drum was sized to hold 30 minutes of inlet volume ($t_{storage}$) to ensure safe operation [21]. The Aspen HYSYS simulation provided the inlet volumetric flow basis of 8.2 sm^3/hr ($\dot{V}_{Flash\ Drum\ Inlet}$).

$$V_{Flash\ Drum} = \dot{V}_{Flash\ Drum\ Inlet} t_{storage}$$

$$V_{Flash\ Drum} = 8.2 \frac{sm^3}{hr} * \frac{30\ \text{min}}{60 \frac{\text{min}}{\text{hr}}} = 4.1\ m^3$$

The diameter and length of the vessel were calculated from these specifications, along with an economical L:D ratio of 5:1 [21]. The Excel Solver software was used to solve the following system of equations.

$$V_{Flash\ Drum} = \pi \left(\frac{D_{Flash\ Drum}}{2} \right)^2 L_{Flash\ Drum}$$

$$L_{Flash\ Drum} = 5 D_{Flash\ Drum}$$

$$\therefore L_{Flash\ Drum} = 5.1\ m, D_{Flash\ Drum} = 1.0\ m$$

For costing of the flash drum, please see the correlation in the next section below used for costing the storage vessel. The material of construction was assumed to be stainless steel 316L and the welding efficiency was assumed to be 80%.

The cross sectional area was calculated based upon the L:D ratio of 5, but additional calculations were performed to ensure that the operating velocity is between the minimum and maximum allowable velocity. The correlations are based upon the density of the vapor and liquid phases and an empirical factor—k—which is based upon whether the system has a mesh pad or not [21]. The system was assumed to not have a mesh pad because it would generate a large pressure drop, which means that the k value was 576 m/hr. The density of each phase was obtained from an Aspen HYSYS simulation of the system (Appendix II).

$$v_{max} = k \sqrt{\left(\frac{\rho_{Liquid} - \rho_{vapor}}{\rho_{vapor}} \right)}$$

$$v_{max} = 576 \frac{m}{hr} \sqrt{\frac{673 \frac{kg}{m^3} - 6.35 \frac{kg}{m^3}}{6.35 \frac{kg}{m^3}}} \frac{1hr}{3600s}$$

$$v_{max} = 1.6 \frac{m}{s}$$

The minimum and design velocity are about 10% and 75% of the maximum velocity [21]. The cross sectional area and volumetric fluid flow rate provided from previous calculations and Aspen HYSYS were used to calculate the velocity going through the system designed with an L:D of 5.

$$v_{min} = 0.1 v_{max}$$

$$v_{design} = 0.75 v_{max}$$

$$v_{L:D=5} = \frac{\dot{V}_{Flash\ Drum}}{\pi \left(\frac{D_{Flash\ Drum}}{2}\right)^2}$$

$$v_{min} = 0.1 \left(1.6 \frac{m}{s}\right) = 0.16 \frac{m}{s}$$

$$v_{design} = 0.75 \left(1.6 \frac{m}{s}\right) = 1.23 \frac{m}{s}$$

$$v_{L:D=5} = \frac{8.15 \frac{m^3}{hr}}{\pi \left(\frac{1.0m}{2}\right)^2} = 0.003 \frac{m}{s}$$

Since the velocity at an L:D of 5 is less than the minimum required velocity, a holding tank on the top of the flash drum should be used to maintain an economical and safe L:D ratio [21].

Storage Vessel Sizing Calculations

As discussed in the Process Description for Ammonia Storage Vessels, this section of the 10 mtpd modular plant was designed to contain 70 metric tons of ammonia, with 85% of the tank volume used for the product. The Maximum Allowable Working Pressure was specified at 250 psig, leading to a safe design pressure of 275 psig. Grade 316 stainless steel was defined as the material of construction (its tensile strength is 20 ksi), a welding efficiency of 0.8 was assumed, and a 2.0 mm corrosion buffer was used. The vessel size was defined as 2.5 m in diameter and 7.5 m in height, so each vessel could feasibly be transported via truck.

The first step in sizing the storage vessels is determining the volume of liquid storage-space needed. Assuming a conservative (low) value for the density of ammonia, 578.8 kg/m^3 (saturated liquid at 40 °C), the volume required for the ammonia product is calculated as follows.

$$V_{liq} = 70000\ kg * \frac{1\ m^3}{578.8\ kg} = 121\ m^3$$

Next, we employ the 85% liquid storage space value to calculate the total contained volume.

$$V_{contained} = (121\ m^3\ liquid) * \left(\frac{1\ m^3\ total}{0.85\ m^3\ liquid}\right) = 142\ m^3$$

The vessel dimensions were already defined, so we can use these to determine how many vessels are needed to meet the volume requirement, as shown below.

$$V_{vessel} = \pi * \left(\frac{D}{2}\right)^2 * H = \pi * (1.25\ m)^2 * 7.5\ m = 37\ m^3$$

$$n_{vessels} = \frac{V_{contained}}{V_{vessel}} = \frac{142\ m^3}{37\ m^3} = 3.8 \rightarrow 4\ vessels\ required$$

Next, the pressure, diameter, tensile strength, and welding efficiency are used to calculate minimum wall thickness requirements based on hoop-stress and longitudinal-stress.

$$Hoop\ Stress\ Equation:\ t_{wall} = \frac{P_i * D}{2 * S * E - 1.2 * P_i}$$

$$Longitudinal\ Stress\ Equation:\ t_{wall} = \frac{P_i * D}{4 * S * E + 0.8 * P_i}$$

$$where, \quad P_i = internal\ gauge\ pressure, \quad D = diameter, \quad S = tensile\ strength,$$

$$and\ E = welding\ efficiency$$

Plugging in values and accounting for corrosion safety factor…

$$t_{wall,hoop} = \frac{(275\ psi) * (2.5\ m)}{(2 * 20000\ psi * 0.8) - (1.2 * 275\ psi)} = 0.022\ m$$

$$t_{wall,longitudinal} = \frac{(275\ psi) * (2.5\ m)}{(4 * 20000\ psi * 0.8) + (0.8 * 275\ psi)} = 0.011\ m$$

$$\therefore t_{wall,safe} = 0.022\ m + 0.002\ m = 0.024\ m = 24\ mm$$

With the wall thickness known, the shell volume and mass can be calculated as shown below.

$$Surface\ Area, A = 2 * \pi * \left(\frac{D}{2}\right)^2 + \pi * D * H$$

$$\therefore A = 69\ m^2$$

$$V_{shell} = A * t_{wall,safe} = (69\ m^2) * (0.024\ m) = 1.6\ m^3$$

Now, plugging in the density of 316 stainless steel, the shell mass is calculated

$$m_{shell} = V_{shell} * \rho_{shell} = 1.6\, m^3 * \frac{8030\ kg}{m^3} = 13100\ kg$$

Storage Vessel Costing Calculations

Similar to the costing calculations for compressors—see Equipment Cost Summary, Compressor Costing—the capital cost of the storage vessels was estimated using a model from matches.com. The specific model used for the storage vessels is called "Vessel: Column, No Internals, Medium." This model gives a range of 1000 to 70000 pounds (shell mass), and this range contains the mass of the shells designed in this project (see unit conversion below). The model from matches.com also provides estimates for multiple materials of construction, conveniently including stainless steel 316. See the outlined costing calculation below.

The input on the website is "vessel weight" in pounds.

$$m_{shell} = 13100\ kg * \frac{2.205\ lb}{kg} = 29000\ lbs$$

$$29000\ lb\ vessel \xrightarrow{medium,\ \ stainless\ steel\ 316} \$247{,}300\ in\ 2014$$

Now, correcting for the 2014 costing index…

$$C_{e,2019} = \left(C_{e,2014}\right)\left(\frac{CEPCI_{2020}}{CEPCI_{2014}}\right)$$

$$C_{e,2020} = (\$247{,}300)\left(\frac{599.5}{576.1}\right) = \$257{,}000\ in\ 2020$$

Appendix II – Aspen HYSYS Flow Sheet and Stream Tables

Figure 6: Includes the Aspen HYSYS flow sheet and stream tables for all the system components in the ammonia synthesis and separation section s of the process.

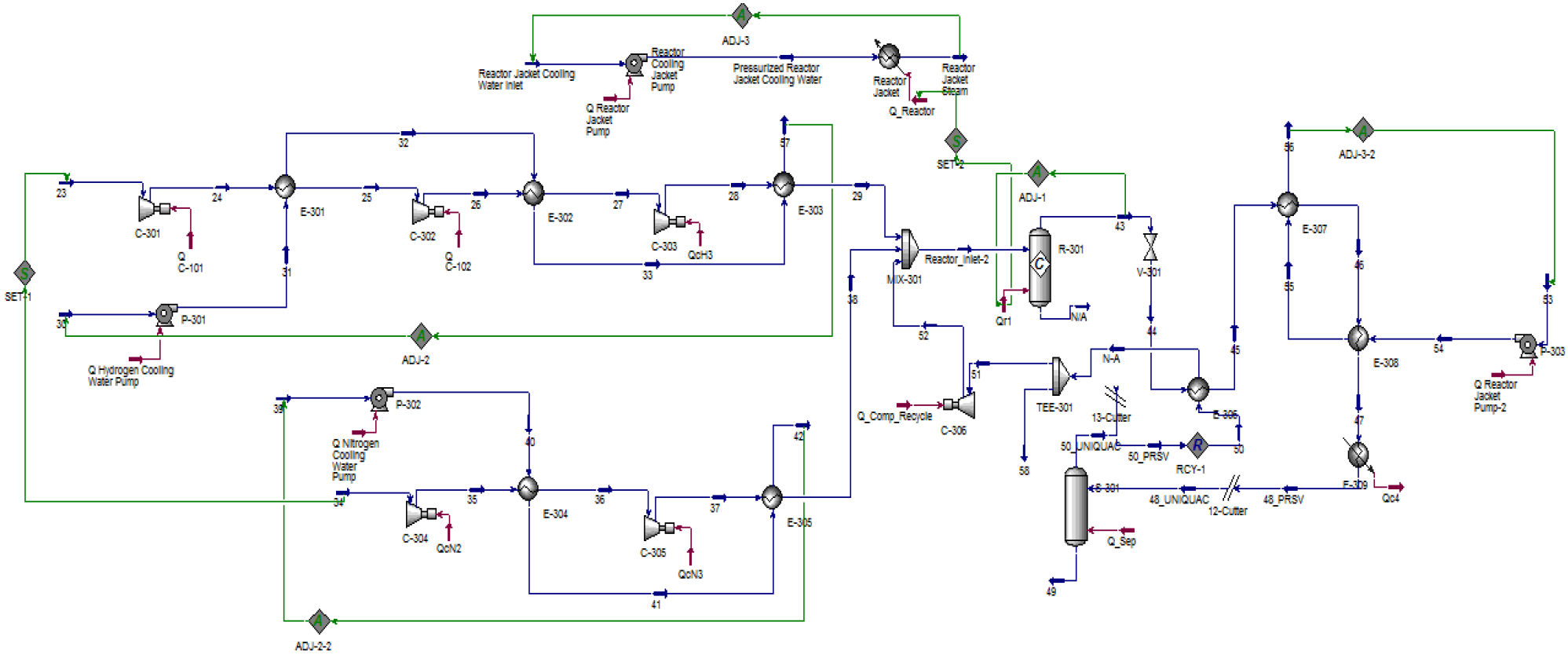

Material Streams

		23	34	35	36	37	43	N/A	48_PRSV	49	50_UNIQUAC	48_UNIQUAC	50_PRSV
Vapour Fraction		1.0000	1.0000	1.0000	1.0000	1.0000	1.0000	0.0000	1.0000	0.0000	1.0000	1.0000	0.9981
Temperature	C	80.00	18.00	411.4	270.0	436.1	380.0	380.0	-16.01	-33.15	-33.15	-16.01	-33.15
Pressure	bar	1.013	4.170	43.00	43.00	86.00	86.00	86.00	13.79	13.79	13.79	13.79	13.79
Molar Flow	kgmole/h	49.50	16.50	16.50	16.50	16.50	272.9	0.0000	272.9	27.40	245.5	272.9	245.5
Mass Flow	kg/h	99.79	462.2	462.2	462.2	462.2	2725	0.0000	2725	466.6	2259	2725	2259
Liquid Volume Flow	m3/h	1.428	0.5732	0.5732	0.5732	0.5732	8.151	0.0000	8.151	0.7575	7.394	8.151	7.394
Heat Flow	kJ/h	7.764e+004	-3916	1.925e+005	1.198e+005	2.059e+005	8.853e+005	0.0000	-2.502e+006	-1.948e+006	-1.325e+006	-2.505e+006	-1.333e+006
		24	26	28	25	27	Reactor_Inlet-2	38	29	50	45	N-A	52
Vapour Fraction		1.0000	1.0000	1.0000	1.0000	1.0000	1.0000	1.0000	1.0000	0.9981	1.0000	1.0000	1.0000
Temperature	C	448.7	449.6	442.8	150.0	170.0	380.0	380.0	380.0	-33.15	290.6	74.44	380.2
Pressure	bar	6.500	25.50	86.00	6.500	25.50	86.00	86.00	86.00	13.79	86.00	13.79	86.00
Molar Flow	kgmole/h	49.50	49.50	49.50	49.50	49.50	301.2	16.50	49.50	244.9	272.9	244.9	235.2
Mass Flow	kg/h	99.79	99.79	99.79	99.79	99.79	2725	462.2	99.79	2253	2725	2253	2163
Liquid Volume Flow	m3/h	1.428	1.428	1.428	1.428	1.428	9.083	0.5732	1.428	7.374	8.151	7.374	7.082
Heat Flow	kJ/h	6.083e+005	6.114e+005	6.071e+005	1.774e+005	2.077e+005	2.370e+006	1.765e+005	5.156e+005	-1.330e+006	9.534e+004	-5.400e+005	1.678e+006
		58	51	46	56	47	Reactor Jacket Steam	32	33	57	31	30	40
Vapour Fraction		1.0000	1.0000	1.0000	1.0000	1.0000	1.0000	0.3053	0.8699	1.0000	0.0000	0.0000	0.0000
Temperature	C	74.44	74.44	246.9	152.0	182.9	152.0	162.0	157.2	152.0	20.06	20.00	20.07
Pressure	bar	13.79	13.79	13.79	5.000	13.79	5.000	6.500	5.750	5.000	7.250	1.013	6.500
Molar Flow	kgmole/h	9.722	235.2	272.9	19.74	272.9	29.68	19.48	19.48	19.48	19.48	19.48	2.147
Mass Flow	kg/h	89.43	2163	2725	355.6	2725	534.7	351.0	351.0	351.0	351.0	351.0	38.68
Liquid Volume Flow	m3/h	0.2928	7.082	8.151	0.3563	8.151	0.5357	0.3517	0.3517	0.3517	0.3517	0.3517	3.876e-002
Heat Flow	kJ/h	-2.144e+004	-5.188e+005	-2.964e+005	-4.693e+006	-8.430e+005	-7.056e+006	-5.127e+006	-4.724e+006	-4.632e+006	-5.558e+006	-5.559e+006	-6.125e+005
		39	41	42	Pressurized Reactor Jacket Cooling Water	Reactor Jacket Cooling Water Inlet	53	54	55	44			
Vapour Fraction		0.0000	0.6290	1.0000	0.0000	0.0000	0.0000	0.0000	0.4631	1.0000			
Temperature	C	20.00	157.2	152.0	20.04	20.00	20.00	20.05	157.2	381.7			
Pressure	bar	1.013	5.750	5.000	5.750	1.013	1.013	6.500	5.750	13.79			
Molar Flow	kgmole/h	2.147	2.147	2.147	29.68	29.68	19.74	19.74	19.74	272.9			
Mass Flow	kg/h	38.68	38.68	38.68	534.7	534.7	355.6	355.6	355.6	2725			
Liquid Volume Flow	m3/h	3.876e-002	3.876e-002	3.876e-002	0.5357	0.5357	0.3563	0.3563	0.3563	8.151			
Heat Flow	kJ/h	-6.125e+005	-5.397e+005	-5.104e+005	-8.466e+006	-8.467e+006	-5.631e+006	-5.631e+006	-5.084e+006	8.853e+005			

Compositions

	23	34	35	36	37	43	N/A	48_PRSV	49	50_UNIQUAC	48_UNIQUAC	50_PRSV
Comp Mole Frac (Hydrogen)	1.0000	0.0000	0.0000	0.0000	0.0000	0.6206	0.6206	0.6206	0.0002	0.6898	0.6206	0.6898
Comp Mole Frac (Nitrogen)	0.0000	1.0000	1.0000	1.0000	1.0000	0.2068	0.2069	0.2068	0.0001	0.2299	0.2068	0.2299
Comp Mole Frac (Ammonia)	0.0000	0.0000	0.0000	0.0000	0.0000	0.1726	0.1725	0.1726	0.9997	0.0803	0.1726	0.0803
Comp Mole Frac (Oxygen)	0.0000	0.0000	0.0000	0.0000	0.0000	0.0000	0.0000	0.0000	0.0000	0.0000	0.0000	0.0000
Comp Mole Frac (H2O)	0.0000	0.0000	0.0000	0.0000	0.0000	0.0000	0.0000	0.0000	0.0000	0.0000	0.0000	0.0000
	24	26	28	25	27	Reactor_Inlet-2	38	29	50	45	N-A	52
Comp Mole Frac (Hydrogen)	1.0000	1.0000	1.0000	1.0000	1.0000	0.7030	0.0000	1.0000	0.6898	0.6206	0.6898	0.6898
Comp Mole Frac (Nitrogen)	0.0000	0.0000	0.0000	0.0000	0.0000	0.2343	1.0000	0.0000	0.2299	0.2068	0.2299	0.2299
Comp Mole Frac (Ammonia)	0.0000	0.0000	0.0000	0.0000	0.0000	0.0627	0.0000	0.0000	0.0803	0.1726	0.0803	0.0803
Comp Mole Frac (Oxygen)	0.0000	0.0000	0.0000	0.0000	0.0000	0.0000	0.0000	0.0000	0.0000	0.0000	0.0000	0.0000
Comp Mole Frac (H2O)	0.0000	0.0000	0.0000	0.0000	0.0000	0.0000	0.0000	0.0000	0.0000	0.0000	0.0000	0.0000
	58	51	46	56	47	Reactor Jacket Steam	32	33	57	31	30	40
Comp Mole Frac (Hydrogen)	0.6898	0.6898	0.6206	0.0000	0.6206	0.0000	0.0000	0.0000	0.0000	0.0000	0.0000	0.0000
Comp Mole Frac (Nitrogen)	0.2299	0.2299	0.2068	0.0000	0.2068	0.0000	0.0000	0.0000	0.0000	0.0000	0.0000	0.0000
Comp Mole Frac (Ammonia)	0.0803	0.0803	0.1726	0.0000	0.1726	0.0000	0.0000	0.0000	0.0000	0.0000	0.0000	0.0000
Comp Mole Frac (Oxygen)	0.0000	0.0000	0.0000	0.0000	0.0000	0.0000	0.0000	0.0000	0.0000	0.0000	0.0000	0.0000
Comp Mole Frac (H2O)	0.0000	0.0000	0.0000	1.0000	0.0000	1.0000	1.0000	1.0000	1.0000	1.0000	1.0000	1.0000
	39	41	42	Pressurized Reactor Jacket Cooling Water	Reactor Jacket Cooling Water Inlet	53	54	55	44			
Comp Mole Frac (Hydrogen)	0.0000	0.0000	0.0000	0.0000	0.0000	0.0000	0.0000	0.0000	0.6206			
Comp Mole Frac (Nitrogen)	0.0000	0.0000	0.0000	0.0000	0.0000	0.0000	0.0000	0.0000	0.2068			
Comp Mole Frac (Ammonia)	0.0000	0.0000	0.0000	0.0000	0.0000	0.0000	0.0000	0.0000	0.1726			
Comp Mole Frac (Oxygen)	0.0000	0.0000	0.0000	0.0000	0.0000	0.0000	0.0000	0.0000	0.0000			
Comp Mole Frac (H2O)	1.0000	1.0000	1.0000	1.0000	1.0000	1.0000	1.0000	1.0000	0.0000			

Energy Streams

		QcN2	QcN3	Qr1	Qc4	Q C-101	Q C-102	QcH3
Heat Flow	kJ/h	1.964e+005	8.609e+004	-1.485e+006	1.659e+006	5.306e+005	4.340e+005	3.995e+005
		Q_Comp_Recycle	Q_Reactor	Q_Sep	Q Hydrogen Cooling Water Pump	Q Nitrogen Cooling Water Pump	Q Reactor Jacket Pump	Q Reactor Jacket Pump-2
Heat Flow	kJ/h	2.197e+006	1.411e+006	-7.683e+005	288.7	31.09	334.0	257.3

Appendix III – Other Supplementary Information

Calculations for the Heat Evolved in the Reactor

The heat evolved from the ammonia synthesis reaction is -91.8 kJ/mol at standard temperature and pressure (via the NIST online webbook). A hypothetical path is required to determine the enthalpy change in the reactor during steady state operation. The figure below shows the hypothetical path used here to determine the heat evolved in the reactor for the ammonia synthesis reaction.

$$3H_{2(g)} + N_{2(g)} \Leftrightarrow 2NH_{3(g)}$$

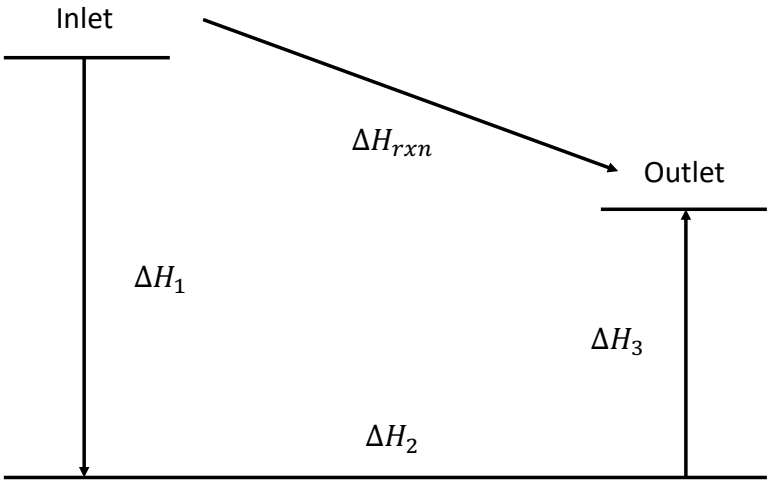

Figure 7: Diagram for the hypothetical path used to calculate the heat evolved from the ammonia synthesis reactor. In the hypothetical path, the reactants are cooled to the standard temperature of 0 ºC, the reaction occurs at standard conditions, and then the products are heated back to the reaction conditions.

The hypothetical path has three steps. The first step is to determine the amount of heat that must be removed from the reactants to go from 380 ºC to 0 ºC. This can be done with the following equation.

$$\Delta H_1 = \left(F_{N_2,2} C_{P,N_2} + \mathrm{F}_{\mathrm{H_2},2} \mathrm{C}_{\mathrm{P,H_2}}\right) \Delta \mathrm{T}_{-}$$

Where $F_{i,2}$ represents the flow rate of species i that is fed to the reactor, $C_{p,i}$ is the heat capacity of species i, and ΔT_{-} is the temperature change from the inlet temperature to standard temperature. In this step, it is assumed that the small amount of ammonia in the feed stream (from the recycle) has a negligible effect on the heat evolved in the reactor. Therefore, it will not be included in the calculation of ΔH_1.

The second step of the hypothetical path accounts for the heat of formation of ammonia at standard temperature and pressure. Ammonia is formed from diatomic hydrogen and nitrogen, which are in their natural states. This means their heats of formation are zero, and only the heat of formation of ammonia needs to be considered.

$$\Delta H_2 = 2F_{NH_3,3}\Delta H^o_{f,NH_3}$$

Where $F_{NH_3,3}$ is the molar flowrate of ammonia formed in the reactor, and $\Delta H^o_{f,NH_3}$ is the heat of formation of ammonia. The equation must be multiplied by 2 to account for the stoichiometric ratio of ammonia synthesis in the reaction.

Finally, the remaining reactants and the products need to heated back to the reactor temperature of 380 ºC.

$$\Delta H_3 = \left(F_{N_2,3}C_{P,N_2} + F_{H_2,3}C_{P,H_2} + F_{NH_3,3}C_{P,NH_3}\right)\Delta T_+$$

Where $F_{i,3}$ represents the flow rate of species i that leaves the reactor, $C_{p,i}$ is the heat capacity of species i, and ΔT_+ is the temperature change from standard temperature to the reaction conditions.

An assumption was made for the heat capacities of each species. The heat capacity of hydrogen and nitrogen does not change significantly with temperature, so the average of the heat capacity at the low and high temperatures was used in these calculations. The heat capacity of ammonia is more dependent on temperature, but there is less ammonia in the system than hydrogen and nitrogen. So the same assumption was made for ammonia's heat capacity. The heat capacities were also assumed to be independent of pressure. The heat capacity data and heat of formation data came from the NIST online webbook. The temperature dependent heat capacity of each species took the following form.

$$C_{P,i} = A_i + B_iT + C_iT^2 + D_iT^3 + E_iT^{-2}$$

Where A_i, B_i, C_i, D_i, E_i are constants for species i, and T is the temperature that the heat capacity is calculated at in Kelvin divided by 1000. The average heat capacity of each species between 0 ºC and 380 ºC was calculated as follows. A sample calculation for nitrogen is shown below.

Table 15: Heat capacity constants from the NIST online webbook that were used in the heat capacity calculations.

	Nitrogen	Hydrogen	Ammonia
A	28.98641	33.066178	19.99563
B	1.853978	-11.363417	49.77119
C	-9.647459	11.432816	-15.37599
D	16.63537	-2.772874	1.921168
E	0.000117	-0.158558	0.189174

Heat capacity for nitrogen gas at 0 ºC:

$$C_{P,N_2,273} = 28.98641 + (1.853978)\left(\frac{273\text{K}}{1000}\right) + (-9.647459)\left(\frac{273\text{K}}{1000}\right)^2 + (16.63537)\left(\frac{273\text{K}}{1000}\right)^3 + (0.000117)\left(\frac{273\text{K}}{1000}\right)^{-2}$$

$$C_{P,N_2,273} = 29.1\frac{J}{mol * K}$$

Heat capacity of nitrogen gas at 380 °C:

$$C_{P,N_2,653} = 28.98641 + (1.853978)\left(\frac{653\text{K}}{1000}\right) + (-9.647459)\left(\frac{653\text{K}}{1000}\right)^2 + (16.63537)\left(\frac{653\text{K}}{1000}\right)^3 + (0.000117)\left(\frac{653\text{K}}{1000}\right)^{-2}$$

$$C_{P,N_2,653} = 30.7\frac{J}{mol * K}$$

As can be seen here, the heat capacity of nitrogen gas barely changes with the 380 °C temperature difference. Therefore, the average of the high and low temperature heat capacities were used in the heat of reaction calculations. The average heat capacities were determined as follows.

$$C_{p,N_2} = \frac{C_{P,N_2,273} + C_{P,N_2,653}}{2}$$

$$C_{p,N_2} = \frac{29.1\frac{J}{mol * K} + 30.7\frac{J}{mol * K}}{2} = 29.9\frac{J}{mol * K}$$

The average heat capacity for each species used in the heat of reaction calculations can be seen in the table below.

Table 16: Average heat capacity of the three species in the heat of reaction calculation. The heat capacity at 0 °C and 380 °C were averaged because the heat capacities of these three species have minimal dependence on temperature.

	$\boldsymbol{C_P\left(\frac{J}{mol * K}\right)}$
Nitrogen	29.9
Hydrogen	29.0
Ammonia	41.0

Now, the enthalpy change in each step of the hypothetical path can be determined. The molar flow rates used in these calculations are from the ammonia synthesis loop material balance hand calculations section.

$$\Delta H_1 = \left[\left(70.2\frac{kmol\ N_2}{hr}\right)\left(29.9\frac{kJ}{kmol * K}\right) + \left(211\frac{kmol\ H_2}{hr}\right)\left(29.0\frac{kJ}{kmol * K}\right)\right](273K - 653K)$$

$$\Delta H_1 = -3.12 * 10^6\frac{kJ}{hr}$$

$$\Delta H_2 = 2\left(28.1\frac{kmol\ NH_3}{hr}\right)\left(-45{,}900\frac{kJ}{kmol\ NH_3}\right)$$

$$\Delta H_2 = -2.58 * 10^6\frac{kJ}{hr}$$

$$\Delta H_3 = \left[\left(56.2\frac{kmol\ N_2}{hr}\right)\left(29.9\frac{kJ}{kmol * K}\right) + \left(169\frac{kmol\ H_2}{hr}\right)\left(29.0\frac{kJ}{kmol * K}\right) + \left(28.1\frac{kmol\ NH_3}{hr}\right)\left(41.0\frac{kJ}{kmol * K}\right)\right](653K - 273K)$$

$$\Delta H_3 = 2.94 * 10^6\frac{kJ}{hr}$$

Finally, the heat evolved in the reactor can be determined by summing the three steps in the hypothetical path.

$$\Delta H_{rxn} = \Delta H_1 + \Delta H_2 + \Delta H_3$$

$$\Delta H_{rxn} = \left(-3.12 * 10^6\frac{kJ}{hr}\right) + \left(-2.58 * 10^6\frac{kJ}{hr}\right) + \left(2.94 * 10^6\frac{kJ}{hr}\right)$$

$$\Delta H_{rxn} = -2.76 * 10^6\frac{kJ}{hr}$$

This is the quantity of heat that must be removed from the reactor to maintain isothermal operation. Now, the quantity of water required to cool the reactor can be calculated using the heat of vaporization of steam at 5 bar (physical property data was obtained from Engineering Toolbox).

$$\dot{m}_w = \frac{-\Delta H_{rxn}}{\Delta H_{vap}}$$

$$\dot{m}_w = \frac{2.76 * 10^6\frac{kJ}{hr}}{2107\frac{kJ}{kg\ H_2O}} = 1{,}310\frac{kg\ H_2O}{hr}$$

Net Present Value 20-year Breakdown

Table 17: Breakdown of the net present value calculation for the 50 mt/day ammonia plant over the 20 year lifetime. A 20-year MACRS depreciation was applied to the plant, which gave the highest NPV compared to shorter schedules. The corporate income tax was taken at 21%. The time value of money was set at 8%. The total capital cost of the plant was spread over the 30-month manufacture and assembly period, which began after the 6-month permit acquisition phase. Money is shown in millions of dollars.

Y	Capital Costs	Gross Profit	MACRS (%)	MACRS ($)	Taxable Income	Taxes Paid	Cash Flow	Present Value
0	0	0	0	0	0	0	0	0
1	-14.15	0	0	0	0	0	-14.15	-13.099
2	-14.15	0	0	0	0	0	-14.15	-12.128
3	-14.15	0	0	0	0	0	-14.15	-11.230
4	0	1.97	0.0375	1.59	0.378	0	1.97	1.448
5	0	1.97	0.07219	3.06	0	0.079	1.89	1.286
6	0	1.97	0.06677	2.83	0	0	1.97	1.241
7	0	1.97	0.06177	2.62	0	0	1.97	1.149
8	0	1.97	0.05713	2.42	0	0	1.97	1.064
9	0	1.97	0.05285	2.24	0	0	1.97	0.985
10	0	1.97	0.04888	2.07	0	0	1.97	0.912
11	0	1.97	0.04522	1.92	0.051	0	1.97	0.845
12	0	1.97	0.04462	1.89	0.076	0.011	1.96	0.778
13	0	1.97	0.04461	1.89	0.076	0.016	1.95	0.718
14	0	1.97	0.04462	1.89	0.076	0.016	1.95	0.665
15	0	1.97	0.04461	1.89	0.076	0.016	1.95	0.616
16	0	1.97	0.04462	1.89	0.076	0.016	1.95	0.570
17	0	1.97	0.04461	1.89	0.076	0.016	1.95	0.528
18	0	1.97	0.04462	1.89	0.076	0.016	1.95	0.489
19	0	1.97	0.04461	1.89	0.076	0.016	1.95	0.453
20	0	1.97	0.04462	1.89	0.076	0.016	1.95	0.419
21	0	1.97	0.04461	1.89	0.076	0.016	1.95	0.388
22	0	1.97	0.04462	1.89	0.076	0.016	1.95	0.359
23	0	1.97	0.04461	1.89	0.076	0.016	1.95	0.333
24	0	0	0.02231	0.95	0	0.016	-0.02	-0.003
							NPV	-21.21
							IRR	-0.007